MODULATION BY NITRIC OXIDE OF PHOTOSYNTHESIS AND MITOCHONDRIAL OXIDATIVE METABOLISM IN MESOPHYLL PROTOPLASTS OF PEA AND INTERACTION WITH GLUTATHIONE METABOLISM IN LEAVES OF *ARABIDOPSIS THALIANA*

A thesis submitted to the University of Hyderabad for the award of Ph. D degree in Plant Sciences

By

SUNIL BABU BOBBA

Department of Plant Sciences
School of Life Sciences
University of Hyderabad
PO Central University, Gachibowli
Hyderabad 500 046
Andhra Pradesh (India)

Regd. No: 04LPPH03

July 2011

University of Hyderabad
School of Life Sciences
Department of Plant Sciences
Hyderabad-500 046

DECLARATION

I, Sunil Babu Bobba, hereby declare that this thesis entitled "**Modulation by nitric oxide of photosynthesis and mitochondrial oxidative metabolism in mesophyll protoplasts of pea and interaction with glutathione metabolism in leaves of *Arabidopsis thaliana***" submitted by me under the guidance and supervision of **Professor A. S. Raghavendra** is an original and independent research work. I also declare that it has not been submitted previously in part or in full to this University or any other University or Institution for the award of any degree or diploma.

Date:

Name : **Sunil Babu Bobba**

Signature :

Regd. No. : **04LPPH03**

University of Hyderabad
School of Life Sciences
Department of Plant Sciences
Hyderabad-500 046

CERTIFICATE

This is to certify that this thesis entitled "**Modulation by nitric oxide of photosynthesis and mitochondrial oxidative metabolism in mesophyll protoplasts of pea and interaction with glutathione metabolism in leaves of *Arabidopsis thaliana***" is a record of bonafide work done by **Mr. Sunil Babu Bobba**, a research scholar for Ph.D. program in Plant Sciences, Department of Plant Sciences, School of Life Sciences, University of Hyderabad under my guidance and supervision.

The thesis has not been submitted previously in part or in full to this or any other University or Institution for the award of any degree or diploma.

Prof. A. S. Raghavendra
(Supervisor)

(Head of the Department)

(Dean of the School)

Dedicated to my parents

Vimala Devi *and* ***Satyanarayana Reddy***

for all the hardships they faced and sacrifices they made

to bring me till this stage.

Acknowledgements

I owe a deep sense of gratitude towards my research supervisor ***Prof. A. S. Raghavendra,*** *FNA, FASc, FTWAS and JC Bose National Fellow, for his guidance, encouragement, suggestions and great support throughout my doctoral study. He is a great human being. I am grateful to you Sir, and thanks for everything*

I avail this opportunity to express profound sense of gratitude to ***Prof. Graham Noctor*** *(Institute de Biotechnologie des Plante, Paris, France) for providing me a chance to work in his lab during my Sandwich Ph. D fellowship and for his thought provoking scientific ideas, optimism and inspiration, which helped me to carry out my research at France.*

My sincere thanks to ***Prof. Attipalli R. Reddy****, Head, Department of Plant Sciences and* ***Prof. M. Ramanatham****, Dean, School of Life Sciences, for providing the facilities necessary for my research. I extend my thanks to former Heads* ***Prof. P.B. Kirti, Prof. Appa Rao Podile*** *and former Dean* ***Prof. A.S. Raghavendra****.*

The noblest profession is being a teacher. They are the pillars that build one's success. I wholeheartedly thank ***Prof. Prasanna Mohanty*** *for his consistent inspiration, patient counsel and valuable advices when needed. Special thanks to,* ***Prof. Attipalli R. Reddy, Dr. Padmasree, Dr. Rajagopal, Prof. Aparna Dutta Gupta*** *and* ***Mr. Durga Prasad*** *(Lecturer, Guntur) for their moral support and suggestions and I also thank all the faculty members of Dept. of Plant Sciences.*

The financial assistance from the ***CSIR****,* ***ICAR****, and* ***Sandwich PhD fellowship*** *from French Embassy in India are gratefully acknowledged. Funding from* ***CSIR, DBT, ICAR-NAIP, DST-DFG, and DST-JC Bose*** *to Prof. A. S. Raghavendra as well as entire umbrella funding from* ***DST-FIST, DBT-CREBB*** *and* ***UGC-SAP*** *to the Department and School are acknowledged. I am thankful to the* ***University of Hyderabad****, Department of Plant Sciences for providing me an opportunity to pursue my Ph.D.*

My heartfelt thanks to ***Dr. Bertrand Gakaire****, for his brotherly gesture, help and support, which made my stay in France to be homely and memorable. I extend my thanks to* ***Dr. Guillaume Queval****, for helping me in executing my research work during my stay in France.*

I would also like to acknowledge ***Prof. Reto J Strasser*** *(University of Geneva, Switzerland),* ***Prof. Govindjee*** *(University of Illinois-UC, USA),* ***Prof. Renate Scheibe*** *(University of Osnabrück, Germany) and* ***Prof. Erwin Grill*** *(Technical University of Munich, Germany) for their useful discussions and helpful suggestions during their visits to our laboratory.*

I am thankful to former lab mates ***Dr. Jhadeswar, Dr. Riazunnisa, Mr. Sudhakar, Dr. Vijay, Dr. Uday, Dr. Dinakar*** *and present lab mates* ***Dr. Bakshu, Dr. Bindu, Dr. Poonam, Sai, Malli, Nupur and Gayatri*** *for providing a conductive and friendly laboratory environment. I thank* ***Mrs. Kalyani*** *for taking care of the lab requirements in time and* ***Mr. Venu*** *and* ***Narasimha*** *for taking care of the plants.*

My Special and wholehearted thanks to my friend and former lab mate ***Dr. K. Apparao,*** *present lab mate* ***Rajsheel*** *for their help, support and cooperation on and off the lab.*

I would like to thank all my long standing friends, who helped me in innumerable ways, both in my 'academic' and 'non-academic' ventures. Thanks to ***Sanjith, Apparao, Eswar, Sunil, Satish, Arjun, Parimala, Srividya,*** *and my "Guntur circle"* ***Ravi, Uday, Samba, Ranga*** *and* ***Adi*** *for their phone calls and emails. I share a very close and special relationship with them.*

I am extremely grateful to my friends ***Prasad, Chaitanya, Roy, Maheedhar, Girish, Sreedhar,*** *and* ***Jayaram*** *for unconditional support and love they provided me all these years. I also feel infinitely happy to express my heartfelt thanks* ***Shankar, Ramakrishna, Nishanth, Srinu, Madhu, Abhay*** *and all* ***my loving friends*** *in School of Life Sciences for their affection and moral support which will remain fresh forever in my memory.*

I owe my heartfelt thanks to my cousins ***Sridhar, Raja, Sasi, Karuna*** *and* ***Hari*** *for making my life happy with their lovely, enjoyable and memorable company.*

With due respect, I express my sense of indebtedness and appreciation to my ever-loving ***Amma*** *and* ***Nanna,*** *for their kind understanding, perseverance and moral support. I am always grateful to my brother* ***Anil Reddy,*** *bhabi* ***Rupa,*** *my sister* ***Sunitha*** *and brother-in-law* ***Ashok Reddy*** *for having faith in my ability and for their understanding, encouragement and support all through the life. I cherish the lovely moments spend with my little nephews and nieces* ***Chinnu, Honey, Lucky*** *and* ***Varshi.***

Words fail me when I try to explain the endless patience, support and faith showed by my better half ***Praveena*** *during the entire period of my study. Life wouldn't have been so beautiful without her.*

Lastly, I would like to give all the honour to ***The Almighty God,*** *for his wisdom, guidance and assurance at all the times.*

Sunil...

Abbreviations

Chl a	: Chlorophyll a
BQ	: Benzoquinone
NO_2^-	: nitrite ion
PQ pool	: Plastoquinone pool
PS I and II	: Photosystems I and II
NADPH	: Nicotinamide adenine dinucleotide phosphate
ATP	: Adenosine-5'-triphosphate
OJIP	: Chlorophyll a fluorescence transients Origin (O)-Intermediate steps 1 and 2 (J-I; also known as I_1-I_2) - Peak (P)
Fv/Fm	: maximal quantum efficiency of Ps II
ROS	: Reactive oxygen species
NO	: Nitric oxide
SNP	: Sodium nitroprusside
CN^-	: Cyanide
cPTIO	: 2-phenyl-4, 4,5,5 tetramethylimidazoline -1-oxyl-3-oxide
DAF-2DA	: 4,5-diaminofluorescein diacetate
COX	: Cytochrome oxidase
AOX	: Alternative oxidase
SHAM	: Salicylhydroxamic acid
LEDR	: Light enhanced dark respiration
Asc	: Ascorbate
GSH	: Glutathione
γECS	: γ-glutamylcysteine synthetase, 1st enzyme of glutathione biosynthesis
GSH1	: gene encoding γECS: Glutaminate cystein ligase
GSH-S	: Glutathione synthetase
GSH2	: gene encoding GSH-S
ggschp	: *Arabidopsis* transgenics over-expressing *E. coli GSH1* in chloroplast

ggscyt	: *Arabidopsis* transgenics over-expressing *E. coli GSH1* in cytosol
cad2	: cadmium sensitive mutant with reduced glutathione content
GR	: Glutathione reductase
GRcyt	: *Arabidopsis* transgenics over-expressing *E. coli GR* in cytosol
GRcyt-	: *Arabidopsis* insertion mutant with reduced GR levels
GRcyt	: gene encoding cytosolic glutathione reductase
GRcm	: gene encoding dual targeted plastidic/mitochondrial isoform of GR
WT	: wild type
Kan	: plant with empty vector carrying kanamycin gene
cAPX	: transcript encoding cytosolic ascorbate peroxidase
AOX1a	: isoform of alternative oxidase
GSTu24	: glutathione S-transferase
RT–PCR	: reverse transcription– polymerase chain reaction
qRT-PCR	: quantitative real time polymerase chain reaction

All the remaining abbreviations are all standard ones and as per *Plant Physiology* issue, 2011, Instructions for contributors, website: http://www.aspb.org.

Further abbreviations related to Chl *a* fluorescence are listed in Table 3.4 in Materials and Methods.

Contents

Chapter 1

Introduction and Review of literature

Chapter 1

Introduction and Review of literature

The diverse physiological and metabolic reactions of the plant cells are tightly coordinated to ensure efficient function. The intracellular crosstalk involving metabolic redox signals is a key factor in the response to environmental challenge, and is central to the physiological outcome of plant responses to stress (Foyer and Noctor, 2003; Noctor, 2006; Pesaresi et al., 2007). Photosynthesis and respiration are the most important metabolic processes associated with carbon and energy metabolism in plants. It has been well recognized that photosynthesis and respiration in the plant cell must be intimately linked, given that respiration relying on photosynthesis for substrate and photosynthesis depends on respiration for a range of compounds (e.g. ATP).

1.1. Physiological and biochemical features of interorganelle interactions

The molecular interaction between the organelles of chloroplasts and mitochondria is studied extensively (Raghavendra and Padmasree, 2003; Yoshida et al., 2006; Sweetlove et al., 2007; Nunes-Nesi et al., 2008; Millar et al., 2011). While the core reaction schemes of the pathways of photosynthesis, respiration, and photorespiration are well defined, it is only recently that the adoption of reverse genetic strategies started to high-light the importance of individual steps (Bauwe et al., 2010; Sweetlove et al., 2010). The rapid exchange of metabolites between chloroplasts, cytosol, peroxisomes and mitochondria forms an important channel of interorganelle communication (Figure 1.1). The feedback from signals of energy-

generating organelles (like chloroplasts and mitochondria) orchestrating quick metabolic adjustments, also helps in the plant responses to environmental changes.

Besides metabolite shuttles, the strong interaction between these organelles is facilitated by multiple factors, which include redox homeostasis and possibly other components. The metabolites formed in the organelles are transported across membranes by either specified translocators or by simple diffusion. Some of the metabolite shuttles may serve multiple functions such as transferring ATP or reducing equivalents or carbon skeletons.

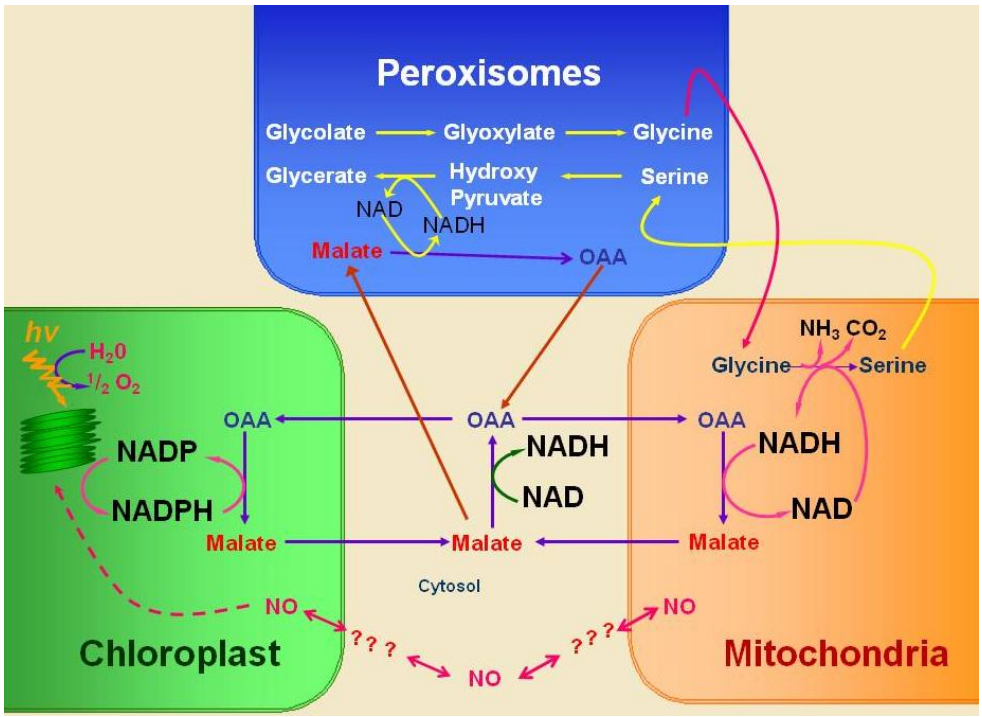

Figure 1.1. Interorganelle interactions in a typical photosynthetic cell. The metabolic processes involving the transfer of energy and redox equivalents, between chloroplast, mitochondrion, peroxisome and cytosol, form the basis of interactions. The present work attempts to examine the role of nitric oxide (NO) in such a system.

The major products exported from chloroplasts of C_3 plants in light are glycolate, triose-P and malate. The carboxylase activity of Rubisco results in the formation of triose-P, while the oxygenase activity of Rubisco leads to the formation of glycolate. Triose-P is exported to cytosol to form sucrose and oxidation to PGA releasing ATP and NADH. The malate released into the cytosol is either oxidized in cytosol to support nitrate reduction or transferred to peroxisomes to support hydroxypyruvate reduction (Atkin et al 2000). The resultant OAA is transported back into chloroplast. Glycolate exported to peroxisomes forms the substrate for photorespiratory metabolism, helping to dissipate excess energy.

Besides ATP, mitochondria exports serine (participates in photorespiratory cycle), oxoglutarate (to supply carbon compounds for N metabolism) and malate (to transfer reducing equivalents to cytosol and peroxisomes). During illumination, the difference in redox potential between chloroplast stroma and cytosol is high (Nunes-Nesi et al 2007). Hence a large amount of malate (as a source of reducing power) is sent into the cytosol in the form of malate or triose-phosphate (Scheibe 2004; Nunes-Nesi et al 2007).

Glycine and glycerate are the major products exported from peroxisomes (Figure 1.2). Glycolate is oxidized to glyoxylate and then to glycine using glutamate in peroxisomes. Glycine is transported into mitochondria, oxidized to yield serine,which in turn exported back to peroxisomes and converted into hydoxypyruvate. Hydroxypyruvate is reduced to glycerate, and is then exported to chloroplast.

Redox signals emanating from the mitochondria are also important in setting the cellular machinery to maintain overall redox balance (Nunes-Nesi et al 2007). Unlike the situation in chloroplasts, ATP produced during oxidative phosphorylation in mitochondria can be transferred directly to cytosol through adenylate translocator (Raghavendra and Padmasree, 2003).

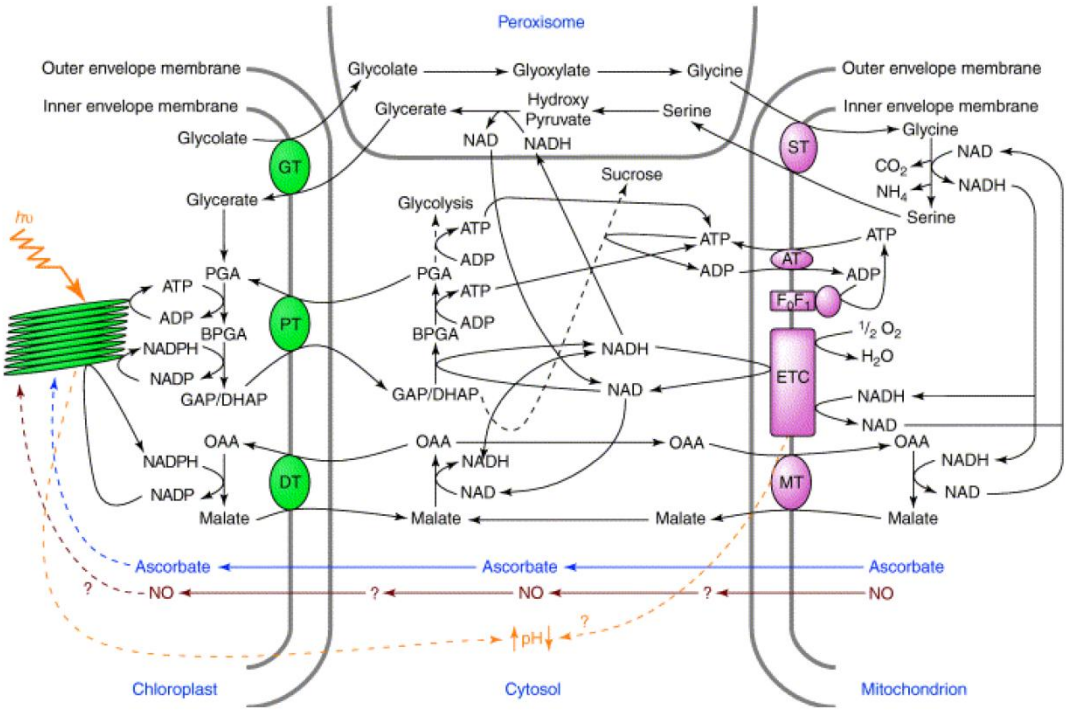

Figure 1.2. Exchange of metabolites and energy/redox between chloroplast, mitochondrion, peroxisome and cytosol, during photosynthesis. These metabolite and energy shuttles form the biochemical basis of interorganelle interaction. **GT**: glycolate/glycerate translocator, **DT:** triose-phosphate/Pi translocator, **MT**: malate/OAA translocator of chloroplast, **ST**: glycine/serine translocator, **AT**: Adenylate translocator, **MT**: malate/OAA translocator of mitochondria, Only the major metabolite exchanges are shown. (Adapted from Raghavendra and Padmasree 2003).

1.2. Mitochondrial contribution for optimal photosynthesis

The tight interaction between photosynthesis and respiration is unique to plant cells. Inhibition of mitochondrial respiration by inhibitors or mutations lowered the photosynthetic activity in tobacco leaves, broad bean and pea protoplasts suggesting that mitochondria provide chloroplasts with flexible strategies to optimize photosynthesis and even protect against photoinhibition (Dutilleul et al. 2003; Fernie et al. 2004; Yoshida et al., 2006). Experiments on transgenic or mutant plants with elevated or reduced levels of respiratory enzymes/components are revealing exciting insights into the function, organization and control of plant respiration.

Inhibition of the mitochondrial respiration alters the cellular redox state and can impair the state transitions of thylakoid membranes (Matsuo and Obokata 2006). The tobacco CMSII mutant deficient in functional complex I displayed markedly reduced rates of photosynthesis (Dutilleul et al., 2003; Priault et al 2006). The increased AOX capacities of transgenic *Arabidopsis* plants, have been shown to decrease the extent of ROS accumulation (Umbach et al 2005). The inhibition of AOX decreased the rates of photosynthetic oxygen evolution and caused a over-reduction of the photosynthetic electron transport system, even under low light (Yoshida et al 2007). These results provided strong evidences for the importance of mitochondrial electron transport, in optimizing photosynthesis.

1.3. Major redox signaling components

To function properly, the living cell needs to monitor, control and maintain an optimal intracellular redox balance. Any disturbance in the intracellular redox balance causes oxidative stress, usually characterized by increased levels of reactive oxygen species (ROS) and/or nitric oxide (NO), resulting in perturbation of cellular function. On the other hand, both ROS and NO play a vital role in intracellular redox signaling by triggering activation of antioxidant resistance mechanisms (Buchanan and Balmer, 2005; Tanou et al., 2009). Both ROS and NO are known to exert a multitude of effects in regulating many key cellular responses in plants (Baudouin, 2011; Mittler et al., 2011).

Reactive oxygen species (ROS)

Generation of ROS (Figure 1.3) from redox reactions of chloroplasts and mitochondria has been identified as an inevitable component of aerobic metabolism (Apel and Hirt 2004; Noctor, 2006; Møller et al. 2007). Four major types of ROS, singlet oxygen ($^1O_2$), superoxide ($O_2^{\cdot -}$), hydrogen peroxide (H_2O_2) and hydroxyl radicals (OH^-), are produced in green tissues during active photosynthesis. In chloroplasts, PSII and PSI (Mehler reaction) are the major sites for the production of singlet oxygen and superoxide radicals (Apel and Hirt 2004). These radicals are potentially dangerous molecules in biological systems, and need to be scavenged efficiently (Haliwell and Gutteridge, 1999). It is essential for plants to restrict also the production of reactive molecules. Chloroplasts possess effective antioxidant machinery such as ascorbate and glutathione, to deal such free radicals. In

mitochondria, complex I, ubiquinone and complex III of electron transport chain are the major sites for the generation of superoxide radicals (Møller 2001; Navrot et al., 2007).

In both chloroplasts and mitochondria, the O_2 radicals are dismutated to H_2O_2, a less toxic form of ROS, by superoxide dismutase (SOD). H_2O_2 is also formed as a by-product of photorespiration during oxidation of glycolate to glyoxylate in

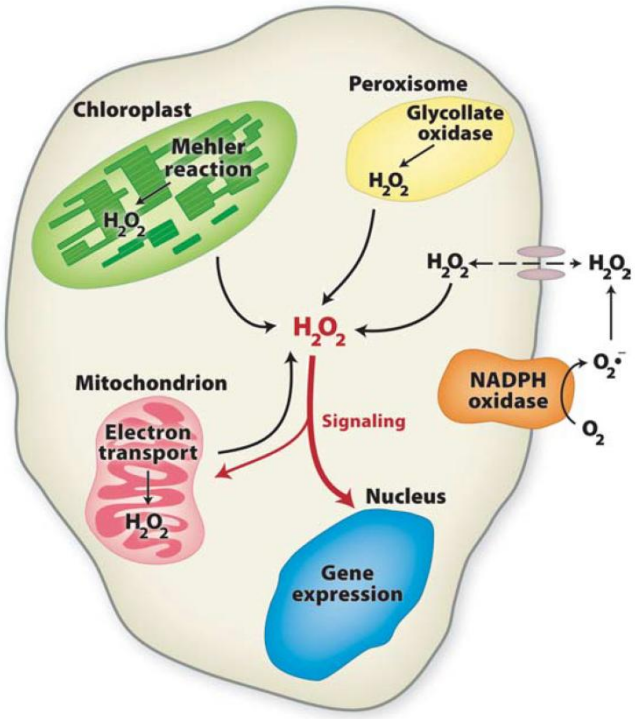

Figure 1.3. H_2O_2 is generated in normal metabolism via the Mehler reaction in chloroplasts, electron transport in mitochondria and photorespiration in peroxisomes. Abiotic and biotic stresses enhance H_2O_2 generation via these routes and also via enzymatic sources such as plasma-membrane-localised NADPH oxidases or cell wall peroxidases. H_2O_2 diffuses freely, perhaps facilitated by movement through peroxiporin membrane channels. (Adapted from Buchanan and Balmer, 2005).

peroxisomes (del Rio et al. 2006). The potential enzymatic sources of H_2O_2 include NADPH oxidase, cell wall peroxidases, amine oxidase, oxalate oxidase and flavin-containing oxidases.

However, despite their potential for causing harmful oxidations, ROS molecules are involved in the control of plant growth, development and acclimatory responses to stress stimuli (Foyer and Noctor, 2005; Jones, 2006; Møller et al., 2007). ROS are, in fact, ideal signaling molecules, since they can diffuse (being small) over short distances (Pitzschke et al., 2006). The efficacy of different ROS signals are determined by the interplay between the ROS production and ROS scavenging systems of the cell. Major ROS-scavenging enzymes of plants include superoxide dismutase (SOD), ascorbate peroxidase (APX), catalase (CAT), glutathione peroxidase (GPX) and peroxiredoxin (PrxR). Together with the antioxidants ascorbic acid and glutathione, these enzymes provide cells with highly efficient machinery for detoxifying O_2 and H_2O_2 (Mittler et al., 2004).

ROS-induced changes might be due to direct effects through redox modification of metabolic enzymes or indirect through changes in transcription factors and subsequently gene expression. ROS can oxidize the redox-sensitive proteins/enzymes directly or indirectly via the ubiquitous redox-sensitive molecules, such as glutathione (GSH) or thioredoxins, which control the cellular redox state in higher plants (Foyer and Noctor, 2009).

Although ROS are generated in chloroplasts, mitochondria and peroxisomes,

the relative contribution of mitochondria to ROS production in green tissues seems to be low (Purvis, 1997). One reason is that plant mitochondria have an unique alternative oxidase (AOX), which minimizes the ROS production, by competing for electrons at ubiquinone. Overproduction of AOX in transgenic cell lines reduced ROS production, whereas antisense cells with reduced levels of the alternative oxidase (AOX) accumulated five times more ROS than control cells (Maxwell et al., 1999). Oxidative stress by added H_2O_2 induced the synthesis of AOX (Wagner and Moore, 1997).

Nitric oxide (NO)

Nitric oxide (NO) is an ubiquitous small gaseous molecule with diverse signaling function in plants (Besson-Bard et al., 2008; Leitner et al. 2009). The presence and synthesis of NO in plant cells is undisputed but the exact source of NO production is not clear (Delledonne et al., 1998; Durner et al., 1998), unlike in mammals, where NO originates from three isoforms of NO synthases (NOS: endothelial NOS, neuronal NOS and inducible NOS) (Alderton et al., 2001). Plants possibly possess multiple sources of NO production either by non-enzymatically or enzymatically (Figure 1.4). The enzymes that can generate NO include Nitrate reductase (NR) (Wilson et al., 2008), NOS-like activity (Wilson et al., 2008; Moreau et al., 2010) and nitrate: NO reductase (Ni-NOR), probably situlated in the plama membrane (Stohr and Ullrich, 2002) and xanthine oxidoreductase (XOR) operating at low oxygen tensions (Rumer et al., 2009). Depending on the physiological context, different sources may be individually or jointly participating in NO production. Recent

evidences demonstrated that mitochondria and plastids are sites for bioactive NO production (Gas et al., 2009; Blokhina and Fagerstedt, 2010). Chloroplasts can synthesize NO from either NO_2^- or Arginine (Jasid et al., 2006).

The effects of NO are mediated through gene regulation and S-nitrosylation. Accordingly, exogenously applied or endogenously produced NO in plant tissues or cell suspensions were reported to modulate the accumulation of the transcripts of numerous putative NO-regulated genes in various plant species. The

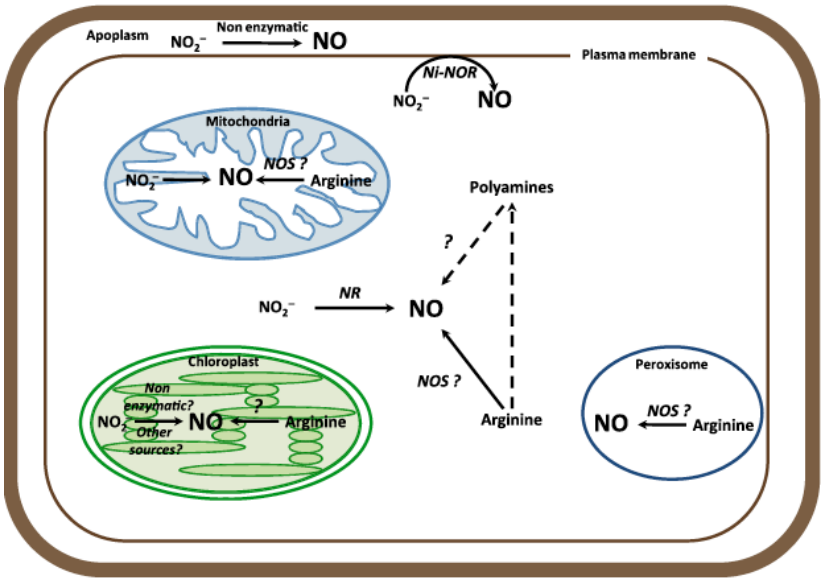

Figure 1.4. Origins of NO in plant cells. The enzymatic conversion of NO_2^- to NO occurs in the cytosol and in the plastids and mitochondria; alternatively, NO_2^- can be converted to NO by non-enzymatic processes in the plastids and in the apoplasm. Arginine-dependent NO production exists in peroxisomes, in mitochondria, in plastids and in the cytosol, and may involve NO synthase-like activities and unidentified enzymes metabolizing polyamines. Abbreviations: **NR**, nitrate reductase; **Ni-NOR**, nitrite–nitric oxide oxidoreductase; **NOS**, putative NO synthase-like enzymes. (Adapted from Baudouin, 2011).

transcriptomic analyses have identified that a significant proportion (about 30%) genes regulated by NO sustain are involved in cellular functions (Besson-Bard et al., 2009b).

Nitric oxide may also be involved in regulating protein function through s-nitrosylation (Lindermayr et al., 2005; Besson-Bard et al., 2008). S-nitrosylation occurs when nitric oxide reacts with the cysteine residue to form S-NO bonds. This is increasingly recognized as a ubiquitous control of protein function in both animals and plants. *Arabidopsis* leaf and cell suspension protein extracts treated with artificially released NO identified several S-nitrosylated proteins. These post-translational modifications can affect the efficiency of a wide array of cellular activities, including metabolism, photosynthesis, redox control, and stress response (Pfannschmidt et al., 1999; Michelet et al., 2005).

NO affects the mitochondrial functionality in plant cells and reduces total respiration due to its inhibitory effect on the cytochrome pathway (Zottini et al., 2002; Millar and Day, 1996). In higher plants, AOX may play a role in NO tolerance, as evidenced by the experiments with tobacco suspension cells, where it has been shown that NO could activate the AOX pathway (Huang et al., 2002). Nitric oxide can also modulate other mitochondrial enzymes, tobacco aconitase. Its inactivation by NO decreases the cellular energy metabolism which may result in reduced electron flow through the mitochondrial respiratory electron transport chain and a subsequent decrease in the generation of ROS (Navarre et al., 2000).

Experiments with isolated thylakoids indicated that NO binding could slow down the rate of electron transfer between Q_A and Q_B (Wodala et al., 2008) or even affect additional sites in PSII (Schansker et al., 2002). Experiments carried out on isolated chloroplasts, thylakoids and intact leaves using different NO donors yielded contradictory results (Hayat et al., 2010). Further work is required to resolve the effects of NO on photosynthetic electron transport and carbon assimilation.

1.4. Antioxidants: focus on glutathione

Redox homeostasis is an essential metabolic response during stress in plant cells. During this process, the accumulation of free radicals such as ROS and NO, are counteracted by the accumulation of antioxidants along with antioxidant enzymes, working together to bring down the ROS levels (Mittler et al., 2004). The non-enzymatic antioxidants include ascorbate (Asc), glutathione (GSH), tocopherols and flavonoids. In the present work, the focus was on Asc and GSH.

Ascorbate

Ascorbate is perhaps the most abundant antioxidant in plants and helps to optimize metabolism and components of redox signaling, photosynthesis and even plant defense (Smirnoff and Wheeler, 2000; Foyer and Noctor, 2009). Subcellular distribution of ascorbate was reported in chloroplasts, mitochondria and peroxisomes as well as in the apoplast (Pignocchi and Foyer 2003).

The interactions between ascorbate, superoxide, hydrogen peroxide and ascorbate peroxisae (APX), in chloroplasts have been extensively studied (Foyer and Halliwell, 1976; Asada, 2006). Ascorbate occurs in a reduced form (ascorbic

acid, Asc) and two oxidized forms mono and dehydroascorbate (MDHA and DHA). The ratio between reduced and oxidized ascorbate is an important factor for plants to adapt against oxidative stress (Foyer and Noctor, 2009). It has recently been suggested that ascorbate participates in the beneficial interactions of chloroplasts and mitochondria (Talla et al., 2011).

Glutathione (GSH)

Glutathione is a tripeptide (γ-glu-cys-gly) and is the predominant low-molecular weight nonprotein thiol in most eukaryotic and prokaryotic cells (Foyer and Noctor, 2005; Meyer, 2008). GSH is also involved in sulfur metabolism, xenobiotic and heavy metal detoxification (Rouhier et al., 2008). GSH is detected virtually in all cell compartments such as cytosol, chloroplasts, endoplasmic reticulum, vacuoles, and mitochondria. The reduced form of glutathione (GSH) exists interchangeably with the oxidized form, glutathione disulfide (GSSG). In plants, the physiological significance of glutathione as an antioxidant and redox buffer (Noctor et al., 2002) makes GSH important for redox signaling.

The pathway of glutathione (GSH) synthesis in plants is well known (Noctor et al., 2002; Mullineaux and Rausch, 2005). Using glutamate, cysteine and glycine, two ATP-dependent enzymes produce GSH via the intermediate, γ glutamylcystein, (γEC, Figure 1.5). The first enzyme, γ-glutamylcysteine synthetase (γECS), is encoded by the *GSH1* gene and the second enzyme, glutathione synthetase (GSH-S) is encoded by *GSH2*. The subcellular localization studies of the Arabidopsis γECS have convincingly demonstrated that the enzyme is restricted to plastids (Wachter

et al., 2005). In contrast, the *GSH2* gene encodes two transcripts. The most abundant is the shorter form, encoding a cytosolic GSH-S, while the longer form encodes a chloroplast-targeted protein (Wachter et al., 2005). Thus, the first step of GSH synthesis is located in the plastid while the second step can occur in both chloroplasts and cytosol. Plastidic γECS and cytosolic GSH-S are linked by γEC export across the chloroplast envelope through transporters (Maughan et al., 2010).

The production of GSH is regulated at multiple levels, with the most important limitation being γECS activity, as observed with the analysis of

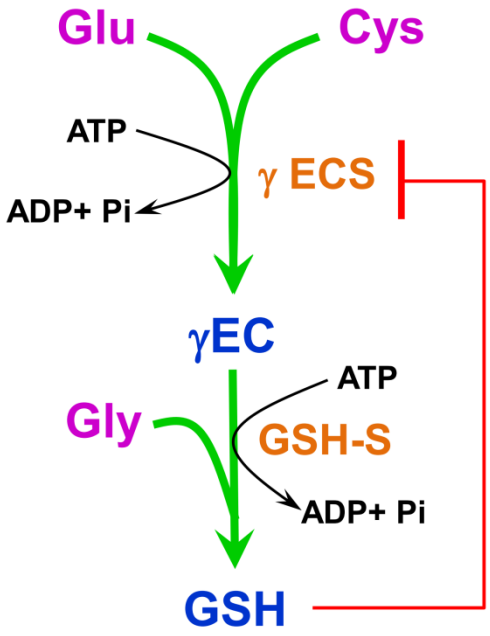

Figure 1.5. Scheme showing production of glutathione using the three constituent amino acids. The regulatory mechanism (feedback inhibition) is shown in red line. **Glu**: Glutamate, **Cys**: Cysteine, **γECS**: γ-glutamylcysteine synthetase, **Gly**: Glycine, **γEC**: γ- glutamylcysteine, **GSH-S**: glutathione synthetase, **GSH**: Glutathione.

Arabidopsis mutants. Complete knockout of *GSH1* or *GSH2* through T-DNA insertions causes an embryonic lethal phenotype (Cairns et al., 2006; Pasternak et al., 2008). The activity of γ-ECS appears to be regulated by cysteine concentration and availability of ATP. Studies using expression of *E. coli* γ-ECS targeted to the poplar chloroplast or cytosol or to the tobacco chloroplast produced increases in leaf GSH (Noctor et al., 1996, Herschbach et al., 2010). Even higher levels of GSH were achieved by combined over-expression of γ-ECS and GSH-S (Creissen et al., 1999). On the other hand, over-expression of GSH-S did not affect glutathione contents (Noctor et al., 1998).

The glutathione is a multifunctional metabolite in plants that is important in redox homeostasis, signaling, defense reactions and stress tolerance. The chemical reactivity of the thiol group of glutathione makes it particularly suitable to serve a broad range of such biochemical functions. Cellular glutathione homeostasis has long been considered as a key element of signaling cascades, transducing information on environmental responses to their respective targets (May et al., 1998).

Glutathione accumulates to high concentrations, under stress situations. Such increase is important for signal transduction and defense against ROS and involves a coordinated activation of genes encoding glutathione biosynthetic enzymes and GR (Xiang and Oliver 1998). These important insights were achieved by the availability of *Arabidopsis* mutants with partial decreases in glutathione contents. The mutants *cad2* (Cobbett et al., 1998), *rax1* (Ball et al., 2004), and *pad2*

(Parisy et al., 2007) all contain mutations in the gene *GSH1*, lead to a reduced overall level of glutathione to 20–50% of wild-type plants. Apparently the mutants didn't show any phenotypic difference with wild type plants, but show increased sensitivity under conditions of stress.

Glutathione keeps the intracellular environment reduced by the detoxification of reactive oxygen species (ROS) (Mayer et al., 2007; Noctor et al., 2011). In plants, ROS are at least partially detoxified through the glutathione-ascorbate-cycle (Noctor and Foyer, 1998). Transient changes in glutathione redox potential were suggested to be part of signaling cascades leading to changes in gene expression during stress responses and developmental processes (Ball et al., 2004; Mayer, 2008). GSH can also react with nitric oxide to form the GSNO derivative, and provide another signaling molecule, to sense both ROS and NO (Lindermayr et al., 2005).

1.5. Antioxidant related enzymes: focus on glutathione reductase (GR)

The enzymatic ROS scavenging system consists of several enzymes like superoxide dismutase (SOD), catalase (CAT), ascorbate peroxidase (APX), monodehydro-ascorbate reductase (MDAR), dehydroascorbate reductase (DHAR), glutathione peroxidase (GPX), and glutathione reductase (GR), which are located in different compartments of the cell (Shao et al., 2008). Within the cell, SODs constitute the first line of defense against ROS. The ascorbate-glutathione (Asc-GSH) cycle that occurs in chloroplasts, cytoplasm, and mitochondria (Noctor and Foyer, 1998) is catalyzed by a set of four enzymes, APX, MDAR, DHAR, and GR.

Glutathione reductase (NADPH: oxidized glutathione oxidoreductase; GR) catalyses the NADPH-dependent reduction of the disulphide bond of oxidized glutathione. GR is localized mainly in the chloroplast in which it represents about 80% of total GR activities in leaf tissues, but is also found in the cytosol, glyoxysomes and peroxisomes (Edwards et al. 1990; Jiménez et al. 1997). GR catalyses the NADPH dependent reaction of disulphide bond of GSSG and is thus important for maintaining the GSH pool (Figure 1.6) (Reddy and Raghavendra 2006; Romero-puertas et al., 2006). Thus, in the ascorbate-glutathine cycle, glutathione acts as recycled intermediate in the reduction of H_2O_2 using electrons derived ultimately from H_2O (Foyer et al., 1997), suggesting that GR plays an important role in the protection of plants against oxidative stress.

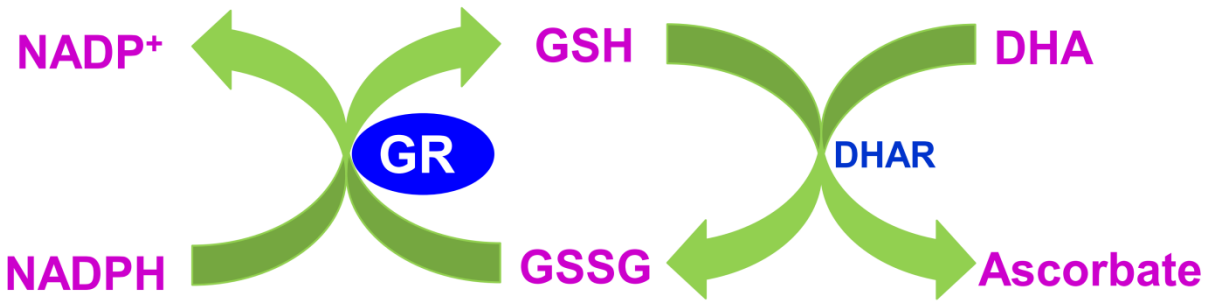

Figure 1.6. Role of glutathione reductase in maintaining cellular redox status. **GSH**: Glutathione reduced, **GSSG**: glutathione disulphide or oxidized GSH, **GR:** Glutathione reductase, **DHA:** Dehydroascorbate, **DHAR:** Dehydroascorbate reductase.

The Arabidopsis genome contains two GR genes. One gene codes for an organellar isoform (*GR2*), which is dual-targeted to chloroplasts and mitochondria (Chew et al., 2003). *GR2* is essential for plant development, which is evident from lethality of deletion mutants in early embryo development (Tzafrir et al., 2004). The second gene encodes for the cytosolic *GR1*. Expression analysis by scrutiny of the Genevestigator microarray database (Zimmermann et al., 2004) shows *GR1* to be responsive to several stress factors.

GR has been over-expressed in a number of plant species and the extractable foliar GR activities were between two and ten times higher than in untransformed plants (Noctor et al., 2011). The poplars over-expressing GR in the chloroplast had extractable GR activities, which were much higher than those of cytosol over-expressors, and this may be due to greater stability of the bacterial enzyme in the poplar chloroplast than in the poplar cytosol (Foyer et al., 1995). The over-expression of GR in the tobacco chloroplast, but not the cytosol, increased both the reduction state and total pool of glutathione (Mullineaux et al., 1994). This strongly implicates chloroplastic GR activity as a factor that influences glutathione levels through controlling the capacity for regeneration of GSH from GSSG.

Stress-tolerant plants exhibited high activities of GR (Mittova et al. 2003). Enhanced chloroplastic GR activity in transgenic plants resulted in increased protection against oxidative stress (Foyer et al. 1995; Pilon-Smit et al. 2000). In addition, decrease in GR activity in tobacco plants increased their sensitivity to

oxidative stress (Aono et al 1995; Ding et al., 2009). However, it is still unclear how GR plays an important role in protecting plants against oxidative stress.

1.6. Experimental systems to study the photosynthesis, key antioxidants and their metabolism

Protoplasts

Plant protoplasts without cell walls offer a versatile cell-based experimental system. Mesophyll protoplasts have been used to study cellular processes and activities such as photosynthesis and respiration (Devi et al., 1992), calcium signaling and regulation, embryogenesis, and the modulation of ion channels by light, stress and hormone responses in various plant species (Sheen, 2001; Davey et al., 2005). Mesophyll protoplasts are routinely isolated from pea and *Arabidopsis* leaves (Riazunnisa et al., 2007) and used for photosynthesis studies. The protoplasts derived from distinct tissues do retain their tissue-and cell-specific features and the advantages of protoplasts, such as high-resolution imaging and the ease of manipulation by exogenous application of chemicals, can be exploited to study highly tissue- or cell-specific processes (Faraco et al., 2011).

Chlorophyll a (Chl a) fluorescence

In photosynthesis research, Chlorophyll *a* fluorescence (Chl *a*) is one of the most widespread methods used in both basic and ecophysiological studies (Strasser et al., 2004; Baker, 2008). It is a non-invasive, reliable and very sensitive tool for measuring, rather quickly, photosynthetic efficiency, particularly of photosystem II (PSII).

When light energy is absorbed by a chlorophyll molecule it is temporarily boosted to a higher energy level. The excitation energy that is captured in the antenna complexes is ultimately transferred to the reaction centres (RC) where it can be converted into chemical energy via photosynthetic processes. When excited chlorophyll pigments cannot transfer their energy to the RCs, they can emit the absorbed energy safely as heat or as fluorescence. Chl *a* fluorescence has a characteristic pattern known as the Kautsky-curve (Kautsky et al., 1960). In dark-adapted leaves, at the onset of illumination, fluorescence rises from the minimum yield Fo (O, open state) to a peak fluorescence level, Fm (P) as RCs are getting closed by charge separations occurring in PSII. When these values from O to the maximal P are plotted on a logarithmic time scale, a typical polyphasic rise with two intermediate steps, denoted as J and I (Strasser and Govindjee 1992) or I_1 and I_2 (Schreiber and Neubauer 1987) are clearly revealed, hence the notation O-J-I-P or O-I_1-I_2-P for the fast rise of the fluorescence transient (Srivastava et al. 1995). The OJIP transients are markedly modulated by stress conditions, in such a way that the signatures can be helpful to identify the type of stress (Tsimilli-Michael and Strasser, 2008).

A procedure for quantification of the O-J-I-P fluorescence transient known as the JIP-test has been developed by Strasser and Strasser (1995). Further analysis of the fluorescence transients from the JIP-test can be used to calculate several phenomenological and biophysical components (Strasser et al., 2004). Another advantage of JIP test is that it can be used with different types of experimental

materials, including leaves, algal suspensions and even mesophyll protoplasts (Sunil et al., 2008; Antal et al., 2009).

Mutants and Transgenic plants

The system of isolating and manipulating single genes through recombinant DNA technology and the method to insert a specific foreign gene into plants enabled scientists to generate transgenic plants to combat several environmental stress conditions. Transgenic plants are extremely useful as proof-of-concept tools to dissect and characterize the activity and interplay of gene networks for different environmental stress conditions. However, care must be taken to check the stability of the transgene over generations. Great progress in our understanding of redox networks and their high level of complexity has come through transgenic studies. Studies with various transgenic plant lines, transcript profiling studies and mutants with altered expression of antioxidant enzymes has provided new insights into the role of these components in plants by allowing direct investigation of their functions and interactions (Maughan and Foyer, 2006; Hanke et al., 2009). Several studies using either transgenic plants or mutants with enhanced or decreased antioxidant capacity have been used to isolate the specific influence of ROS and antioxidants in the regulation of gene expression (Allen et al., 1997; Hanke et al., 2009).

1.6. Focus of the present work

The present study has been designed to examine the effects of NO on the patterns of photosynthesis, respiration and on the cross talk between chloroplasts and

mitochondria. Initially, the responses of photosynthesis and respiration were studied in mesophyll protoplasts as well as leaves of pea. Later experiments were focused to elucidate the interaction of NO with glutathione metabolism in *Arabidopsis thaliana* using transgenics and mutants. The objectives and approach of the present work are described in detail in the next chapter.

*****

Chapter 2

Objectives and Approaches

Chapter 2

Objectives and Approaches

2.1. Specific objectives of the present study

The regulatory role of nitric oxide and its importance as a secondary messenger in several biochemical and physiological processes in plants has been studied extensively (Baudouin, 2011). However, there is not much work available on the effects of NO on photosynthetic parameters and its possible role to mediate organelle interaction between chloroplasts and mitochondria. With the above scenario in background, the objectives of present work are as follows:

1. To assess the functional integrity and performance of mesophyll protoplasts of pea (*Pisum sativum*) during isolation using chlorophyll a (Chl a) fast transient analysis as a tool.
2. To study the effects of NO and H_2O_2 on the activities of photosynthesis, dark respiration and on the cross-talk between chloroplasts and mitochondria.
3. To investigate the possible targets of NO in chloroplast components using fast Chl *a* fluorescence transients of OJIP curves.
4. To identify the homozygous *Arabidopsis* lines over-expressing the genes of glutathione metabolism
5. To elucidate the interaction of NO signaling with glutathione metabolism in *Arabidopsis thaliana* using relevant transgenics and mutants.

The rationale of our experiments are described below

2.2. Plant material: Pea and Arabidopsis

Pea (*Pisum sativum*) is a mesophytic plant that is easy and fast to grow. Owing to their small size, pea plants can be grown in a large number in a relatively small area. Being a typical C_3 plant, it is widely used for physiological and biochemical studies as it offer a very good experimental material in the form of intact leaves, leaf discs/leaf slices, isolated protoplasts and organelles. Isolation of active mesophyll protoplasts from pea leaves is easy and rapid (Devi et al., 1992).

Arabidopsis has been selected as research model plant, because the genome of *Arabidopsis* is relatively small and its genome is well characterized. The plant's small size and rapid life cycle are additional advantages. Further, the availability of wide spectrum of mutants and transgenics, as well as established protocols for isolation of protoplasts, transient expression of recombinant proteins offers a wide scope for experiments in physiology, biochemistry and molecular biology.

We have used two experimental systems in our study: mesophyll protoplasts of pea and leaves of *Arabidopsis*. Protoplasts offer a good model to study intracellular, but not intercellular signaling. To study the NO intercellular signaling, transcript analysis in whole plant is necessary. In the present study, we have therefore used protoplasts to examine the role of NO and H_2O_2 as biochemical signals during organelle interaction and to identify the possible targets of NO in chloroplastic components. The *Arabidopsis* leaves were used in the experiments dealing with the interactions of NO with glutathione metabolism, including enzyme and metabolite assays, transcript expression.

2.3. Use of SNP as NO donor and other metabolic modulators

The origin of NO in plants and the concentrations, at which it exerts its functions, is still debated. To study the NO dependent responses in plants, the best strategy is to trigger NO burst in protoplasts/plants, using NO donors, such as sodium nitroprusside (SNP). Treatment with SNP releases NO, particularly in presence of light (Floryszak-Wieczorek et al., 2006). But, apart from NO, SNP may also release CN^- as a byproduct, which can affect photosynthesis severely. During the experiments related to photosynthesis, the possibility of CN^- effect was crosschecked using cPTIO, a scavenger of NO.

Metabolic inhibitors were instrumental in the elucidation of metabolic pathways and regulatory steps *in vivo*. We have used classic mitochondrial inhibitors to restrict mitochondrial oxidative functions. These inhibitors are: antimycin A (inhibitor of complex III of the cytochrome pathway of mitochondrial electron transport), salicylhydroxamic acid (SHAM) (inhibitor of AOX). In view of the possible unspecific side effects of inhibitors, we used these test compounds at very low concentrations, so as to minimize the general perturbation of the metabolic system.

2.4. Application of Chl a fluorescence as a tool

Chl *a* fluorescence is a highly sensitive, non-destructive, and reliable tool for measuring photosynthetic efficiency, particularly of photosystem II (PSII) *in vivo* as well as *in vitro* (Lazár 2006). The oxygenic photosynthetic organisms show polyphasic rise in Chl a fluorescence with time, consisting of a sequence of phases

denoted as OJIP (Strasser et al 2000). Any perturbation in chloroplast structure and function would alter these fluorescence transients (Strasser et al., 2004). The OJIP transients reflect changes in electron transport in PS II over a wide range of time, from microseconds to seconds that allow us to evaluate the sub-characteristics of PS II, such as energy trapping, electron transport (Strasser et al., 2004; Stirbet and Govindjee, 2011). This is perhaps the first study to use Chl a fluorescence, as a tool to monitor the functional status and photochemical performance of protoplasts.

2.5. Use of *Arabidopsis* transgenic lines for the study of NO interaction with glutathione metabolism

Evidences has emerged that the GSH biosynthetic pathway is stimulated in response to NO in both animal and plant cells (Gegg et al., 2003; Innocenti et al., 2007). The glutathione-NO adduct (GSNO) can regulate NO availability in plant cells, with the help of GSNO reductase (GSNOR) (Rusterucci et al. 2007; Lee et al. 2008).

Transgenic plants with altered levels of glutathione expression would offer an excellent system, to study the interaction of NO with glutathione metabolism. In our study, we have used homozygous lines of *Arabidopsis thaliana* plants over-expressing bacterial GR in cytosol and these plants were subjected to NO treatment, hydroponically. A glutathione mutant (*cad2*) and GR insertion mutant (*GRcyt*) were also included for comparison. The transcript changes of the genes (related to glutathione metabolism and few known stress marker genes) in response to NO were followed using quantitative RT-PCR (qRT-PCR).

The data generated by the above approaches would increase our understanding of NO's role in photosynthesis and its interaction with glutathione metabolism during cellular signaling. The information can help to define NO's place within the complex signaling pathways in plants. The results and discussion are organized into five chapters, corresponding to five objectives mentioned, at the beginning of this chapter.

*****

Chapter 3

Materials and Methods

Chapter 3

Materials and Methods

3.1. Plant material

Plants of pea (*Pisum sativum* L., cv. Arkel) were raised from seeds, procured from Pocha Seeds Pvt. Ltd. Pune, India (Figure 3.1A).

The seeds of transformed *Arabidopsis thaliana* lines were obtained from material originally developed by Dr. Lise Jousnin, Institut National de la Recherché Agronomique (INRA), Versailles, France. These were the original T1 after selection on kanamycin. These lines included those transformed to over-express *Escherichia coli* genes of glutathione reductase in the cytosol (*GRcyt*) and for gamma-glutamylcysteine synthase (γ*ECS*, first enzyme of glutathione biosynthesis) in cytosol (γcyt) and chloroplast (γch). The plants were transformed by the floral-dip method using *Agrobacterium tumefaciens* mediated transformation (Clough and Bent, 1998). The biochemical characterization was done on plants grown from T1 seeds and subsequent SNP treatments were performed on plants grown from T3 seeds. The seeds of *Arabidopsis thaliana* mutant lines carrying T-DNA insertions in the *GR1* gene (At3g24170) were obtained from the Nottingham Arabidopsis Stock Centre (http://nasc.nott.ac.uk) (Table 3.1).

3.2. Plant growth and sampling

The pea seeds were soaked in water overnight, surface sterilized with 0.2% (v/v) sodium hypochlorite solution for 30 min and then washed for 1h under running tap water. The seeds were kept covered in a moist black cloth at 25 °C until germination

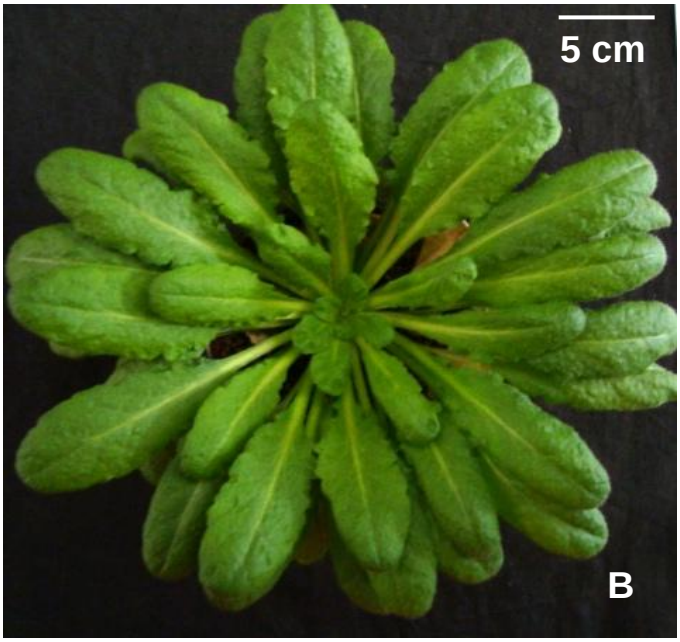

Figure 3.1. (A) 8 to10 day-old plants of pea (*Pisum sativum* cv. Arkel) grown in the green house. (B) 4 week-old plants of *Arabidopsis thaliana* (ecotype-Columbia) used in the experiments.

Table 3.1. The *Arabidopsis thaliana* plants used in the present study

Nomenclature	Enzyme over-expressed	Function	Remarks
Col-0	Wild type (Columbia)		
ggschp	*γECSchp*	Over-expression of γ-glutamylcysteine synthetase from *E.coli* in the chloroplast	γch+ 1 to 10 (= 10 different lines)
ggscyt	*γECScyt*	Over-expression of γ-glutamylcysteine synthetase from *E.coli* in the cytosol	γ+ 1-5, 7-10, 11 (= 10 different lines)
GRcyt	*GRcyt*	Over-expression of glutathione reductase from *E.coli* in the cytosol	GRcyt+ 1-2, 4-5, 7-16 (= 15 different lines)
GRcyt-	mutant with a T-DNA insertion in cytosolic GR gene	30-40% decrease in total leaf GR capacity	
cad2	mutant deficient in γ-glutamylcysteine synthetase	20-30% of WT glutathione contents	

(usually 3 days). Vigorously germinating seeds were sown in plastic trays filled with soil and farmyard manure (3:1) and were watered twice daily. The plants were grown in a green house at average temperatures of 30 °C day/ 25 °C night and a natural photoperiod of approximately 12 h. The second to fourth pair of fully unfolded leaves were picked from 8-15-dayold plants and used for isolation of mesophyll protoplasts.

The seeds of *Arabidopsis thaliana* were preconditioned/imbibed on whatmann® filter paper moistened with water in a Petri dish for 2 days at 4 °C in dark to break dormancy. These seeds were then sown in soil in 7-cm pots in the controlled environment growth chambers and maintained at 8 h light/16 h dark photoperiod at an irradiance of 120-150 μE m^{-2} s^{-1} at 20 °C/18 °C and 65% humidity (Veljovic-Jovanovic et al., 2001).

Table 3.2. The composition of nutrient solution used for watering *Arabidopsis* plants.

Macronutrients	**(mM/l)**	**Micronutrients**	**(μM/l)**
KNO_3	5.0	$FeSO_4 .7H_2O$	50 (in 50 mM Na_2EDTA)
KH_2PO_4	2.5	$MnSO_4 .4H_2O$	60
$MgSO_4$	2.0	$ZnSO_4 .4H_2O$	7
$Ca(NO_3)_2$	2.0	$CuSO_4 .5H_2O$	0.1
		H_3BO_4	49
		KI	4.5
		$Na_2MoO_4 .2H_2O$	1.0
		$CoCl_2$	0.1

The nutrient solution (Table 3.2) was given twice per week up to 4 weeks (Figure 3.1B). Samples of approximately 100 mg fresh weight rosette leaf material were collected, taking care to exclude material from the stem and hypocotyl. Following weighing, samples were introduced into 2 ml eppendorf tubes, rapidly frozen in liquid nitrogen, and stored at -80 °C until further analysis. Each sample was either a mixture of 1 leaf each from 3 plants in a pot (enzyme assays) or a pool of 2-3 leaves from single plant (for RT-PCR assay). All samples were taken 4 h into the photoperiod.

3.3. Preparation of mesophyll protoplasts (MCP)

A typical protoplast preparation is shown in Figure 3.2. The mesophyll protoplasts were isolated from pea leaves by minor modifications of the procedure of Devi et al. (1992). The lower (abaxial) epidermis of leaves was stripped off with the help of forceps. The midrib was discarded and the leaves were cut into small pieces of approximately 1 cm^2 size. These leaf pieces were floated on preplasmolysis medium (Table 3.3) with the peeled lower surface touching the medium in the petri-dish. After 30 min, the preplasmolysis medium was carefully removed and the leaf strips were subjected to enzymatic digestion (Table 3.3). The leaf pieces were digested for 30 min under low light intensities of 50-100 $\mu E\ m^{-2}\ s^{-1}$ at 30 °C (Devi et al., 1992; Saradadevi and Raghavendra, 1992).

After digestion, the digestion medium was gently removed with a pasture pipette and washing medium (Table 3.3) was added to the petri-dish containing the digested leaf pieces. The petri-dish was tapped and swirled gently to release the

protoplasts into the medium. All further operations were done at 4 °C. The suspension was filtered through a nylon filter of 60 µm pore size (Saryu Textiles, Mumbai, India) to remove the debris and the filtrate was centrifuged at 500 rpm for 5 min. The supernatant was discarded and the pellet was washed thrice using washing medium to remove broken protoplasts. The washing was done by suspending the protoplast pellet in washing medium, centrifuging at 500 rpm for 3 min and discarded the supernatant. Finally, the pelleted protoplasts were washed once with suspension medium (Table 3.3). The final pellet was suspended in 0.5 ml of suspension medium, mixed gently and left on ice. The protoplasts were handled carefully throughout the experiments.

The intactness of protoplasts was routinely assessed by either staining with fluoresceine diacetate (FDA) or assaying glycolate oxidase (Nishimura et al., 1985). The intactness ranged from 80 to 90%. The intactness of chloroplasts, assayed by using ferricyanide reduction (Walker, 1988), ranged from 80-90%.

3.4. Estimation of chlorophyll

Chlorophyll was estimated in mesophyll protoplasts by extracting into 80% (v/v) acetone (Arnon, 1949). An aliquot of 12.5 µl of protoplast suspension was added to 5 ml of 80% (v/v) acetone and mixed well using a cyclo-mixer. The absorbance of acetone extract was measured at 652 nm (A_{652} - to determine chlorophyll) and 710 nm (A_{710} - to correct for turbidity), using a spectrophotometer (Shimadzu UV-1700).

The chlorophyll concentration in the protoplast preparation was calculated using the following formula:

$$\text{Chl (mg ml}^{-1}\text{ of protoplast suspension)} = (A_{652} - A_{710}) \times 11.11$$

The room temperature absorption spectrum of isolated protoplasts was recorded using a Shimadzu UV 1801 spectrophotometer.

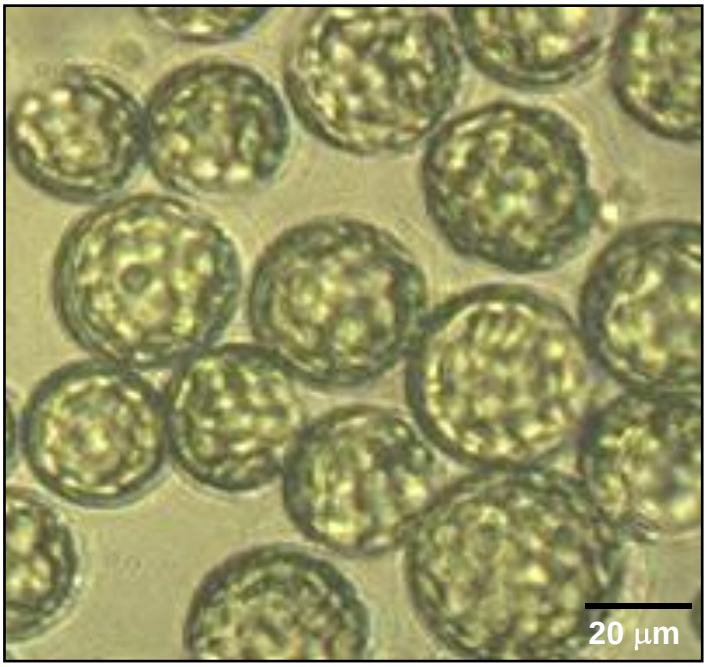

Figure 3.2. Photomicrograph of mesophyll protoplasts isolated from leaves of pea (*Pisum sativum*) suspended in reaction medium containing 0.4 M sorbitol (iso-osmoticum).

Table 3.3. Media used for protoplast isolation, indicating the final concentrations of components.

preplasmolysis medium	Sorbitol	0.3 M
	$CaCl_2$	1 mM
	MES (pH 6.0)	10 mM
Digestion medium	Sorbitol	0.4 M
	$CaCl_2$	1 mM
	EDTA	0.25 mM
	MES (pH 5.5)	10 mM
	Cellulase Onozuka R-10	2.0 % (W/V)
	Macerozyme R-10	0.2 % (W/V)
	BSA	0.25 % (W/V)
	Sodium ascorbate	10 mM
Washing medium	Sorbitol	0.4 M
	$CaCl_2$	1 mM
	MES (pH 6.0)	10 mM
Suspension medium	Sorbitol	0.4 M
	$CaCl_2$	1 mM
	$MgCl_2$	0.5 mM
	HEPES (pH 7.0)	10 mM
Reaction medium	Sorbitol	0.4 M
	$CaCl_2$	1 mM
	$MgCl_2$	1 mM
	HEPES (pH 7.5)	10 mM

3.5. Monitoring photosynthesis and respiration

The rates of photosynthetic O_2 evolution (on illumination) and respiratory O_2 uptake (in darkness) of the mesophyll protoplasts were monitored polarographically using a Clark type O_2 electrode (DW2, Hansatech Ltd., King's Lynn, UK). The Calvin cycle activity of the mesophyll protoplasts was measured as rate of bicarbonate dependent O_2 evolution, where as for photochemical activities: the oxygen evolution was assayed in the presence of 5 mM glycolaldehyde (an inhibitor of Calvin-Benson cycle), with or without 1 mM *p*-benzoquinone (*p*-BQ, for PSII activity, transfer of electrons from H_2O to *p*-BQ), or 10 mM $NaNO_2$ (PSII + PSI activity).

The mesophyll protoplasts equivalent to 10 µg Chl were loaded to oxygraph chamber containing the reaction medium (Table 3.3). An illumination of 700 µE m^{-2} s^{-1} was provided by a 35 mm slide projector (with Philips Focusline projection lamp, 24 V/150 W) to monitor $NaHCO_3$/*p*-BQ/$NaNO_2$ dependent photosynthetic O_2 evolution (Figure 3.3A). While 1.0 mM $NaHCO_3$ was added to the reaction medium before measurement of respiratory O_2 uptake, 1.0 mM *p*-BQ was added to the reaction medium, just before light was switched on after measurement of dark respiratory O_2 uptake. Oxygen content in the electrode chamber was pre-calibrated at 25 °C with air saturated water (assumed to contain 252 nmoles of oxygen ml^{-1}) using sodium dithionate (Walker, 1988). A typical recorder trace of respiratory O_2 uptake and photosynthetic O_2 evolution is shown in Figure 3.3B.

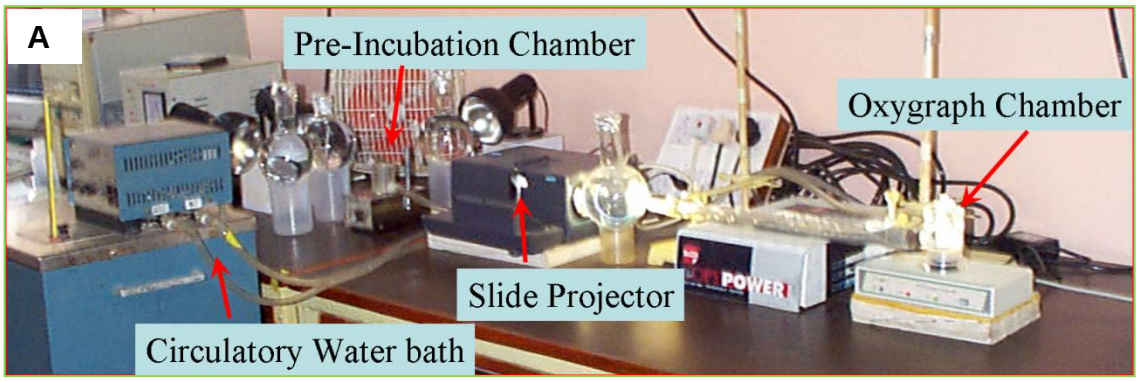

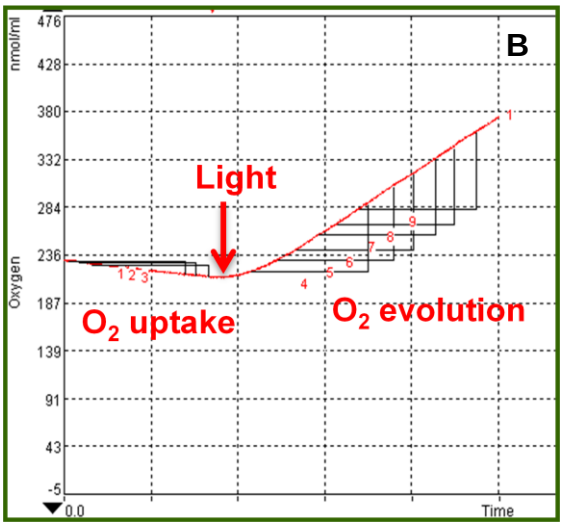

Figure 3.3. A: Experimental setup of the oxygen electrode to measure photosynthesis or respiration. B: A typical recorder trace of respiratory O_2 uptake and photosynthetic O_2 evolution by mesophyll protoplasts of pea at 25 °C.

3.6. Treatment of protoplasts with test compounds

Protoplasts were pre-incubated in darkness for 5 min prior to illumination, with the test compounds. The respiratory inhibitors Antimycin A (inhibitor of COX pathway/ complex III of mitochondria) and SHAM (inhibitor of AOX pathway of mitochondria) or substrates, sodium nitroprusside (SNP, releases NO) and hydrogen peroxide (H_2O_2 as a source of ROS) or modulating compounds (cPTIO, specific NO scavenger) were added to the reaction medium, at the required final concentrations, while pre-incubating.

3.7. Measurement of fast Chl a fluorescence induction kinetics

A Plant Efficiency Analyzer (Handy PEA, Hansatech Instruments Ltd., King's Lynn, Norfolk, England) was used to measure the chlorophyll a fluorescence (O-J-I-P) transients (Figure 3.4A). Protoplast samples at selected stages of isolation were transferred into a 1.5 ml eppendorf tube kept in darkness for 5 min and then examined for Chl *a* fluorescence transient pattern, using the procedure of Strasser et al. (2004). The OJIP transients were induced by 1 s illumination with an array of three light emitting diodes focused on a circle of 5 mm diameter of the sample surface. The peak wavelength of the emitted light is at 650 nm and the maximum light intensity is ~3000 µE m^{-2} s^{-1}. The detector is a fast response PIN photodiode with RG9 long pass filter. This filter prevents the red light emitted by the LEDs from reaching the fluorescence detector. The fluorescence signal received by the sensor unit during a recording is digitized in the control box using a fast analogue/digital converter (12 bit resolution).

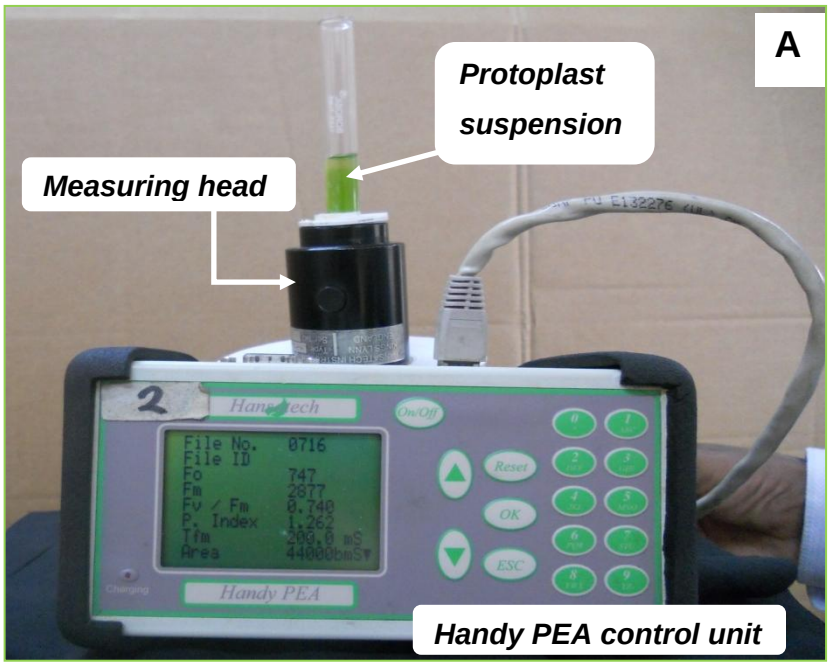

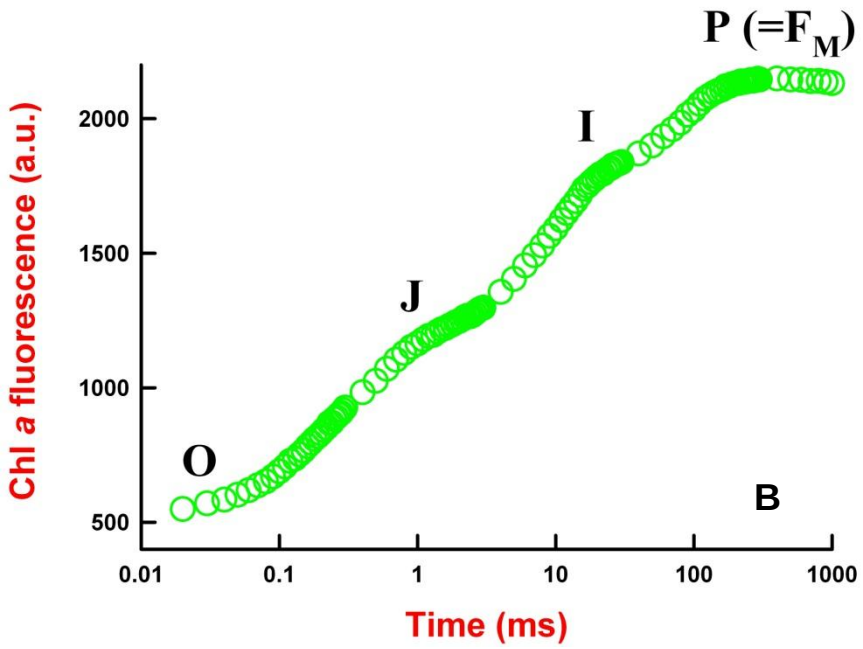

Figure 3.4. (A) Handy PEA fluorometer. (B) Typical patterns of OJIP transients from protoplasts.

A typical set of original transient traces are presented in Figure 3.4B. At each step, the Chl content and protoplast numbers may differ. Therefore, the transients in selected figures were normalized, so as to present comparative changes in the kinetics of OJIP phase, if any, during isolation procedures or treatment. For SNP treatments, protoplasts were pre-illuminated (50 μE m^{-2} s^{-1}) with or without SNP, for specified time points (0-30 min). As a control, protoplasts were dark incubated for the same time points. After stipulated time intervals, samples were dark-adapted and then transients were recorded. The fast fluorescence kinetics (F_0 to F_M) were recorded from 10 μs to 1 s. For the first 300 μs fluorescence is sampled at 10 μs intervals. This provides excellent time resolution of minimal fluorescence intensity (Fo) and the initial rise kinetics. The fluorescence intensity at 10 μs was considered as F_0 (Strasser and Strasser, 1995). The maximal quantum efficiency of PS II (Fv/Fm) was determined from the Handy PEA.

3.8. Analysis of the fast Chl a fluorescence transients using the JIP-test

The chlorophyll a fluorescence induction curves (O–J–I–P) were analyzed according to the JIP test, developed by Strasser and Strasser (1995). The translation of the measured parameters using Biolyzer software (courtesy, R. Rodriguez and R. Strasser, University of Geneva) into JIP-test parameters provided information on the stepwise flow of energy through PS II at different levels. The JIP test enables the calculation of several phenomenological and biophysical expressions for quantifying the energy fluxes and energy ratios through photosystem II. From the

Table 3.4. Characteristic points of OJIP transients and formulae used for calculation of selected JIP-test parameters in our study, with short explanations (from Strasser et al., 2004).

Fluorescence Parameters	**Remarks**
Extracted parameters	
F_0	Minimal Chl *a* fluorescence (at ~ 10 µs), when all PS II RCs are open
F_J, F_I and F_P	Fluorescence intensity at J-step (at ~2 ms), I-step (at ~30 ms) and P-step (at ~1000 ms)
F_M	Maximal fluorescence, when all PS II RCs are closed
Performance index	
$PI_{ABS} = \frac{}{} \times \frac{}{} \times \frac{}{}$	Performance index (PI), calculated as combined measurement of the amount of photosynthetic reaction centers, the maximal energy flux which reaches to the PS II reaction centers and the electron transport at the onset of illumination on absorption basis.
Specific energy fluxes	
$ABS/RC = M_0 \times (1/V_J) \times (1/\varphi_{P0})$	Absorption flux per RC
$TR_0/RC = M_0 / V_J$	Trapped energy flux per RC at t = 0
$ET_0/RC = M_0(1/V_J) \times \psi_0$	Electron transport flux per RC at t = 0
$DI_0/RC = (ABS/RC) - (TR_0/RC)$	Dissipated energy flux per RC at t=0
Phenomenological energy fluxes	
$ET_0/CSm = (ABS/CS_0) \times \varphi_{E0}$	Electron transport flux per CS at t=m
$TR_0/CSm = (ABS/CS_0) \times \varphi_{P0}$	Trapped energy flux per CS at t=m
$DI_0/CSm = ABS/CS_0 - TR_0/CS_0$	Dissipated energy flux per CS at t=m
ABS/CSm	Absorption flux per CS at t=m
$RC/CSm = \varphi_{P0}\ (ABS/CS_0) \times (V_J/M_0)$	Density of RCs (Q_A- reducing PS II reaction centers

OJIP transient, the measured parameters (F_o, F_m, $F_{300\mu s}$, F_J, F_I, tF_m etc.) were used to the calculation and derivation of a range of new parameters. The detailed derivation for the formulae for the various energy fluxes and for the flux ratios in the JIP test is derived from Strasser et al., 2004) and listed in Table 3.4.

3.9. Monitoring NO levels in protoplasts

The intracellular level of NO in protoplasts was measured using a NO specific fluorescent dye 4,5-diaminofluorescein–diacetate (DAF-2DA), as described previously (Kojima et al., 1998). The membrane permeable DAF-2DA can be used for real time bioimaging of NO with fine temporal and spatial resolution (Kojima et al. 1998). DAF-2DA, after entering into the cells is hydrolyzed by intracellular esterase activity releasing free DAF-2, which does not leak into the medium. At physiological pH, DAF-2 is relatively non-fluorescent. However, in the presence of intracellular NO, It rapidly forms a fluorescent triazolofluorescein (DAF-2T), a highly fluorescent compound (Figure 3.5). The other advantage of using DAF-2DA for cellular imaging is its visible excitation wavelength is less damaging to cell.

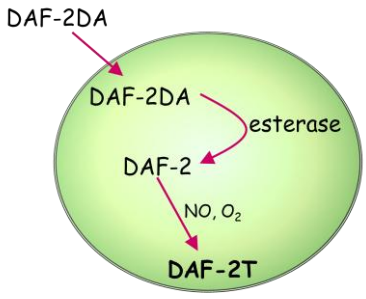

Figure 3.5. A schematic view of the mode of DAF-2DA action in the cell.

Protoplasts were pre-loaded with the 20 µM/ml DAF-2DA in suspension medium containing 10 mM HEPES-KOH buffer (pH 7.0) supplemented with 0.4 M sorbitol, 1 mM $CaCl_2$, 0.5 mM $MgCl_2$. The samples were incubated for 30 min in the dark at 25 °C on an orbital shaker, followed by washing twice in the same buffer for 3 min each at 500 rpm.

The protoplasts containing the DAF-2DA dye were loaded into the oxygraph chamber and subjected to SNP treatments, under the conditions of light and dark. After specified time points, the protoplasts were taken on a microscopic slide and the intra cellular NO production (fluorescence from DAF-2T) as well as the chloroplast autofluorescence were monitored under a confocal laser scanning microscope (TCSSP-2; Leica, Heidelberg, Germany) with an excitation 488nm, emission 510-530 nm.

3.10. Estimation of antioxidants and assay of glutathione reductase

Glutathione and ascorbate can be measured in the same acid extracts. Typical whole tissue values in healthy leaves are 200-1000 nmol g^{-1} FW (glutathione) and 1-10 µmol g^{-1} FW (ascorbate).

Extractions

All extraction steps were performed at 4 °C or below using an extraction medium/FW ratio of 1 ml/100 mg. Samples were ground in liquid nitrogen and then extracted into 1ml of 0.2 N HCl. The homogenate was transferred to eppendorf tubes and were centrifuged at 16,000 *g* for 10 min at 4 °C. An aliquot of 0.5 ml supernatant is taken into fresh tube and neutralized as follows. First, 50 µl of 0.12 M

NaH_2PO_4 (pH 5.6) was added, followed by the stepwise addition of aliquots (about 100 µl each time) of 0.2 M NaOH. The sample was vortexed after each addition, and the pH was verified with pH indicator papers. The final pH of all the neutralized acid extracts of the samples was between 5 and 6, requiring approximately 0.4-0.5 ml of 0.2 M NaOH. Care was taken for not to exceed the pH 7, to avoid oxidation of the sample.

3.10.1. Total Glutathione Analysis:

Total glutathione was measured by the recycling assay initially described by Tietze (1969), and modified by Noctor and Foyer (1998). The method relies on the NADPH- driven, GR-dependent reduction of 5,5′-Dithiobis(2-nitrobenzoic acid) (DTNB, Ellman's reagent), monitored at 412nm. The sulfhydryl group of GSH reacts with DTNB and produces a yellow colored 5-thio-2-nitrobenzoic acid (TNB, reduced DTNB). The rate of TNB production is directly proportional to the concentration of GSH in the sample.

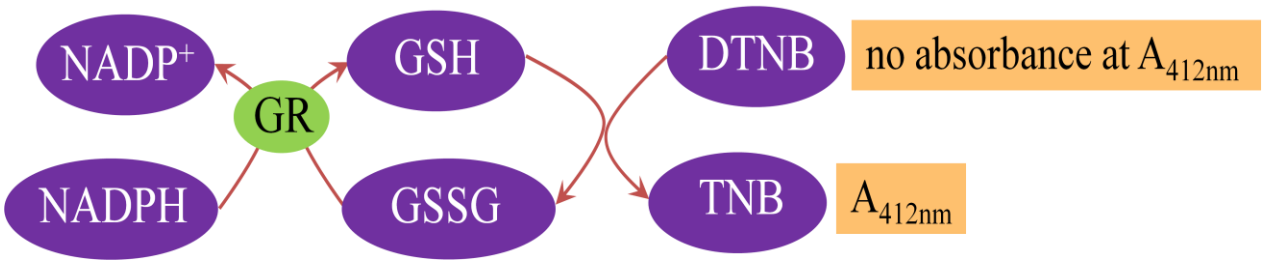

Figure 3.6. A schematic view of the principle of total glutathione assay.

Thus, there is no net consumption of glutathione in the reaction (Figure 3.6). Because, inclusion of GR in the assay means that glutathione cycles between the reduced and oxidized forms and the assay measures both GSH and GSSG without any distinction (i.e. Total glutathione).

Assay:

GR was freshly prepared each day by centrifugation of $(NH_4)_2SO_4$ suspension of yeast GR (1.6 mg ml^{-1}) at 10,000 *g* for 2 min at 4 °C. The supernatant was carefully decanted and the pellet was re-suspended in 2.56 volumes of 0.12M NaH_2PO_4-6 mM EDTA buffer (pH 7.5) to get a final GR concentration of 100U ml^{-1}.

To measure total glutathione, 10 µl- 20 µl neutralized extract was used. The reaction mixture contained, 910-920 µl of 0.12 M NaH_2PO_4 -6 mM EDTA buffer (pH 7.5), 10 µl of 50 mM NADPH, 50 µl of 12 mM DTNB. Reference cuvette contained everything but leaf extract (buffer volume adjusted accordingly). The reaction was started by the addition of 10 µl GR. After mixing the samples by shaking, the increase in absorbance at 412 nm was monitored for 10 min. Total glutathione was calculated over the first 90s by reference to standards run concurrently (0 to 1 nmol GSH in the cuvette) and unknowns and standards were corrected for GSH-independent reduction of DTNB by subtraction of the mean value of triplicate blank assays (without GSH).

3.10.2. Ascorbate assay:

Ascorbate was measured by a method adapted from Foyer et al. (1983) and Veljovic-Jovanovic et al. (2001). This assay measures the decrease in absorbance

at265nm upon the addition of ascorbate oxidase (AO), which converts reduced ascorbate (ASC) to non-absorbing oxidized forms (Figure 3.7). ASC is measured without pretreatment of extracts; ASC and the relatively stable oxidized form, dehydroascorbate (DHA), are measured together as "total ascorbate" after conversion of DHA to ASC by incubation with thiols such as dithiothreitol (DTT).

AO was dissolved in 0.12 M NaH_2PO_4 (pH 5.6) at 40 U ml^{-1}, divided into aliquots of 0.2 ml, and stored at –20 °C. Each day, an aliquot was freshly thawed and unused enzyme was discarded at the end of the experiment.

To assay ASC, triplicate aliquots of 50-100 µl neutralized supernatant (unless stated otherwise) were introduced into cuvette containing 0.9 ml of 0.2 M NaH_2PO_4 (pH 5.6). Reference cuvette should contain everything but leaf extract (adjusted buffer volume accordingly). The solutions were mixed well and then A_{265} was recorded and 10 µl AO (2 U ml^{-1}) was added. Solutions were remixed by shaking, and the decrease in A_{265} value was monitored In general, a stable value was reached within 1 to 2 min. Values were taken 5 min after the addition of AO.

To assay total ascorbate, 0.1 ml neutralized supernatant was first added to 0.14 ml of 0.12 M NaH_2PO_4 (pH 7.5) and 10 µl of 25 mM DTT, and solutions were incubated for 30 min at room temperature unless stated otherwise. Triplicate aliquots of this solution were then assayed as described for ASC. The difference in A_{265} before and after the addition of AO is converted to ascorbate content by taking ε_{265}=14 mM-1 cm-1 (1nmol in 1 ml = 0.014).

3.10.3. Glutathione reductase (GR, E.C. 1.6.4.2):

Glutathione reductase (GR) activity was determined by spectrophotometric analysis based on the method of Foyer and Halliwell (1976). GR catalyzes the NADPH-dependent reduction of glutathione disulfide ($GSSG_{oxd}$) to glutathione (GSH).

The oxidation of NADPH to NADP+ is accompanied by a decrease in absorbance at 340 nm. Since GR is present at rate limiting concentrations, the rate of decrease in the A_{340} is directly proportional to the GR activity in the sample. The reaction is thus measured by the decrease in absorbance at 340 nm using the extinction coefficient 6220 M^{-1} cm^{-1} for NADPH. One unit of glutathione reductase oxidizes 1 µmol of NADPH per minute at 25 °C, pH 7.5.

To assay GR, samples were ground in liquid nitrogen and then extracted into 1 ml of 0.1 M NaH_2PO_4-1 mM EDTA (pH 7.5). The homogenate was transferred to eppendorf tubes and centrifuged at 16,000 *g* for 10 min at 4 °C. 500 µl of supernatant is collected and loaded onto NAP-5 columns. The desalted elutant is used for the enzyme assay. The reaction mixtures contained 0.9 ml of 0.1M NaH_2PO_4 - 1 mM EDTA (pH 7.5), 10 µl of 50 mM oxidized glutathione (GSSG) and 10 µl of 10 mM NADPH (adjusted buffer volume accordingly). Triplicate aliquots of 25-100 µl of the desalted extracts were assayed.

3.11. Total RNA isolation and Reverse transcriptase PCR (RT-PCR) analysis

3.11.1. RNA extraction:

Total RNA samples were extracted from 4 weeks old Arabidopsis leaves using a TRIzol® isolation reagent (Invitrogen).

Homogenization:

The leaf samples (harvested, quickly frozen and stored at -80 °C) were ground to a fine powder using a mortar and pestle. This leaf powder was homogenized with TRIzol® (for 100 mg leaf tissue, add 1.5 ml of TRIzol reagent), mixed well and harvested into eppendorf tubes. The samples were incubated at room temperature for 5 min and then centrifuged at 12000 *g* for 10 min at 4 °C to remove the cell debris.

Phase separation:

The clear supernatant was carefully transferred to a fresh 2 ml eppendorf tube and chloroform (0.3 ml of chloroform for 1 ml TRIzol® reagent) was added. The tubes were capped securely and vortoxed for 15 sec and incubated at 25-30 °C for 5 min. The samples were centrifuged again at 12000 *g* for 15 min at 4 °C. After centrifugation, the mixture separated into a lower red, phenol-chloroform phase, an interphase, and a colorless upper aqueous phase.

RNA Precipitation:

The upper aqueous phase was carefully transferred to a fresh 2 ml eppendorf tube without disturbing the middle phase. To this, 0.6 volume (of TRIzol® + chloroform used initially) Isopropyl alcohol and 0.1 volume of 3 M potassium

acetate (KoAC) was added and incubated at 30 °C for 10 min. The samples were then centrifuged at 12000 *g* for 10 min at 4 °C and the supernatant was discarded.

RNA wash

The pellet (RNA) was washed with 70% alcohol (flick the tube to wash) and then centrifuged at 12000 *g* for 5 min at 4 °C to re-pellet the RNA at the bottom of the tube. Repeated the washing again and the pellet was air dried for 10-15 min at room temperature. The air dried pellet was re-suspended in 30-50 µl of RNase free diethyl pyrocarbonate (DEPC) treated water (DEPC-H_2O). An aliquot was put into the spectrophotometer to determine RNA concentration and quality at A_{260} and A_{280}. For optimal spectrophotometric measurements, RNA aliquots were 1:80 diluted with DEPC-H_2O. The RNA quantification was done using the following formula:

$$\text{RNA concentration } (\mu g\ ml^{-1}) = 40 \times A_{260} \times \text{dilution factor}$$

where RNA extinction coefficient = 40 (1 OD at 260 equals 40 µg /ml RNA)

The A_{260}/A_{280} ratio gives the purity of the RNA (ratio should be between 1.8 -2.1).

3.11.2. cDNA synthesis:

For cDNA synthesis, 1 µl (containing 0.5 µg) of Oligo$(dT)_{12\text{-}18}$ (Invitrogen) was added to 1 µg of total RNA and the final volume was adjusted to 18.5 µl with RNase free water. The sample was mixed well and incubated in a thermal cycler at 75 °C for 5 min, snap frozen in ice for 2 min and spin briefly. The cDNA was synthesized using 200 units M-MLV Reverse Transcriptase (Promega) in a buffer containing 0.1M dithiothreitol and 25 mM each of dNTPs (in a total volume of 6.5

µl= 5 µl of 5x RTase buffer+ 1 µl RTase+0.5 µl dNTP mix). The reaction was proceeded at 42 °C for 50-60 min in a water bath and was stopped at 70°C for 10 min. 2 µl of cDNA was used as template for PCR amplification.

3.11.3. Semi-quantitative RT-PCR:

Gene specific primers (Table 3.5) were designed for γECS and GR on the basis of the published sequence (Blattner et al., 1997 and EcoCys, http://ecocyc.org) using Primer3 software (Rozen and Skaletsky (2000), http://fokker.wi.mit.edu/primer3/input.htm). cDNA samples were standardized by PCR for actin content.

To ensure similar amplification conditions, 20bp-long oligonucleotides were used as primers, which had a uniform GC content of approximately 45-55% and yielded products of 400 to 600bp. The PCR conditions were optimized empirically by testing various annealing temperatures.

The PCR reaction mixture (Invitrogen) contained (for 1 reaction of 20 µl total volume)

10x buffer	2 µl
25 mM $MgCl_2$	2 µl
Fwd primer	0.2 µl - 0.5 µl
Reverse primer	0.2 µl - 0.5 µl
cDNA	2 µl
10x dNTP (2.5 mM)	2 µl
H_2O	11.4 µl - 10.8 µl
Taq polymerase (1 unit)	0.2 µl

Table 3.5. The sequence of the primers used for RT-PCR amplification.

Oligonucleotides	Sequence
γECS	5′-AGA-CGG-TAA-GAG-GCT-GCA-AA-3′ (sense) 5′-GGG CAG AGA AAG TCA GAT CG-3′ (antisense)
GR	5′-ATA CCG ATG GTA GCC TGA CG-3′ (sense) 5′-AAA GCC AAT GCC GTG AAT AC-3′ (antisense)
Actin2	5′-TTC CCT CAG CAC ATT CCA GCA G-3′ (sense) 5′-TTA ACA TTG CAA AGA GTT TCA AGG-3′ (antisense)

The PCR cycling conditions comprised

1.	94 °C	4 min	initial denaturation	
2.	94 °C	1 min	denaturation	} 30 cycles from step 2- 4
3.	52 °C	1 min	annealing	
4.	72 °C	2 min	extension	
5.	72 °C	10 min	final elongation	

As an internal (constitutive) control, PCR was performed simultaneously using *Actin2* primers and amplification products were resolved by electrophoresis.

3.11.4. Agarose gel electrophoresis:

Electrophoresis was carried on 1% (w/v) agarose gels. The gel was polymerized in 1x TBE buffer (89 mM Tris base, 89 mM Boric acid, 2 mM EDTA, pH 8.0). The required quantity of agarose (500 mg) was suspended in appropriate volume of 1 x TBE (50 ml) and boiled (in a microwave oven) for solubilization. The solution was allowed to cool till 60-65 °C to which, ethidium bromide (0.5 µg/ml) was added. The gel was poured into a horizontal gel electrophoresis system, into which the well comb was placed and left to polymerize at room temperature.

The PCR products were loaded with 4 µl bromophenol blue (BPB) dye (loading dye) before being loaded into the wells of the gel. Then the samples (about 12 µl) were directly loaded on to gel. DNA smartladder (Eurogentec) was used as molecular weight marker, which on standard loading of 5 µl yields 14 regularly spaced bands from 200 bp to 10000 bp. The size of each band is an exact multiple of 100bp. Electrophoresis was carried out in the same buffer (1x TBE) at a voltage 5V/ cm^2 until the dye reached $^3/_{4^{th}}$ of the length of the gel. All the ethidium bromide gels were visualized using UV-transilluminator and analyzed using UVP-gel documentation system. The PCR amplified an approximately 0.5 kb fragment of the gene of interest.

3.12. Kanamycin selection and characterization of homozygous lines

The most commonly used marker for selection of transgenic *Arabidopsis* is resistance to the antibiotic kanamycin. Resistance to kanamycin is conferred by a bacterial gene encoding the enzyme neomycin phosphotransferase (NPT). In this protocol, kanamycin-resistant seedlings are selected on solid medium.

About 0.1 ml of Arabidopsis seeds were placed in microcentrifuge tube and were surface sterilized in Bayrochlore/ethanol (1:24 v/v) for 5 min, followed by brief rinsing in ethanol. The seeds were finally washed twice with sterile distilled water and then air dried in laminar hood. The surface sterilized seeds plated on half-strength Murashige & Skoog Basal Medium (MS medium, Sigma) solid medium (pH 5.8) containing 0.8% agar, 50 mg l^{-1} kanamycin monosulfate and 1% (w/v) sucrose as described (Harrison et al., 2006). The plates were sealed with

parafilm® tape and stratified for two days in dark at 4 °C to break dormancy and to promote uniform germination. After 2 days, the plates were transferred to culture room and exposed to a continuous white light (120 µE m^{-2} s^{-1}) at 22 °C with adequate light. Transformed Kan-resistant plants were counted after 12days of culture, which will be visible as green seedlings with long roots, while untransformed seedlings will be yellowish with short or no roots. The kanamycin resistant seedlings were gently pulled out of the agar (removed the residual agar with a forceps) and transferred to soil for further growth.

Seeds were harvested from T3 plants and another round of kanamycin selection was carried out for selecting stable T4 homozygous lines of γECSchp, γECScyt and GRcyt transgenic plants. Each set of kanamycin selection was repeated thrice. These T4 plants were characterized and used for SNP treatments.

3.13. Genotyping of T4 GRcyt lines

Genomic DNA from the selected T4 plants was isolated using a small piece (5 mm^2) of leaf (frozen in liquid nitrogen), ground to fine powder and homogenized in extraction buffer (0.2 M Tris pH 7.5, 0.25 M NaCl, 25 mM EDTA and 0.5% SDS). The homogenized sample was centrifuged at 10000 *g*/4°C/10 min. About 200 µl of the supernatant is collected into a fresh eppendorf tube and equal volume of isopropanol was added to supernatant and centrifuged again at 10000 *g*/10 min at room temperature. Supernatant was discarded and the pellet was collected and washed with 70% ethanol, air dried and finally suspended in TE buffer.

The PCR reaction mixture (Promega) contained (for 1 reaction of 25 µl total volume)

5x GoTaq® Reaction Buffer	5 µl
dNTP mix (5 mM)	1 µl
25 mM $MgCl_2$	4 µl
Fwd primer	1 µl
Reverse primer	1 µl
GoTaq® polymerase (5 U/µl)	0.25 µl
DNA	2 µl
Nuclease free H_2O	10.75 µl

For PCR, Thermocycler® (MJ Research) was used and the cycling conditions comprised

1.	94 °C	3 min	initial denaturation	
2.	94 °C	30 sec	denaturation	} 36 cycles from step 2- 4
3.	60 °C	30 sec	annealing	
4.	72 °C	1 min	extension	
5.	72 °C	5 min	final elongation	

The amplified PCR products were resolved by electrophoresis and were visualized, analyzed using UVP-gel documentation system. The PCR amplified an approximately 0.5-kb fragment of the gene of interest.

3.14. Hydroponics culture of Arabidopsis plants

For growing the Arabidopsis plants hydroponically, the seeds were surface-sterilized and germinated on sterile agar plates (square 115 x 15 cm) containing ½ strength MS basal salts, 0.8% agar and 1% (w/v) sucrose. The plates were cold

stratified at 4 °C for 2 days in dark for synchronized germination and then grown vertically for 10 days in growth chambers prior to transfer to liquid growth medium. The growth conditions in the culture room were: 8 h light/16 h dark photoperiod, temperature of 22 °C and relative humidity of 70%.

Hydroponic culture was carried out using sterile 200 µl polyurethane tip boxes, which were used as mini-greenhouses. A sheet of medical adhesive tape was used to seal the top portion of the box and holes were cut through the tape to provide adequate space between the neighboring plants.

After 10-days, the seedlings were taken out from agar medium and the roots were rinsed in distilled water and carefully placed into the micro tip box (one plant/hole) containers (capacity of 0.5 L) filled with nutrient solution (Hoagland and Arnon, 1950). The hydroponic nutrient solution consisted of 1/4 strength Hoagland's macronutrients and full-strength micronutrients (Table 3.6). The solution was neutralized to pH 5.6 with 1 M KOH and maintained the plants for 2 weeks in the growth. The solution in the tanks was aerated and replaced with fresh nutrient media every 4 days to limit growth of microorganisms.

SNP treatments were given to four week old plants (Figure 3.7), by supplementing the nutrient solution with required concentration of SNP for required time points.

3.15. Treatment of Arabidopsis plants with SNP

For SNP treatments, T4 lines of GRcyt overexpressors and other plants were grown hydroponically. After 24 days, individual plants were carefully transferred to 10 ml

test tubes with Hoagland's solution. Treatments were performed after 2 days of plant acclimatization in the tubes. Nutrient media is supplemented with or without 1 mM SNP. As a negative control, 1 mM potassium ferrocyanide was used. Time scan of the experiment was carried out. Phenotypes were observed in 2 independent experiments. Samples were collected at 0 h, 3 h, 6 h and 12 h. Fresh weight was taken and immediately frozen in liquid nitrogen for subsequent qRT-PCR analysis. Untreated controls were harvested in parallel, at the same time points. Each treatment consisted of 3 individual plants per sample per treatment and qRT-PCR analysis was undertaken on two biological repeats.

3.16. Quantitative real-time PCR (qRT-PCR) and Transcript analysis

Total RNA was extracted from whole rosette leaves (80-100 mg) of triplicate plants per treatment using Trizol (Invitrogen) method as described above. RNA (1 µg) was reverse-transcribed using the SuperScript™ First-Strand Synthesis System for RT-PCR (Invitrogen).

qRT-PCR analysis was performed as in Queval et al. (2007). Gene specific primers for γECS, GR and other known stress inducible genes were designed according to available gene sequences (http://mips.gsf.de) and sequence specificity was checked on the TAIR webpage (http://www.arabidopsis.org). The genes tested for expression levels by qRT-PCR and their primer sequences are listed in Table 3.8.

qRT-PCR analysis was performed in duplicate on 10 ng cDNA using primers at 250 nm, 5 µl LightCycler® 480 SYBR Green I Master, in a final volume of 10.25 µl,

Table 3.6. The composition of Hoagland's nutrient solution used in our experiments.

Ingredients	Nutrient	Stock conc. (mM)	Conc./ml 1x (mM)	Final conc. 0.25x (mM)	Vol to take for 1 lit (ml)
		Macronutrients*			
KH_2PO4	P	200	1	0.25	1.25 ml
KNO_3	N/ K	1000	5	1.25	1.25 ml
$Ca(NO_3)_2.4H_2O$	N	800	4	1	1.25 ml
$MgSO_4.7H_2O$	S, Mg	400	2	0.5	1.25 ml
Fe-EDTA**	Fe	25	0.25	0.06	2.40 ml
		Micronutrients mix***			
			1x final (mM)		
$CuSO_4.5H_2O$	Cu	1.5	1.5 µM		1 ml
$ZnSO_4.7H_2O$	Zn	2	2.0 µM		
$MnSO_4.H_2O$	Mn	10	10 µM		
H_3BO_3	B	50	50 µM		
MoO_3	Mo	0.1	0.1 µM		
KCl	Cl	50	50 µM		

* Macronutrients are prepared separately in 200 ml volume each

** Fe-EDTA is prepared in amber colour bottle

*** Micronutrients stock is prepared in 200 ml (all the nutrients are in the same stock, amber colour bottle)

Figure 3.7. Hydroponics culture design and hydroponically grown Arabidopsis plants. (A) Plants were grown hydroponically as described for 4 wk on Hoagland's nutrient solution. (B) Close-up view of plants grown on hydroponic culture**.**

Table 3.8. Sequences of genes used for expression analysis by qRT-PCR and their primer sequences**.**

Gene function	Gene locus	Oligonucleotide sequence
Putative glutathione transferase (***GSTU24***)	AT1G17170	5′-TCCATAGCTGGTTTGCAGTG-3′ (fwd) 5′-TAGCGACGCTCTCTCTCTCC-3′ (rev)
Alternative oxidase 1a precursor (***AOX1A***)	AT3G22370	5′-GTTTCGTCTCACGAGGCTTT-3′ (fwd) 5′-TCGTCGGAGCTCTAGTCCAT-3′ (rev)
Ascorbate peroxidise (***APX1a***)	AT1G07890	5′-GCACTATTGGACGACCCTGT-3′ (fwd) 5′-GCAAACCCAAGCTCAGAAAG-3′ (rev)
1-aminocyclopropane-1-carboxylate oxidase (***ACC oxidase***)	AT5G43450	5′-CGTGGAGCATAGGGTACGAC-3′ (fwd) 5′-TTTGGAGAAAGACTCGAGCTAAAG-3′ (rev)
Glutamate-cysteine ligase (***GSH1***)	AT4G23100	5′-TCCCAGTTACTGGCTTAAAGACTC-3′ (fwd) 5′-CCTGTTCTGACCACTTCATCG-3′ (rev)
Glutathione synthetase (***GSH-S***)	AT5G27380	5′-AAAGAAGGAGAGGAAGGAAACG-3′ (fwd) 5′-CTGAGGTAAGCACCATAGACACC-3′ (rev)
Chloroplastic glutathione reductase (***GRchp***)	AT3G54660	5′-CCACACACTGTTGATGTAGATGG-3′ (fwd) 5′-GCTTGGAAGGCAAATCAAGC-3′ (rev)
Cytosolic glutathione reductase (***GRcyt***)	AT3G24170	5′-TGGACGCCAGGAAAAGAC-3′ (fwd) 5′-TTGGTTGCTCCACACTTGAG-3′ (rev)
Actin2	AT3G18780	5′-CTGTACGGTAACATTGTGCTCAG-3′ (fwd) 5′-CCGATCCAGACACTGTACTTCC-3′ (rev)

using a LightCycler® 480 Real-Time PCR System (Roche, http://www.roche-applied-science.com) according to the manufacturer's protocol. PCR conditions were 2 min at 50 °C, 10 min at 95 °C, and 50 cycles of 15 sec at 95 °C, 20 sec at 60 °C and 15 sec at 72 °C. Fold change in RNA expression was estimated using threshold cycles. Results were processed with LC-480 Software using the second derivative to obtain Cp values normalized to an internal reference. *Actin2* was used as an internal control to normalize the expression data of the selected genes (Queval et al., 2007).

Replications

The data presented are the average values (±SE) of results from three to four experiments conducted on different days.

Chemicals and Materials

Cellulase (Onozuka R-10) and Macerozyme R-10 (pectinase) were procured from Yakult Honsha Co. Ltd., Tokyo, Japan. Antimycin A, SHAM, *p*-BQ, glycolaldehyde, cPTIO, reduced and oxidized glutathione, DTNB, DAF-2DA, NADPH, MES, sodium ascorbate, and all the enzymes used for the spectrophotometric assays were procured from Sigma-Aldrich Corporation, USA. Ascorbate oxidase was from Roche Applied Science, Mannheim, Germany. All other chemicals and materials were of analytical grade and were purchased from the following companies: Sisco Research Laboratories, Loba Chemie, Himedia Laboratories and Qualigens, all from Mumbai. All the primers were synthesized by Eurogentec (Angers, France).

*****

Chapter 4

Application of fast chlorophyll *a* fluorescence transient (OJIP) analysis to monitor functional integrity of pea (*Pisum sativum*) mesophyll protoplasts during isolation

Chapter 4

Application of fast chlorophyll *a* fluorescence transient (OJIP) analysis to monitor functional integrity of pea *(Pisum sativum)* mesophyll protoplasts during isolation

4.1. INTRODUCTION

Plant protoplasts form unique, single cell and versatile system for use in a variety of biochemical, biophysical and physiological experiments (Davey et al., 2005; Yoo et al., 2007; Faraco et al., 2011). They find use in tissue culture, plant transformation and in other fields of modern plant biology and biotechnology. The protoplasts, which represent cell wall less mesophyll cells, have been isolated from a variety of tissues from both monocotyledonous and dicotyledonous plants. The yield and efficiency besides the intactness are important for protoplast isolation.

Application of chlorophyll (Chl *a*) fluorescence fast transient analysis is a simple and useful non-invasive tool to monitor chloroplast function *in vivo* as well as *in vitro* (Lazar 2006). The fast OJIP transient and its quantification by the JIP test provide a sensitive and reliable test for the functionality of photosynthetic system and vitality of green, tissues (Strasser et al., 2004; Prakash et al., 2003; Strauss et al., 2007). The Chl *a* fluorescence transients, both fast and slow, are used extensively in studies on various aspects of plant biology from physiology, biotechnology to eco-physiology (Strasser et al., 2004; Davey et al., 2005; Strauss et al., 2007). These Chl *a* fluorescence transients have the potential to be exploited in studies on plant protoplasts.

Isolation of intact mesophyll protoplasts from leaves involves short but physiologically stressful steps, such as enzymatic digestion at acidic pH and alternate periods of light and darkness (Devi et al., 1992). During such isolation procedure, the bioenergetic organelles of chloroplasts and mitochondria could experience metabolic disturbances. Our laboratory has developed an extremely efficient procedure for isolating intact mesophyll protoplasts from pea *(Pisum sativum)* leaves for routine studies on photosynthesis and respiration (Devi et al., 1992; Sunil et al., 2008). In addition, a fast and reliable procedure for isolation of metabolically active mesophyll protoplasts from model plant *Arabidopsis thaliana* has recently been developed (Riazunnisa et al., 2007).

In this chapter, we have used for the first time the fast Chl *a* fluorescence transients for monitoring and assessing the functional photochemical performance of mesophyll protoplasts at different stages of isolation from pea (*Pisum sativum*) leaves. Our results demonstrate the similar photosynthetic performance of isolated mesophyll protoplasts to that of intact leaves.

4.2. RESULTS

4.2.1. Mesophyll cell protoplasts from pea plants

The protoplast preparation required about an hour and involved dark-light adaptations (Figure 4.1). After isolation, the intact protoplasts were separated by centrifugation. The micrograph in Figure 4.2A demonstrates that before centrifugation, there were some broken fragments. The centrifugation step did not cause any further breakage of the protoplasts (Figure 4.2B). The room temperature absorption spectrum (Figure 4.2C) of protoplasts exhibited typical

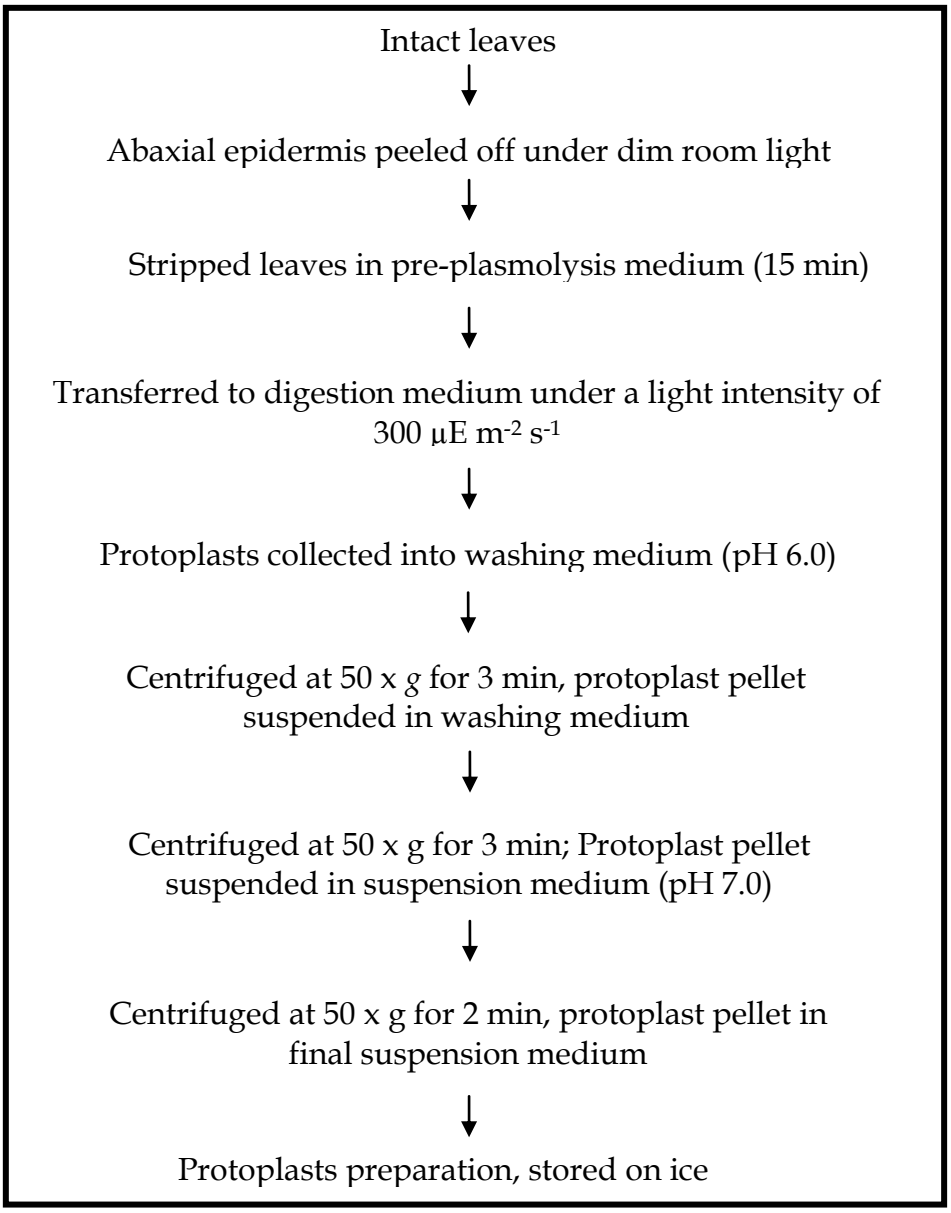

Figure 4.1. The different steps and treatments involved in isolation of mesophyll protoplasts of pea leaves.

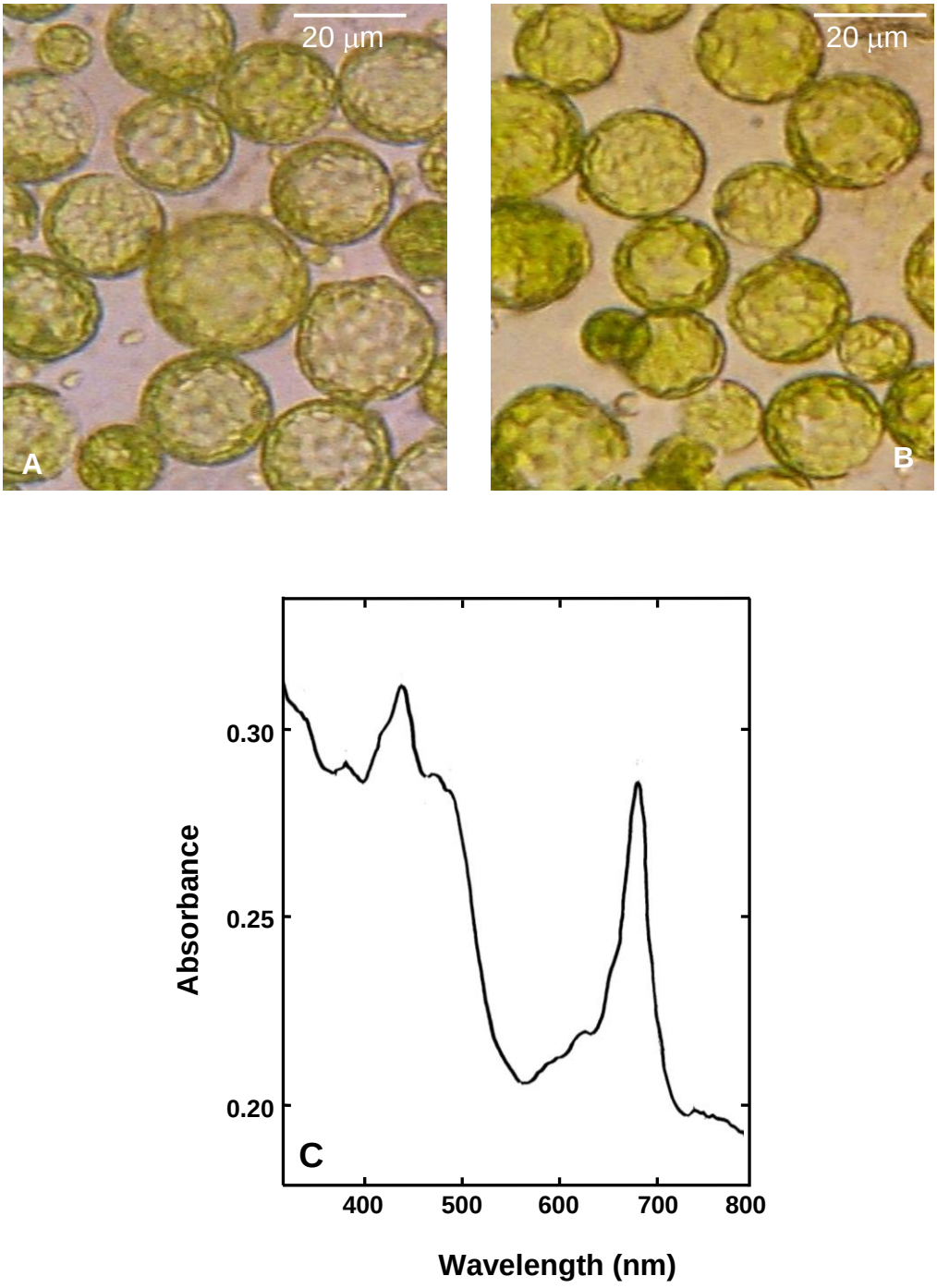

Figure 4.2. Appearance and absorption spectrum of mesophyll protoplasts of pea (*Pisum sativum*). (A): Micrograph of mesophyll protoplasts in washing medium before centrifugation step; (B): Micrograph of mesophyll protoplasts after final centrifugation and kept in suspension medium and (C): Absorption spectrum of mesophyll protoplasts in suspension medium.

peaks corresponding to Chl *a*, Chl *b* and carotenoids. A comparison of Chl *a* fluorescence transient curve measured during the isolation procedure with the transients of intact leaves provided a good test for the functional integrity of the photosynthetic electron transport chain. Because of the need for quick monitoring of Chl *a* fluorescence transients at frequent intervals, we measured only OJIP transients in this study (Table 4.1).

4.2.2. Bicarbonate dependent O_2 evolution by mesophyll protoplasts

Table 4.2 shows the oxygen evolution ability of same set of protoplasts preparation used for the measurement of the OJIP-transients. A high rate of photosynthetic oxygen evolution, even without any added bicarbonate, is a consistent feature of our protoplast preparations. The rate of benzoquinone (BQ)-dependent O_2 evolution, which reflects PSII activity, was significantly higher than that with 1 mM $NaHCO_3$, which represents a measure of PSI + PSII + Calvin cycle (Table 4.2).

The isolated mesophyll protoplasts were metabolically very active and evolved O_2 on illumination. Such photosynthetic O_2 evolution was stimulated by the increased levels of added bicarbonate. Maximum photosynthetic O_2 evolution was seen in the presence of 1 mM bicarbonate and thereafter there was a slight decrease in the rate when the bicarbonate concentration reached to 10 mM (Figure 4.3). The respiratory oxygen uptake showed marginal variation with varying concentrations of bicarbonate.

Table 4.1. List of symbols used to describe technical fluorescence parameters, calculated from OJIP measurements

Fo	Minimal Chl *a* fluorescence (at ~ 20 µs)
F_J	Fluorescence intensity at j-step (at ~ 2 ms)
F_I	Fluorescence intensity at i-step (at ~ 30 ms)
F_P	Fluorescence intensity at p-step (at ~ 1000 ms)
F_M	Maximal fluorescence intensity
F_t	Fluorescence at a given time
V, Relative variable fluorescence	$(F_t-F_O)/ (F_M-F_O)$

(Further details in Appendix I - II in Prakash et al., 2003)

Table 4.2. Photosynthetic oxygen evolution (µmol mg^{-1} Chl h^{-1}) by mesophyll protoplasts of pea before and after centrifugation of protoplast suspension in presence or absence of 1 mM benzoquinone (BQ) or glycolaldehyde (5 mM) or bicarbonate (1 mM). Data represent means of three independent experiments ± SD.

Step	No BQ or Glycolaldehyde		BQ + Glycolaldehyde	
	Without HCO_3^-	HCO_3^-	Without HCO_3^-	HCO_3^-
Before centrifugation	59 ± 1.5	113 ± 2.0	190 ± 2.5	233 ± 1.6
After centrifugation	64 ± 2.6	121 ± 2.2	236 ± 3.4	248 ± 2.5

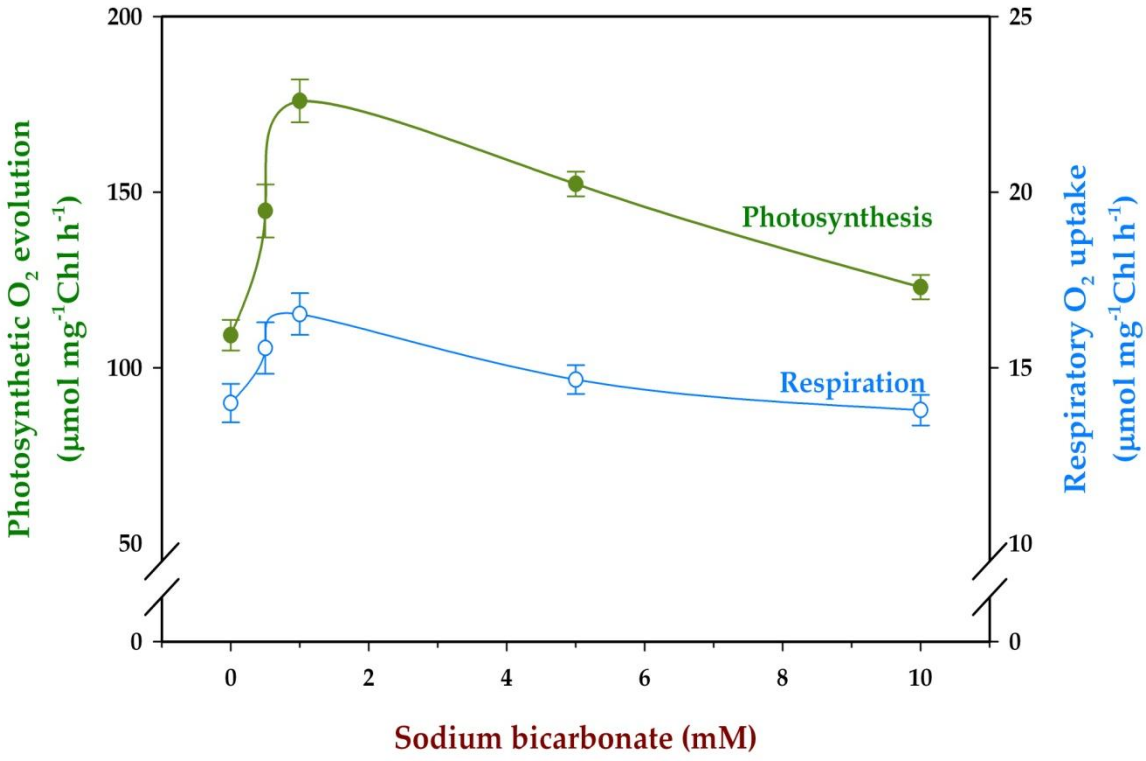

Figure 4.3. Photosynthetic and respiratory rates in mesophyll protoplasts of pea in response to varying concentrations of bicarbonate. Bicarbonate was added to 1 ml of reaction medium (*see materials and methods*) and mesophyll protoplasts equal to 10 mg of chlorophyll. The protoplasts were then monitored for respiration (in dark for 5 min) and photosynthesis (illuminated at 700 µE m^{-2} s^{-1} for 10 min) at 25 °C.

4.2.3. Chl a fluorescence (OJIP) transients obtained from pea protoplasts in comparison with those of leaves

Figure 4.4 shows the typical Chl *a* fluorescence fast OJIP transients, recorded from 5 samples starting from pea leaves (control), peeled leaf segments, enzyme-digested preparations including washing and suspension steps during the isolation procedure. The basic level of fluorescence would vary with the amounts of Chl in the same sample as well as the duration of exposure to light or darkness (Walker, 1988; Schansker et al., 2006). These differences in Chl fluorescence could be overcome by normalizations to Fo, Fi or Fm of the fast transient. These normalizations make a comparison of the shapes of fluorescence transients within the same figure easier. Large numbers of repetitive measurements were made to monitor if any rapid occurrence of changes in OJIP kinetics but the typical curves of samples at different intervals revealed no major changes during isolation procedure.

4.2.4. Effect of digestion on Chl *a* fluorescence (OJIP) transients

Figure 4.5A shows the Chl fluorescence transients of peeled leaf pieces (without epidermis), while these measurements made after 0, 10, 20 and 30 min of digestion are shown in Figure 4.5B. The Chl fluorescence transients measured after 30 min of digestion (Figure 4.5B) showed a rise in J peak, as indicated by high F_J-value, possibly owing to a more reduced PQ pool.

4.2.5. Effect of washing and centrifugation on OJIP transients

Figure 4.6A shows a comparison between transients measured at the end of digestion (after 30 min) and soon after the suspension of protoplasts in washing medium (pH 6) (see the isolation steps in Figure 4.1). The results showed that the

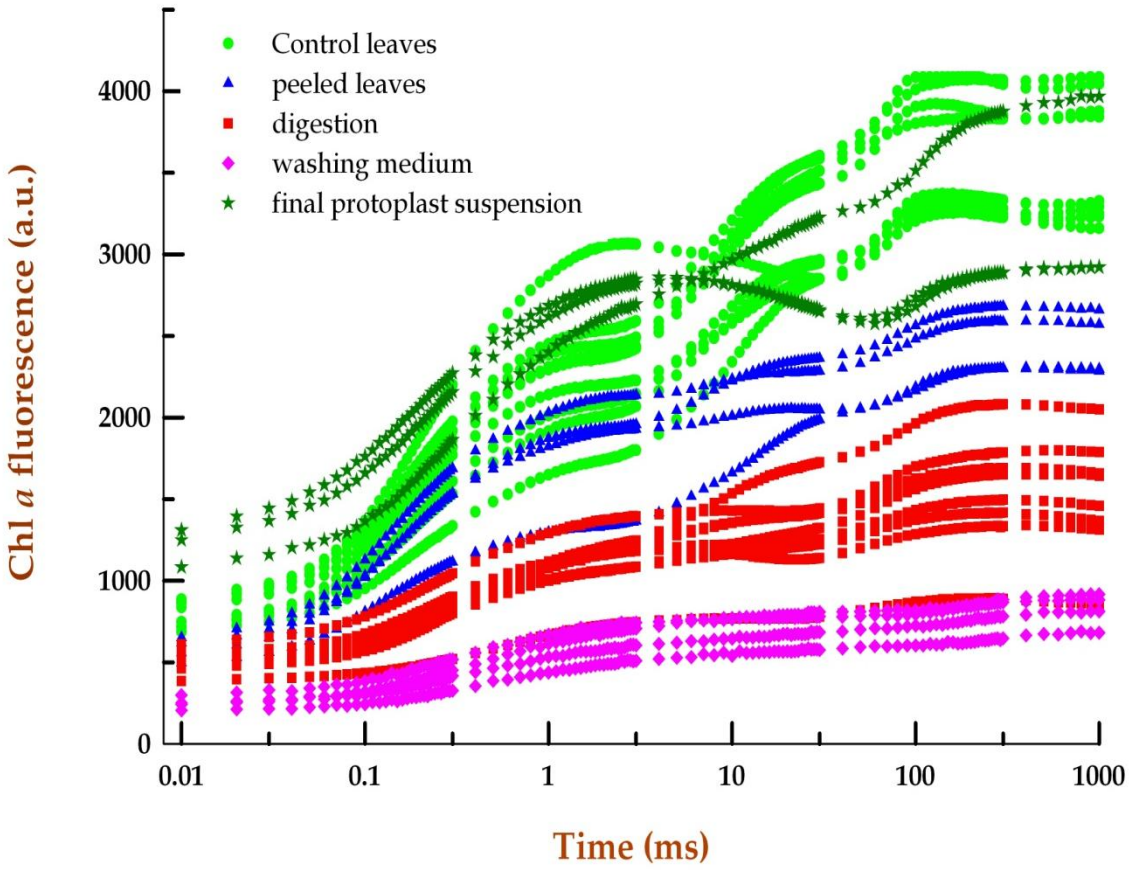

Figure 4.4. Typical set of fast Chl *a* fluorescence OJIP transient measurements made during protoplast isolation (see, Figure 4.1). Raw OJIP transient traces (arbitrary units, a.u.) as recorded by Handy PEA are shown. Green: Pea leaves from green house as well as their detached leaf segments; Blue: peeled leaves before digestion; Red: peeled leaf segments in digestion medium at different times of digestion in light; Pink: samples incubated in washing medium; Dark green: final protoplast suspension.

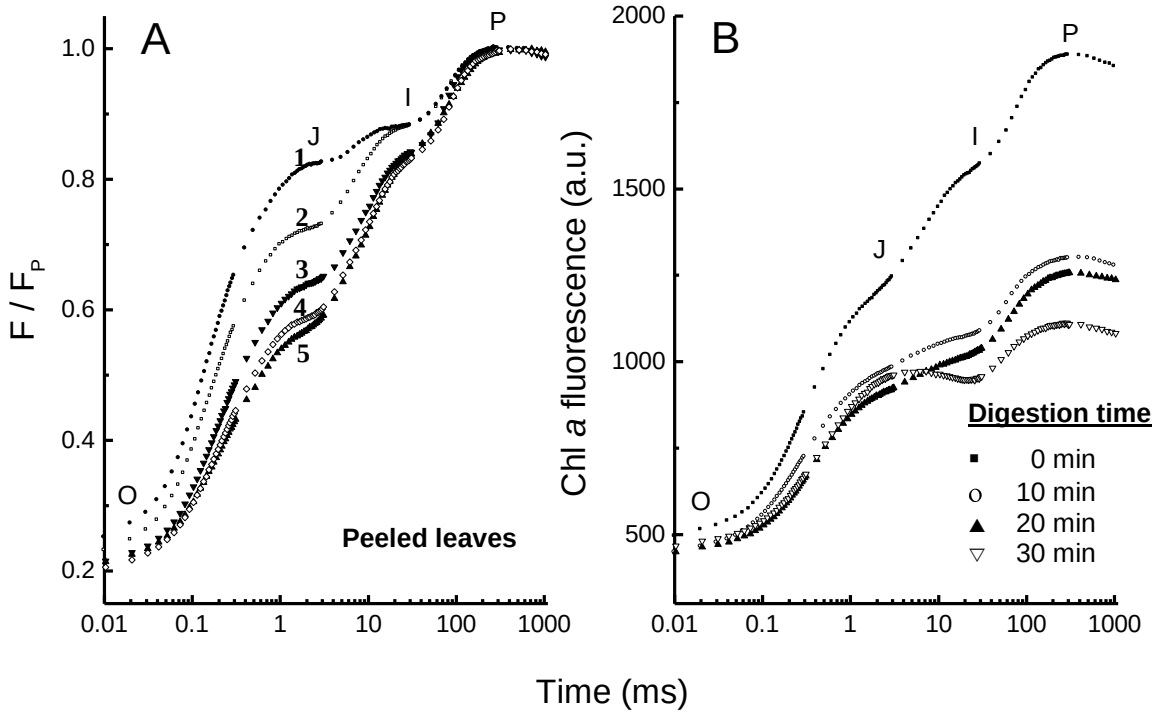

Figure 4.5. Chl *a* fluorescence fast OJIP transients recorded during the first two steps of protoplasts isolation. (A): Measurements with abaxial epidermis peeled leaf segments kept in dim light (<10 µE m^{-2} s^{-1}) at room temperature (24 °C); samplings were examined at different time intervals in different peeled samples marked as 1 to 5. The curves were normalized at P level of the transients. (B): Stripped leaf samples in digestion medium: samples were measured at 0 to 30 min, at 10 min intervals (loss in signal amplitude and change in the time course is noticeable due to enzymatic digestion). The terminology is described in Table 4.1.

washing of protoplasts affected the kinetics of Chl *a* fluorescence, while slowing down of the initial rise (the amplitude of the OJIP-transient in the washing medium was large). The lower F_J relative intensity in the trace 2 (protoplasts in washing medium) indicated that the PQ pool was mostly in oxidized state. The OJIP-transients measured after the subsequent centrifugation step were similar to the ones measured before centrifugation, except that the initial fluorescence rise was fast (Figure 4.6B). Thus, centrifugation of the protoplasts at 50 x g had no harmful effect on fluorescence kinetics of the protoplasts (Figure 4.6B). A strong recovery of the initial OJIP-kinetics was observed on transfer of the protoplasts to an iso-osmotic suspension medium (pH 7) at the end of the washing procedure (Figure 4.6C). This transient of protoplasts showed only minor differences with the OJIP-transient of the source leaves.

4.2.6. Effect of pre-illumination on OJIP transients

The differences between the OJIP transient at the end of the digestion step and the transient of the sample suspended in washing medium shows that the IP-rise started later when the protoplasts were kept in the washing medium and the fluorescence intensity continued rising until the end of the 1 s illumination. In contrast, after digestion, a maximum fluorescence level was reached after 300 ms of illumination (Figure 4.7A). The effect of illumination and temperature on the OJIP-transients in leaves was showed in Figure 4.7B. At the beginning of the protoplast isolation, the leaves were kept in ice-cold water. This caused a decrease in the extent of Chl *a* fluorescence (particularly the second half of the OJ-rise) in leaves kept at 0 °C, compared to the leaves kept at 25 °C. However,

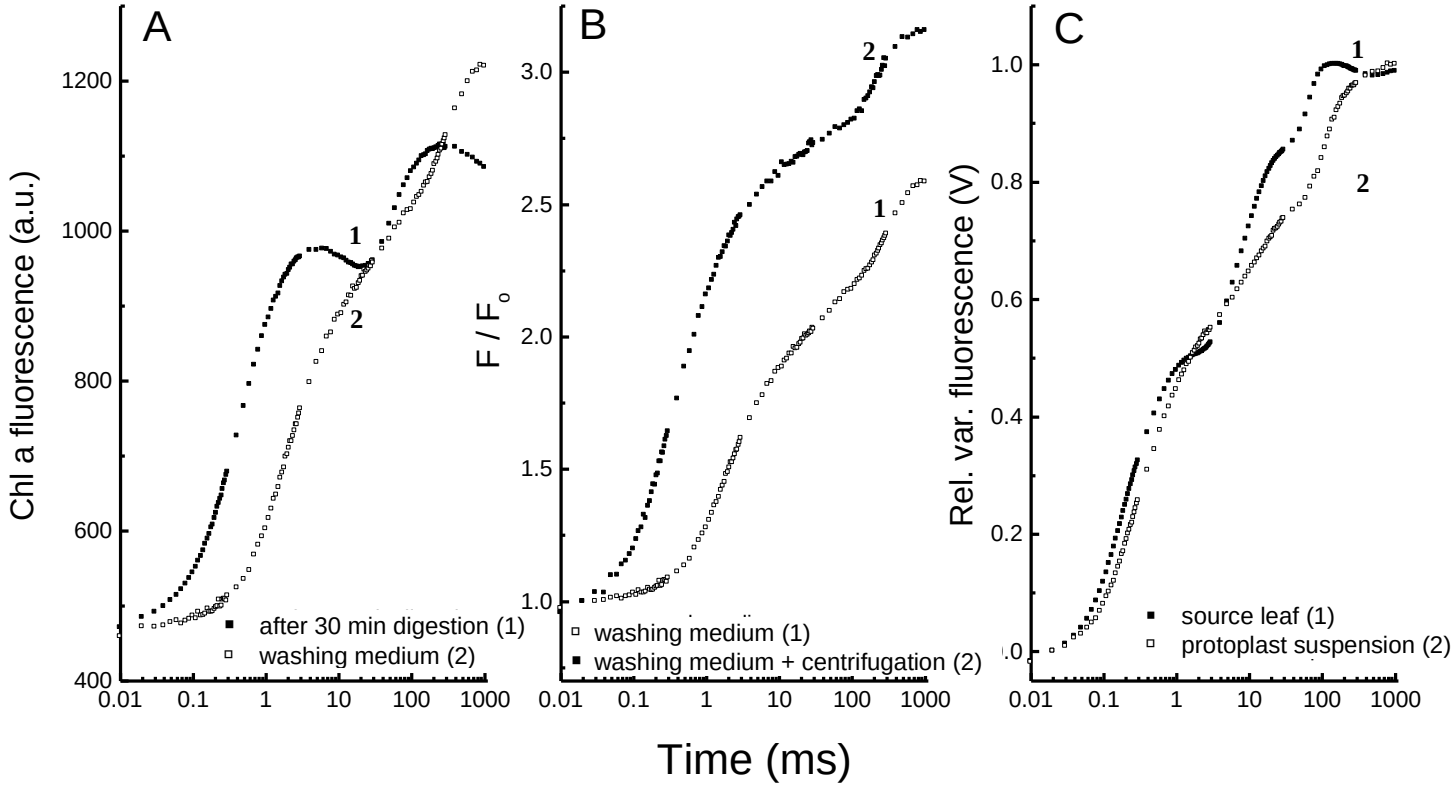

Figure 4.6. Chl *a* fluorescence fast transient of protoplasts samples at washing and centrifugation steps. (A): Protoplasts at the end of digestion (Curve 1) and after re-suspension in the washing medium (Curve 2); (B): protoplasts in washing medium, before centrifugation (Curve 1) or after centrifugation (Curve 2). Both these traces were normalized at F_O; (C): OJIP transient curves of leaf (1) and final protoplast suspension (2), normalized at F_O and at F_M. The curves 1 and 2 represent averages of 3 to10 measurements. The terminology is described in Table 4.1.

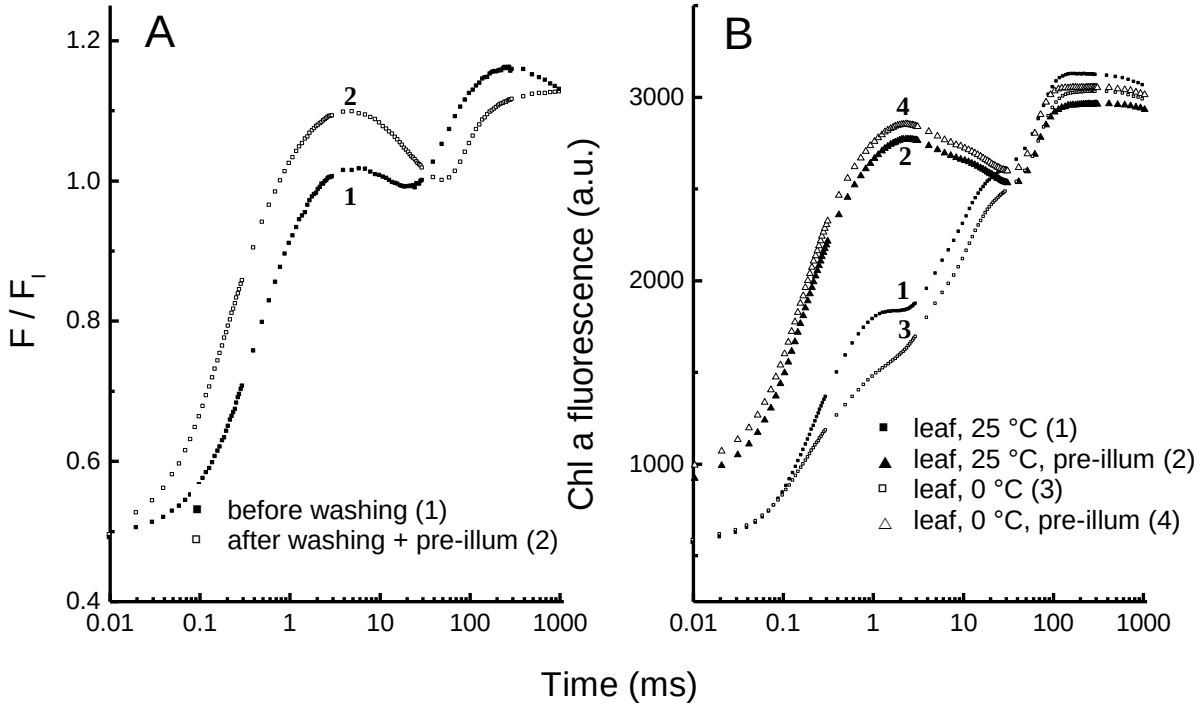

Figure 4.7. Effect of pre-illumination on fluorescence fast transient of protoplasts and leaf segments. (A): Fluorescence transients of protoplasts before and after washing; (B): Fluorescence transients of leaf segments kept at 25 °C (curves 1 and 2) or at 0 °C (curves 3 and 4). The characteristics of leaf segments without pre-illumination (curves 1 and 3) or with pre-illumination (curves 2 and 4) are shown separately. The terminology is described in Table 4.1.

the OJIP transient curves of leaves become quite similar when a second light pulse was given 10 s after the first, the temperature effect was disappeared.

4.3. DISCUSSION

The fast Chl *a* fluorescence OJIP transient is a powerful tool for assessing the photochemical electron transport activities as well as the overall vitality and physiological performance of oxygenic photosynthetic organisms and their tissues (Krause and Weis, 1991; Govindjee, 1995; Joshi and Mohanty, 1995; Strasser et al., 2004; Strauss et al., 2007).

4.3.1. Protoplasts maintained the functional integrity and performance

Although the intactness of protoplasts was assessed routinely during our studies, the functional integrity of the mesophyll protoplasts has to be ascertained, as the digestion involves exposure to acidic pH and high osmoticum. Rapid non-invasive spectroscopic method like Chl *a* fluorescence analysis can, therefore, be beneficial to monitor the photosynthetic performance of protoplasts during the isolation. The isolated mesophyll protoplasts maintained their integrity and photosynthetic status very well, and their functional performance was quite good. The marked uptake of oxygen in darkness and the oxygen evolution in light (Figure 4.3) indicated the active operation of respiration and photosynthesis, respectively.

4.3.2. Protoplast isolation procedure affected the kinetics of OJIP transients

An important cause of variability in Chl fluorescence transients time course is due to change in the F_J-intensity that is ascribed to differences in the chloroplast PQ-pool redox state (Schansker et al., 2006). Despite the fact that the abaxial

peeling was done in dim room light (<10 μE m^{-2} s^{-1}), a partially reduced PQ-pool was observed in leaves whose epidermis is stripped off (Figure 4.5A). Since the leaf pieces were illuminated during digestion, the fluorescence amplitude was suppressed (Figure 4.5B), possibly due to non-photochemical quenching. Such type of effect of light, on the OJIP-transients was reported in an earlier study (Schansker et al., 2006).

Room temperature Chl *a* fluorescence in higher plants gets emanated from chloroplasts and the Chl *a* fluorescence transient (Kautsky transient) reflects the photo reduction of electron transport carriers of two interactive photosystems and also the development of transthylakoid proton gradient which ensures the coupling of electron transport to ATP synthesis (Govindjee, 1995; 2004). The intactness and integrity of chloroplasts ensures retention of both fast O-J-I-P phase as well as slow P-S-M-T phases of Kautsky transient. These phases are reliable criteria of the functional integrity of chloroplasts *in vivo* and *in situ* (Govindjee, 1995; Schreiber et al., 1995). Any perturbation of chloroplast structure and function would alter these fluorescences (Krause and Weis, 1991; Prakash et al., 2003; Strasser et al., 2004). Generally isolated intact chloroplasts do not retain their functional ability for a long time because of CO_2 and Pi limitations (Walker, 1988). However, intact protoplasts isolated from the pea mesophyll cells in the present study retained their CO_2 fixation ability, respiratory and photosynthetic control and metabolic fluxes, during their isolation and for several hours thereafter. Thus, the protoplasts may be quite useful for studies on chloroplast-mitochondrial interactions, metabolic fluxes

and modulation of metabolites as well as on cellular signaling (Padmasree et al., 2002). Earlier studies on Chl fluorescence properties of barley protoplasts demonstrated a slow decline in their redox state, transthylakoid pH gradient and phosphate metabolism (Quick and Horton, 1984; 1986).

The protoplast suspension exhibited a slight slowdown of the kinetics up to the J-step and a much smaller contribution of the JI-phase to the whole transient (Figure 4.6A). The smaller contribution of the JI-phase could be a side-effect of the illumination during digestion. Light-induced changes in the amplitude of the JI-phase have been suggested to be related to changes in the LHCII-phosphorylation state (Schreiber et al., 1995; Schansker et al., 2006). The slower rise up to the J-step could be related to this process. However, the reason for the slower IP-rise remains to be elucidated.

Part of the differences between the OJIP-transients of protoplasts before and after the washing step (Figure 4.7A) could be attributed to differences in the PQ-pool redox state. A brief (1s) pre-illumination given 10s before the fluorescence measurement can cause a reduction of the PQ-pool (Schansker et al., 2005; Toth et al., 2007). Such a 'pre-illumination' pre-treatment given to protoplasts kept in washing medium made the OJIP-transients of protoplasts after washing (Figure 4.7A) quite similar to the transients measured at the end of the digestion treatment. The decrease in Chl a fluorescence at 0 °C could be due to the fact that the second transient was measured in the presence of a reduced PQ-pool and therefore the OJ-rise was not affected by temperature-dependent electron transport between Q_A and Q_B (Krause and Weis, 1991;

Govindjee, 1995; Strasser et al., 2004). However, some warming-up of the leaf during the measurement could also not be excluded. The transients in Figure 4.7A indicated that slow rise kinetics up to the J-step largely disappeared, if the PQ-pool was pre-reduced by a pre-illumination flash.

In the present study, we measured only the fast OJIP phase fluorescence transients which can monitor only light driven electron flow involving two photosystems from H_2O to FNR. However, the slow fluorescence phases of the transient would be extremely useful to also characterize the transthylakoid ΔpH development and state transitions and CO_2 fixation (Govindjee, 1995). These transient changes and changes in other spectroscopic features would be quite appropriate for further elucidating and probing the metabolic functions of protoplasts.

4.4. CONCLUSIONS

1. The present study provides a novel feature of protoplast functional ability that can be followed during the course of isolation from leaves by using a non-invasive technique, Chlorophyll *a* fluorescence transient (OJIP) analysis. The monitoring of Chl *a* fluorescence was rapid and provided information on the light driven electron flow involving two photosystems from H_2O to FNR.
2. The mesophyll protoplasts retained their CO_2 fixation ability and respiratory and metabolic fluxes during isolation and for several hours thereafter. These characteristics made the protoplasts a useful system for studies on organellar interactions, modulation of metabolic fluxes as well as on cellular signaling.

3. The OJIP transients, monitored using a Handy PEA, showed clearly that our preparative steps were gentle and none of the steps seemed to alter the integrity and photosynthetic status of protoplasts. Microscopic examination and electron transport assays supported these conclusions. The functional performance of protoplasts was very similar to that of the intact leaves.
4. We propose that the Chl *a* fluorescence OJIP transients could be used as a quick non-invasive test to assess the functional integrity and physiological performance of the protoplasts.

*****

Chapter 5

The possible role of nitric oxide (NO) and reactive oxygen species (ROS) as biochemical signals during the cross-talk between chloroplasts and mitochondria

Chapter 5

The possible role of nitric oxide (NO) and reactive oxygen species (ROS) as biochemical signals during the cross-talk between chloroplasts and mitochondria

5.1. INTRODUCTION

The key compartments within plant cells, not only mitochondria and chloroplasts but also the peroxisomes and cytosol, appear to be in a state of metabolic equilibrium. Disturbance of any of these compartments disrupts the metabolism of whole cell, including the photosynthetic carbon assimilation (Gardestrom et al., 2002; Raghavendra and Padmasree, 2003). The metabolic interaction between chloroplasts and mitochondria has been extensively studied. There is overwhelming evidence for the importance of these interactions in photosynthesis and respiration, at both biochemical and molecular levels (Matsuo and Obokata, 2006; Noguchi and Yoshida, 2008; Nunes-Nesi et al., 2008).

In illuminated leaves, intracellular metabolism is dynamically modulated depending on environmental changes. Under such conditions, the rapid exchange of metabolites between the organelles forms an important channel of communication. The reduction-oxidation (redox) cascades of the photosynthetic and respiratory electron transport chains not only provide the driving forces for metabolism but also generate redox signals, which orchestrates metabolic adjustment, regulating energy production/utilization, while integrating the plant responses to environmental changes (Pesaresi et al., 2007; Foyer and Noctor, 2009).

The redox control of gene expression within chloroplasts and mitochondria, demonstrates that redox signaling is a primary function of these organelles (Allen, 1993). Other important redox signals that can modulate the intracellular crosstalk are Reactive Oxygen Species (ROS), Nitric Oxide (NO), ascorbate and cytosolic pH (Raghavendra and Padmasree 2003).

The highly reactive radicals of ROS and NO are generated as byproducts of various metabolic pathways, localized in different cellular compartments and turn out to be key molecules in regulating many cellular responses in plants (Neil et al., 2002; del Rio et al., 2006; Navrot et al., 2007). Being readily diffusible, NO and ROS reach a variety of intracellular and extracellular targets. For example, ROS and NO may act directly on targets such as protein thiol groups that are susceptible to nitrosylation or oxidation (Lindermayr et al., 2005; Pitzschke et al., 2006). These post-translational modifications can affect the efficiency of photosynthesis and other plant metabolic processes, resulting in changes in the redox state and modification of metabolism (Michelet et al., 2005; Pfannschmidt et al., 2009). Genes regulated by H_2O_2 (Vandenabeele et al., 2003), NO (Parani et al., 2004; Grun et al., 2006) or both (Zago et al., 2006) have been identified in plants.

There is considerable work on the responses of photosynthetic metabolism to the accumulation of ROS, particularly under high light, water stress and salt stress (Miller et al., 2010; Dinakar et al., 2010; Mubarakshina et al., 2010). However, similar work with NO is quite limited. The present work is an attempt to assess the role of NO and ROS during the biochemical crosstalk between chloroplasts and

mitochondria in mesophyll protoplasts of *Pisum sativum*. The isolated protoplasts offer an excellent model system to study different aspects of metabolism and particularly the interactions between photosynthesis and respiration. The consequence of exogenous application of sodium nitroprusside (SNP, NO donor) and H_2O_2 on the pattern of photosynthesis and respiration were studied. Experiments were also conducted to study the effects of inhibitor-modulation of mitochondrial oxidative metabolism in presence of NO and H_2O_2 on photosynthesis in protoplasts of pea.

5.2. RESULTS

The respiratory and photosynthetic activity of the mesophyll cell protoplasts were measured using a clark-type O_2 electrode. The steady state rates (150 μmol mg^{-1} Chl h^{-1}) of photosynthetic O_2 evolution, attained after a lag period of 3 min illumination, were stable over a time period of 20 min. However, so as to avoid errors due to perturbations in the stability of mesophyll protoplasts at 25 °C, all treatments in the present study were restricted to a time period of 10 min illumination.

5.2.1. Effect of NO on photosynthesis and Respiration

Incubation of plant tissues with SNP (as a chemical donor of NO) can increase the NO levels in tissues. We therefore studied the patterns of the photosynthesis and respiration at varying concentrations of externally added SNP in mesophyll protoplasts of pea. The pre-incubation of mesophyll protoplasts with SNP caused severe inhibition in the CO_2 dependent O_2 evolution, while not exhibiting any significant effect on the rate of respiratory O_2 uptake (Figure 5.1). Photosynthesis

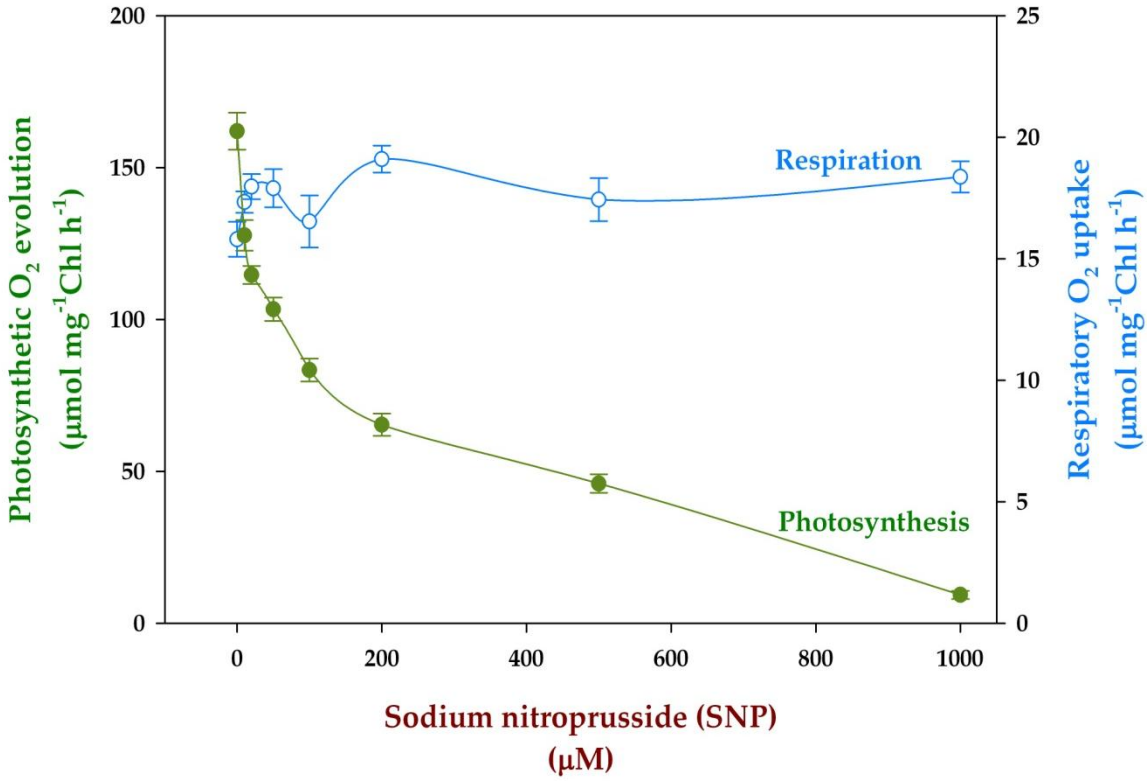

Figure 5.1. The effect of sodium nitroprusside (SNP), which releases nitric oxide, on photosynthesis and respiration of mesophyll protoplasts of pea with 5 min treatment. The protoplasts were then exposed to light (700 μmol m^{-2} s^{-1}).

was progressively suppressed in a concentration dependent manner, from 162 to 9.3 μmol O_2 mg^{-1} Chl h^{-1}. At 100 μM SNP, about 50% inhibition of photosynthesis was observed.

In order to verify that NO was the primary cause for this inhibition, the protoplasts were pre-treated with 2-phenyl-4,4,5,5 tetramethyllimidazoline 1-oxyl-3-oxide (cPTIO, a NO specific scavenger). The inhibition of photosynthesis by SNP was completely reversed by cPTIO, which indicates that the inhibition of photosynthesis by SNP was solely due to nitric oxide but not by other byproducts of SNP (Figure 5.2). By itself, cPTIO had no effect on the photosynthesis.

5.2.2. Effect of H_2O_2 on photosynthesis and Respiration

The exogenous application of H_2O_2 (to enhance the internal ROS levels) to mesophyll protoplasts elicited a contrasting response from photosynthesis and respiration, when compared to the effect of NO. When protoplasts were treated with different concentrations of H_2O_2, their respiratory O_2 uptake was markedly decreased (from 17.6 to 2.8 μmol O_2 mg^{-1}Chl h^{-1}) in a concentration dependent manner (Figure 5.3). In contrast, the effect on photosynthesis was much less than that on respiration. At 100 μM H_2O_2, the decrease in respiration was about 75%, where as the inhibition was only about 15% in photosynthesis. When the concentration of H_2O_2 was raised to 200 μM, marked inhibition of both photosynthesis (50%) and respiration (85%) occurred.

When checked as a function of incubation duration, the rate of respiration in absence of H_2O_2 changed only slightly by 20 min (Figure 5.4). In contrast, when

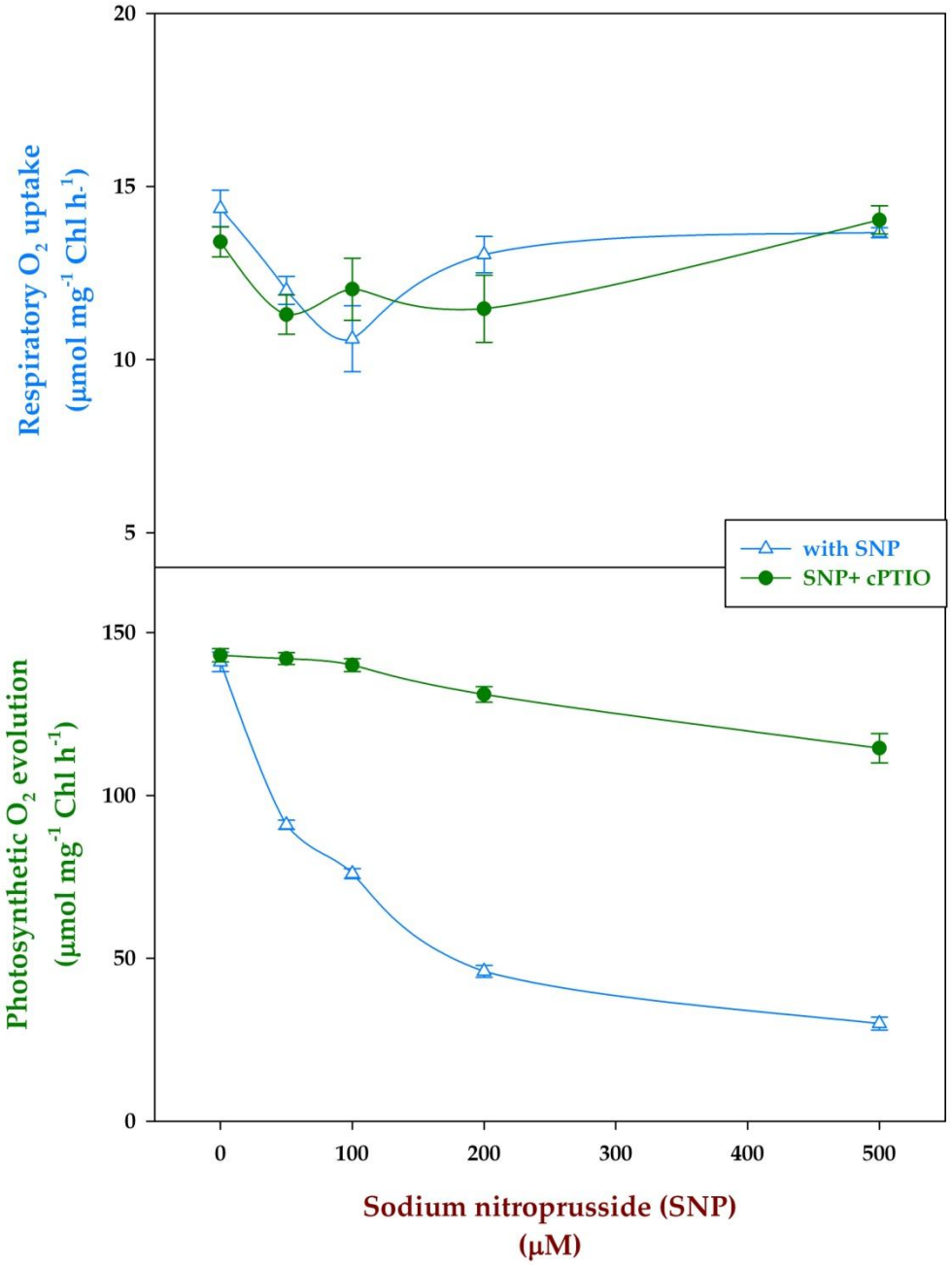

Figure 5.2. The protection due to the cPTIO against inhibition of photosynthesis and respiration by NO (released by SNP). The protoplasts were pre-treated with cPTIO for 5 min and the photosynthesis and respiratory activities were taken in presence of SNP.

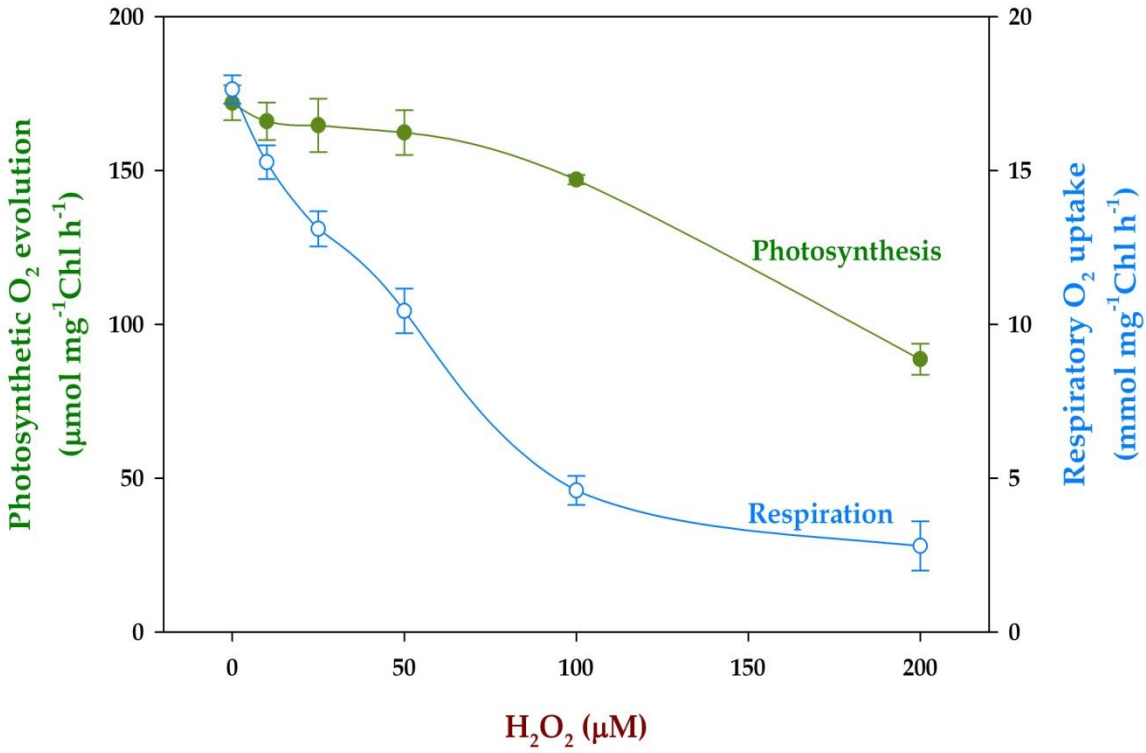

Figure 5.3. The effect of H_2O_2 on photosynthesis and respiration, when exposed to different concentrations of H_2O_2 during a 5 min pre-treatment. The protoplasts were then exposed to light (700 μE m^{-2} s^{-1}).

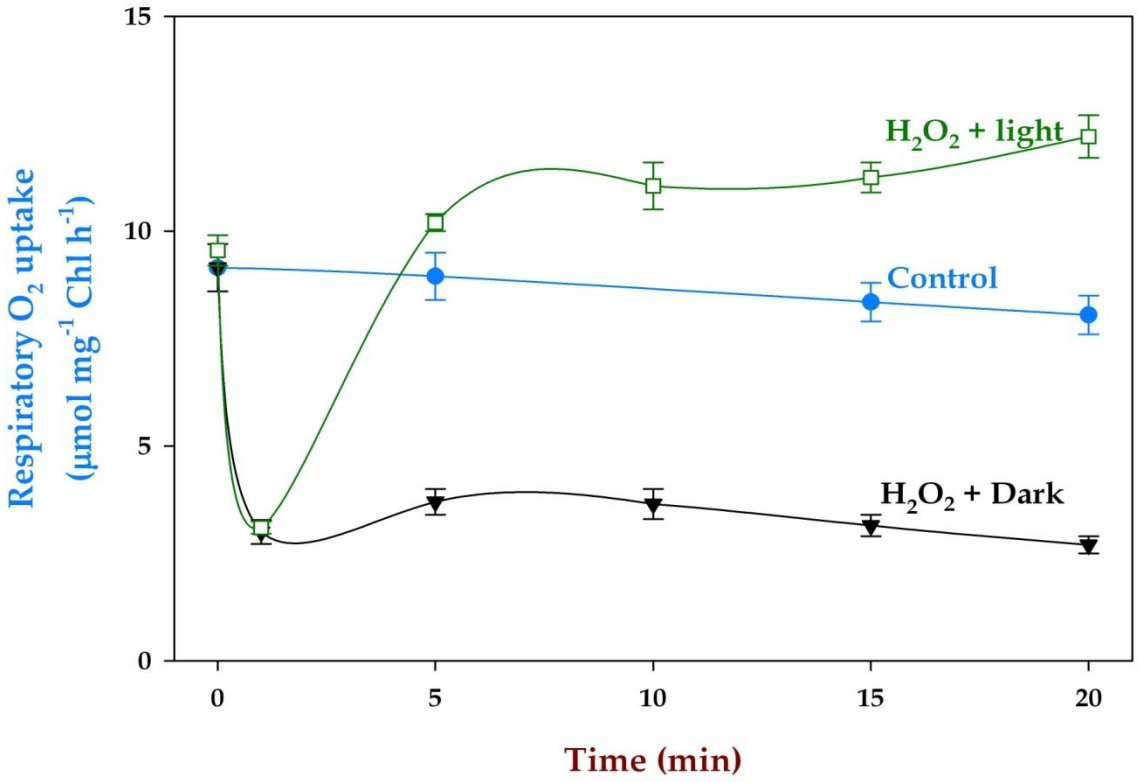

Figure 5.4. Pattern of changes in respiratory rate, with time in mesophyll protoplasts of pea, treated with 100 µM H_2O_2. The protoplasts were pre-incubated with H_2O_2 in dark or light (50 µE m^{-2} s^{-1}) for different time points and then rate of O_2 uptake was measured using Clark-type electrode at specified time points.

treated with 100 μM H_2O_2 in dark, the respiratory performance of protoplasts was severely decreased already by 70% in a minute of incubation. However, when H_2O_2 treatment was given under illumination (50 μE m^{-2} s^{-1}), the respiration decreased by one minute, but then went on to increase up to 20 min (Figure 5.4).

5.2.3. Effect of mitochondrial inhibitors on photosynthesis and respiration

The effect of mitochondrial inhibitors Antimycin A (inhibitor of COX pathway/ complex III of mitochondria) or SHAM (inhibitor of AOX pathway of mitochondria) on photosynthetic carbon assimilation (at optimal conditions: 1 mM bicarbonate and a light of 700 μE m^{-2} s^{-1}) or respiration of pea mesophyll protoplasts were examined.

At the range of concentrations, used in the present study, Antimycin A had only a marginal effect on respiration. In contrast, , the rate of photosynthetic O_2 evolution decreased markedly from 132 to 30 μmol O_2 mg^{-1} Chl h^{-1}, as the concentration of Antimycin A was raised (0 to 0.5 μM). For example, at 100 nM of Antimycin A, the decrease in respiratory O_2 uptake was 20%, where as photosynthesis went down by as much as 60% (Figure 5.5).

Subsequently, the effect of SHAM in mesophyll protoplasts was ascertained by monitoring both the respiratory and photosynthetic rates in the presence of a wide range of concentrations of SHAM (0 to 0.5 mM). When pre-incubated with SHAM, the rates of respiration of mesophyll protoplasts decreased marginally.

On the other hand, the photosynthesis decreased drastically from 130 (no SHAM) to 51 μmol O_2 mg^{-1} Chl h^{-1}, with 500 μM SHAM (Figure 5.6). Even at 200 μM

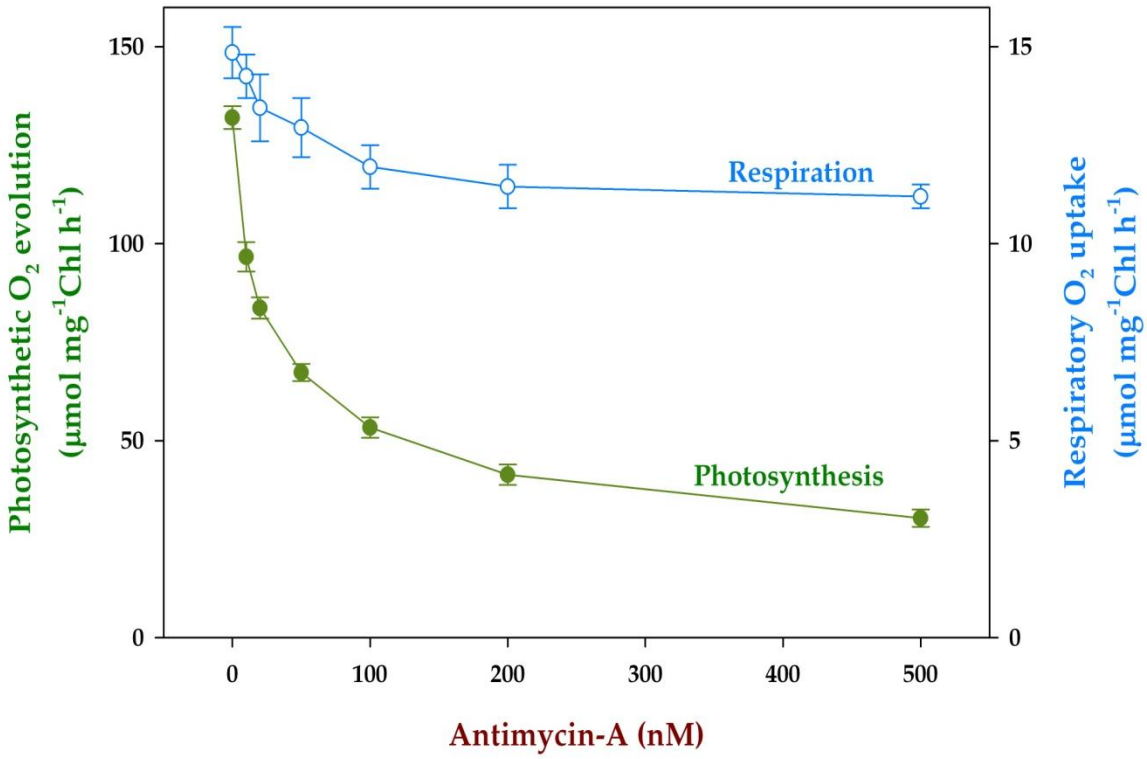

Figure 5.5. Effect of Antimycin A, an inhibitor of cytochrome pathway, on photosynthesis and dark respiration in mesophyll protoplasts of pea. The protoplasts were pre-incubated with the indicated concentrations of Antimycin in darkness for 5 min at 25 °C and then the respiratory O_2 uptake or photosynthesis was monitored.

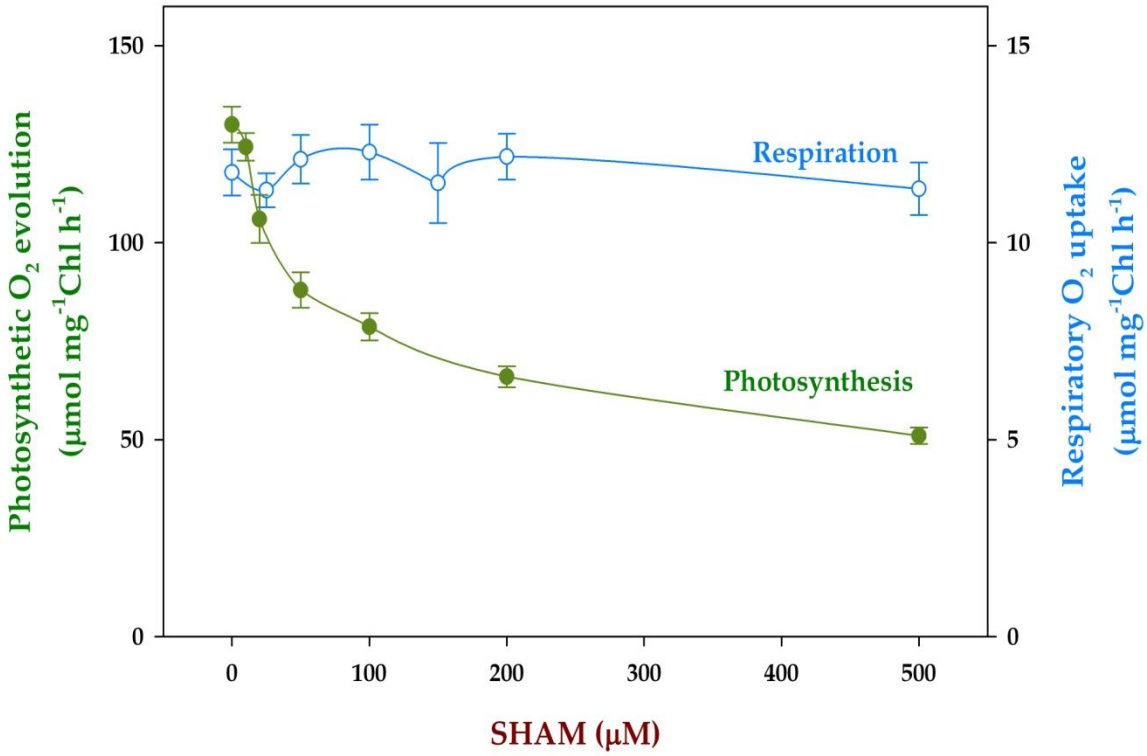

Figure 5.6. Effect of SHAM, an inhibitor of alternative pathway, on photosynthesis and dark respiration in mesophyll protoplasts of pea. The protoplasts were pre-incubated at 25 °C with the indicated concentrations of SHAM in darkness for 5 min and then the respiratory O_2 uptake or photosynthesis was monitored.

SHAM, photosynthesis decreased by 50%, while the respiration did not change significantly.

5.2.4. Effect of SNP (source of NO) on protoplasts during restricted mitochondrial electron transport

The marked inhibition of photosynthesis by the classic mitochondrial inhibitors in contrast to only a marginal effect on respiration (Figures 5.5 and 5.6) is a strong indication of the inter-dependence of chloroplast and mitochondria. To elucidate the role of NO during such interaction, we have pre-treated protoplasts with SNP and then the rate of respiration and photosynthesis was measured in presence of mitochondrial inhibitors.

The presence of 100 μM SNP decreased the rate of photosynthesis by 45%. Similarly, the presence of Antimycin A and SHAM caused about 50% inhibition in photosynthesis. The sensitivity of photosynthesis to these classic mitochondrial inhibitors was marginally decreased in presence of SNP (Table 5.1). None of these mitochondrial inhibitors either alone or in combination with SNP or cPTIO had any significant effect on respiratory activity of protoplasts (Table 5.2).

5.2.5. Effect of H_2O_2 on photosynthesis of protoplasts in relation to restricted mitochondrial electron transport

The presence of 100 μM H_2O_2 decreased the rate of protoplast photosynthesis by <20%. Similarly, the presence of mitochondrial inhibitors Antimycin A and SHAM caused an inhibition of photosynthetic rate by about 45% to 60% (Table 5.3).

Table 5.1. Sensitivity of photosynthesis to mitochondrial inhibitors in presence of SNP and/or NO modulators. The protoplasts were incubated in dark at 25 °C for 5 min without (control) or with SNP along with mitochondrial inhibitors (50 nM of Antimycin-A or 200 μM of SHAM).

	Photosynthetic O_2 evolution (μmol mg^{-1}Chl h^{-1})		
	No inhibitor	Antimycin A	SHAM
Control	137 ± 4.0 (100)	70 ± 4.1 (51)	72 ± 4.5 (53)
cPTIO	139 ± 5.9 (100)	84 ± 5.4 (60)	83 ± 3.2 (60)
SNP	76 ± 6.7 (100)	44 ± 3.2 (58)	47 ± 2.4 (62)
SNP+ cPTIO	131 ± 3.4 (100)	72 ± 2.2 (55)	85 ± 6.1 (65)

★ values in parenthesis indicate the percentage control without Antimycin A or SHAM(%).

Table 5.2. Sensitivity of respiration to mitochondrial inhibitors in presence of SNP and/or NO modulators. The protoplasts were incubated in dark at 25 °C for 5 min without (control) or with SNP along with mitochondrial inhibitors (50 nM of Antimycin-A or 200 μM of SHAM).

	Respiratory O_2 uptake (μmol mg^{-1}Chl h^{-1})		
	No inhibitor	Antimycin A	SHAM
Control	16.7 ± 0.8 (100)	16.6 ± 1.0 (99)	16.2 ± 1.4 (97)
cPTIO	16.2 ± 1.1 (100)	15.8 ± 0.8 (98)	19.1 ± 0.6 (118)
SNP	17.8 ± 1.1 (100)	18.2 ± 0.9 (102)	17.1 ± 1.0 (96)
SNP+ cPTIO	17.5 ± 0.8 (100)	16.5 ± 0.7 (94)	18.7 ± 0.4 (107)

★ values in parenthesis indicate the percentage of control without Antimycin A or SHAM(%)

However, the sensitivity of photosynthesis to mitochondrial inhibitors, Antimycin A and SHAM was significantly less in the presence of H_2O_2 than that in the absence. In presence of H_2O_2 the inhibition of photosynthesis by Antimycin A and SHAM was suppressed to 30% to 40%.

5.2.6. Effect of H_2O_2 on photochemical activities of protoplasts

It is possible that the presence of H_2O_2 may interfere directly with the photochemical electron transport activities in protoplasts. We have measured BQ and NO_2^- dependent O_2 evolution after ensuring that CO_2 dependent O_2 evolution is suppressed by including in the assay medium contained 5 mM glycolaldehyde (inhibitor of CO_2 fixation). para-Benzoquinone (*p*BQ) is an artificial electron acceptor used to examine the PSII activity, where as $NaNO_2$ is used to monitor the whole chain activity. However, there was not much change (<5%) in the photochemical activities of either PS I or PS II of protoplasts in presence of externally added H_2O_2 (Table 5.4).

5.3. DISCUSSION

Mitochondrial oxidative metabolism modulates the coordination between different components of photosynthetic carbon assimilation in chloroplasts such as generation and use of assimilatory power (ATP and NADPH), induction of photosynthesis and maintenance of metabolites (Igamberdiev et al. 1998; Padmasree et al., 2002; Yoshida et al. 2006, 2007). In present study, we focused on the pattern changes in photosynthesis and respiration in response to NO and ROS,

Table 5.3. Sensitivity of photosynthesis to mitochondrial inhibitors in presence of H_2O_2. The protoplasts were incubated in dark at 25 °C for 5 min without (control) or with H_2O_2 along with mitochondrial inhibitors (50 nM of Antimycin-A or 200 μM of SHAM).

	Photosynthetic O_2 evolution (μmol mg^{-1}Chl h^{-1})		
	No inhibitor	Antimycin A	SHAM
Control	127 ± 3 (100)	70 ± 2 (55)	52 ± 1 (41)
H_2O_2	104 ± 3 (100)	71 ± 3 (68)	58 ± 3 (56)

★ values in parenthesis indicate the percentage control without Antimycin A or SHAM(%)

Table 5.4. Sensitivity of photochemical reactions to the exogenous application of H_2O_2

	Photosynthetic O_2 evolution (μmol mg^{-1} Chl h^{-1})		
	no H_2O_2	H_2O_2 (100 μM)	% inhibition by H_2O_2
Control	131 ± 2.03	110 ± 4.58	16 %
Glycolaldehyde	0	0	-
Glycolaldehyde + BQ*	242.7 ± 6.01	233 ± 6.43	4 %
Glycolaldehyde+$NaNO_2$**	18.5 ± 0.90	17.9 ± 1.64	3 %

* Dependent on PS II alone

** Dependent on Ps II and PS I

when the mitochondrial oxidative metabolism is restricted. These studies are expected to validate the roles of NO and ROS as possible biochemical signals during the cross-talk between chloroplast and mitochondria.

NO and ROS are of great relevance in physiology of plants under both natural and stress conditions. These two molecules have emerged as ubiquitous components of signal transduction in plants (Besson-Bard et al., 2008; Tanou et al., 2009). Most of the earlier studies were aimed at investigating the effect of NO and H_2O_2 on gene transcription level (Polverari et al. 2003; Vanderauwera et al., 2005; Zago et al., 2006; Ahlfors et al., 2009) or post-translational modifications of proteins. We have employed SNP as the NO releaser and H_2O_2 as a source of ROS in our study and experiments were done using *Pisum sativum*. L. mesophyll protoplasts.

5.3.1. Differential inhibition of photosynthesis and respiration by SNP

When protoplasts were exposed to SNP, there was significant inhibition in the rate of photosynthesis. The inhibition of photosynthesis was concentration dependent (Figure 5.1) and could be reversed by supplying the NO scavenger cPTIO (Figure 5.2) indicating that the observed inhibition was due to the rise in NO. Previous research suggested that NO gas decreased net photosynthesis rates in oat (*Avena sativa*) and alfalfa (*Medicago sativa*) leaves (Hill and Bennett, 1970). Lum et al. (2005) have identified a number of intracellular targets of NO besides in chloroplasts, along with mitochondria and peroxisomes. They found that with 6 h of incubation, SNP decreased the amount of Rubisco activase and the β-subunit of the Rubisco

subunit-binding protein in mung bean (*Phaseolus aureus*). Jasid et al. (2006) showed that chloroplasts exposed to $ONOO^-$ increased lipid radical content by 34% and reduced both the O_2 evolution rate and the Φ_{PSII}, indicating damage to the electron transport activities of thylakoid membranes. Wodala et al. (2008) observed that NO could influence (decrease) the photosynthetic electron transport chain directly and PS II was an important site of NO action.

In contrast to high sensitivity of photosynthesis, the respiratory rate was only marginally affected due to SNP treatment of protoplasts (Figure 5.1). As per the earlier reports, in carrot cell suspension cells, NO reduced total respiration by 50% and this effect was accomplished by cell death (Zottini et al., 2002). Similarly in isolated soybean cotyledon mitochondria, NO treatment resulted in cytochrome pathway inhibition, and the inhibition was relieved upon NO removal (Miller and Day, 1996). A main reason for not observing any effect on respiration in our study might be the short time of NO exposure (5 min) to the cells. It is also possible that AOX may confer NO tolerance and compensate COX pathway inhibition. This observation is concurrent with the observation of Huang et al, (2002), where it has been shown that NO exposure to tobacco suspension cells could activate the AOX pathway.

Since our results show that elevated NO affects the photosynthetic performance of mesophyll protoplasts, we conclude that chloroplasts are one of the early targets of NO in the plant cell. Our result supports the earlier reports, that chloroplasts could be one of the primary sub cellular targets for NO (Lum et al.

2005; Jasid et al., 2006; Gas et al., 2009).

5.3.2. Effect of H_2O_2 on photosynthesis and respiration

The exposure of mesophyll protoplasts to H_2O_2 resulted in a response quite opposite to the effect of NO. The H_2O_2 treatment showed a significant inhibition of respiration, while the extent of inhibition was marginal or little on photosynthesis (Figure 5.3). Such response is quite intriguing, because of the fact that photoactive chloroplasts generate considerable ROS in light. Further the chloroplast/peroxisome systems are estimated to generate about 90% of the total H_2O_2 in a photosynthetically active plant cell (Foyer and Noctor, 2000). It is possible that chloroplasts have efficient H_2O_2 scavenging systems like ascorbate peroxidase and glutathione that prevent the harmful effects of H_2O_2. An array of antioxidant response systems, designed for the control of the cellular redox state, impart tolerance to plants at high H_2O_2 levels (Apel and Hirt, 2004; Foyer and Noctor, 2005). Thus, the generation as well as the scavenging systems of H_2O_2 in plant cells would ultimately pronounce the effect on metabolism. When the concentration of H_2O_2 is raised to 200 μM, a marked inhibition of both photosynthesis (50%) and respiration (85%) occurred (Figure 5.3). We feel that when the respiratory metabolism is severely affected, it leads to a decrease in photosynthetic rates of protoplasts. Our results support the concept of strong dependence of chloroplasts on mitochondria (Padmasree and Raghavendra, 2001).

The sensitivity of respiration in absence of H_2O_2 didn't change much over the time period up to 20min (Figure 5.4). In contrast, when protoplasts were treated

with 100 μM H_2O_2 in dark, their respiratory performance was severely decreased (70%) in a time dependent manner. While in low light, H_2O_2 treatment initially resulted in decrease of respiration but then dramatically increased with the time of treatment (Figure 5.4), which could be a possible effect of light enhance dark respiration (LEDR). LEDR is a characteristic feature in plants and has been demonstrated in protoplasts as well as in leaves (Reddy et al., 1991; Tcherkez and Farquhar, 2005). Atkin et al. (1998) showed that LEDR is noticeable even in low intensities of light (3 μE m^{-2} s^{-1}).

Our results show that the inhibitory effect of H_2O_2 is much stronger on respiration than that on photosynthesis, suggesting mitochondria could be one of the primary targets for ROS in plant cell.

5.3.3. Effect of restricted mitochondrial metabolism on photosynthesis

The importance of mitochondrial metabolism in optimizing photosynthesis is ascertained by examining the effects of mitochondrial inhibitors Antimycin A (inhibitor of COX pathway) and SHAM (inhibitor of AOX pathway) on photosynthetic carbon assimilation. The non-specific effects of both AA and SHAM were minimized by using very low concentrations, which do not disturb directly photosynthetic reactions (Padmasree et al., 2002). At the range of concentration used in the present study, both the Antimycin A and SHAM caused remarkable decrease in the rates of photosynthetic oxygen evolution in mesophyll protoplasts in a concentration dependent manner (Figure 5.5 and 5.6). These results confirm the essentiality of mitochondrial oxidative metabolism for photosynthetic carbon

assimilation. The presence of Antimycin A marginally decreased respiration (by <15%) but on exposure to lower levels of SHAM, caused a marginal increase in respiration (Figure 5.6). It is known that mitochondrial electron transport through the AOX pathway is enhanced when the electron flow through the cytochrome pathway is either inhibited or saturated (Millar et al., 1995). In agreement with these earlier observations, the presence of SHAM alone at low concentrations increased the respiratory O_2 uptake (Padmasree and Raghavendra, 2001).

Even a marginal interference in electron transport through COX or AOX pathway of mitochondrial respiratory chain causes a significant drop in photosynthetic carbon assimilation (Padmasree and Raghavendra, 1999; Dutilleul et al., 2003; Yoshida et al., 2006). For example, a decrease of <15% in the rate of respiration caused an inhibition of 50% in photosynthesis in the presence of Antimycin A (Figure 5.5). Our results reaffirm that mitochondrial metabolism is not only beneficial but also crucial for optimal functioning of photosynthesis.

5.3.4. Influence of NO on the sensitivity of photosynthesis to mitochondrial inhibitors

The results from the present study and past work from our laboratory and literature demonstrates that any perturbation in the operation of the mitochondrial oxidative electron transport leads to disturbances in the sustenance of photosynthesis. The well-known basis of inter-organelle interaction is the exchange of metabolites between them. However there could be other possible signals like NO, ROS and ascorbate, which can fine-tune these interactions (Raghavendra and Padmasree,

2003; Noctor et al., 2007). However, during our experiments, we could not find any strong evidence for the role of NO during interactions, as the sensitivity of photosynthesis to mitochondrial inhibitors was only marginally decreased in presence of SNP (Table 5.1). It is possible that chloroplasts, as the site of several antioxidant systems, are responsible for this marginal recovery but not NO, as observed with the use of NO scavenger, cPTIO. But further studies need to be done to clearly find out the role of NO as a biochemical signal during cross talk between chloroplast and mitochondria.

5.3.5. H_2O_2 decreased the sensitivity of photosynthesis to mitochondrial inhibitors marginally

The presence of H_2O_2 appeared to decrease the sensitivity of photosynthesis to mitochondrial inhibitors, particularly SHAM. Pre-treatment of protoplasts with mitochondrial inhibitors resulted in 50-60% inhibition in photosynthesis. In presence of H_2O_2, the inhibition of photosynthesis by mitochondrial inhibitors was suppressed to 30-40% (Table 5.3). This could be due to the fact that inhibition of electron transport in mitochondria could result in over reduction of respiratory complexes and lead to generation of ROS. This ROS can diffuse to cellular compartments and can relay the information of over reduction of electron transport in mitochondria and chloroplasts. Moreover chloroplasts are known to have better ROS scavenging capacity because of abundance levels of ascorbate and glutathione (Foyer and Noctor, 2003; Apel and Hirt, 2004).

The role of ROS on the photochemical activities were checked and found out that there is not much change in the photochemical activities of protoplasts in presence of externally added H_2O_2. H_2O_2, at this concentration didn't affect the electron transport activities of PS I or PS II (Table 5.4). Our results, revealed that H_2O_2 affected chloroplasts and mitochondria, rather differentially and that the effect on photosynthesis is on carbon assimilation reactions. The cross-talk between chloroplasts and mitochondria becomes less pronounced in presence of H_2O_2. It is therefore possible that the intracellular level of H_2O_2 may be one of the important factors during cross talk between chloroplasts and mitochondria.

5.4. CONCLUSIONS

1. Elevated levels NO (by SNP) severely inhibited the photosynthetic performance of mesophyll protoplasts of pea, while exhibiting marginal/no effect on dark respiration, indicating that chloroplasts could be one of the sensitive targets of NO in the plant cell.
2. NO did not alter much the sensitivity of photosynthesis by mitochondrial inhibitors, as evidenced with the use of SNP, and/or a scavenger of NO, cPTIO. Further studies need to be done to elucidate the role of NO during inter-organelle interaction.
3. The addition of external H_2O_2 caused marked inhibition of dark respiration, while exhibiting only marginal inhibition of photosynthesis; suggesting mitochondria could be one of the immediate targets for ROS in plant cells.

4. Further, H_2O_2 appeared to decrease the sensitivity of photosynthesis to mitochondrial inhibitors, particularly SHAM, suggesting that H_2O_2 perhaps acts as a stress signal, mediates crosstalk between chloroplasts and mitochondria.

*****

Chapter 6

Targets of NO in chloroplast components of pea protoplasts studied using fast transients of OJIP fluorescence curves

Chapter 6

Targets of NO in chloroplast components of pea protoplasts studied using fast transients of OJIP fluorescence curves

6.1. INTRODUCTION

In photosynthesis research, chlorophyll *a* (Chl a) fluorescence is one of the most widespread parameter used to assess the functionality of chloroplast during basic and ecophysiological studies (Papageorgiou and Govindjee 2004). Chl *a* fluorescence is a highly sensitive, non-destructive, and reliable tool for measuring photosynthetic efficiency, particularly of photosystem II (PSII) *in vivo* as well as *in vitro* (Lazár 2006; Stirbet and Govindjee, 2011). Such fluorescence provides information on the ability of a plant to tolerate environmental stresses and the extent of damage to the photosynthetic apparatus; if any (Baker, 2008).

At the onset of illumination, Chl *a* fluorescence of dark-adapted cells exhibits complex kinetics with several inflection points (O, J, I and P) with time, known as OJIP transients (Kautsky et al., 1960). These OJIP transients reflect changes in electron transport in PS II over a wide range of time, from microseconds to seconds, that allow us to evaluate the sub-characteristics of PS II, such as energy trapping, electron transport (Strasser et al., 2004; Stirbet and Govindjee, 2011). During OJIP transients, all the reaction centers are open at the minimal fluorescence (Fo) and are closed at maximum fluorescence (Fm). A versatile JIP test has been developed for the quantification of OJIP fluorescence transients into several phenomenological and biophysical expressions of PSII (Strasser and Strasser, 1995).

Chloroplasts are the site of not only carbon/nitrogen metabolism, but also reactive oxygen species (ROS) production. The ROS as well as NO/related species, being active radicals can affect a wide range of downstream signals through their effects on chloroplasts (Asada, 2006; Moller et al., 2007; Hayat et al., 2010). Being a readily diffusible free radical, NO reacts with a variety of intracellular and extracellular targets. In biological systems, NO reacts with thiol- and metal-containing proteins and can regulate the activity of proteins through post-translational modifications that include S-nitrosylation (Abat et al., 2008; Lindermayr et al., 2010). These post-translational modifications can affect chloroplastic/mitochondrial electron transport components and subsequently the efficiency of photosynthesis and other plant metabolic processes (Michelet et al., 2005; Foyer and Noctor, 2009). Recent studies have indicated that chloroplasts can be significant sources of NO (Jasid et al., 2006; Gas et al., 2009). In the cellular organelles, NO may play a dual role of protection and damage, depending on the concentration and physiological conditions.

In Chapter 5, it has been shown that NO severely affects the photosynthesis quite quickly. This chapter describes the efforts made to study the changes in the different components of photosynthetic electron transport and identify the possible targets of NO within chloroplasts. Protoplasts were pre-treated with or without sodium nitroprusside (SNP), which releases NO within the cell for specified time points, up to 20 min. Their photosynthetic activities were monitored, in terms of O_2 evolution and Chl *a* fluorescence transients. We have further investigated the

pattern and kinetics of NO release from SNP and PS II photochemistry in elevated NO conditions, to understand the influence of NO on photosynthetic reactions in protoplasts.

6.2. RESULTS

All the observations were made using mesophyll protoplasts of pea plants. These mesophyll protoplasts were quite functional and were as active as the leaves (described in Chapter 4).

6.2.1. Patterns of NO production on incubation with SNP

The pattern of NO release in response to light and time was monitored using DAF-2DA fluorescence (specific for NO) in protoplasts under a confocal microscope. The endogenous level of NO in control protoplasts (without SNP treatment) was quite low. The red fluorescence is due to chlorophyll auto-fluorescence. The exogenous application of SNP enhanced the NO levels in protoplasts, particularly in light.

On illumination, the SNP treated protoplasts showed enhanced levels of NO, both in terms of number of fluorescing protoplasts and intensity of the fluorescence in them (Figure 6.1). The step-wise increase in NO fluorescence levels from 5-30 min was quite visible (Figure 6.1). A close up examination of DAF-2DA fluorescence in SNP treated protoplasts indicated that there was a marked increase in NO levels from 5 to 30 min (Figure 6.2), and only a marginal increase occurred during dark treatments (Figure 6.3).

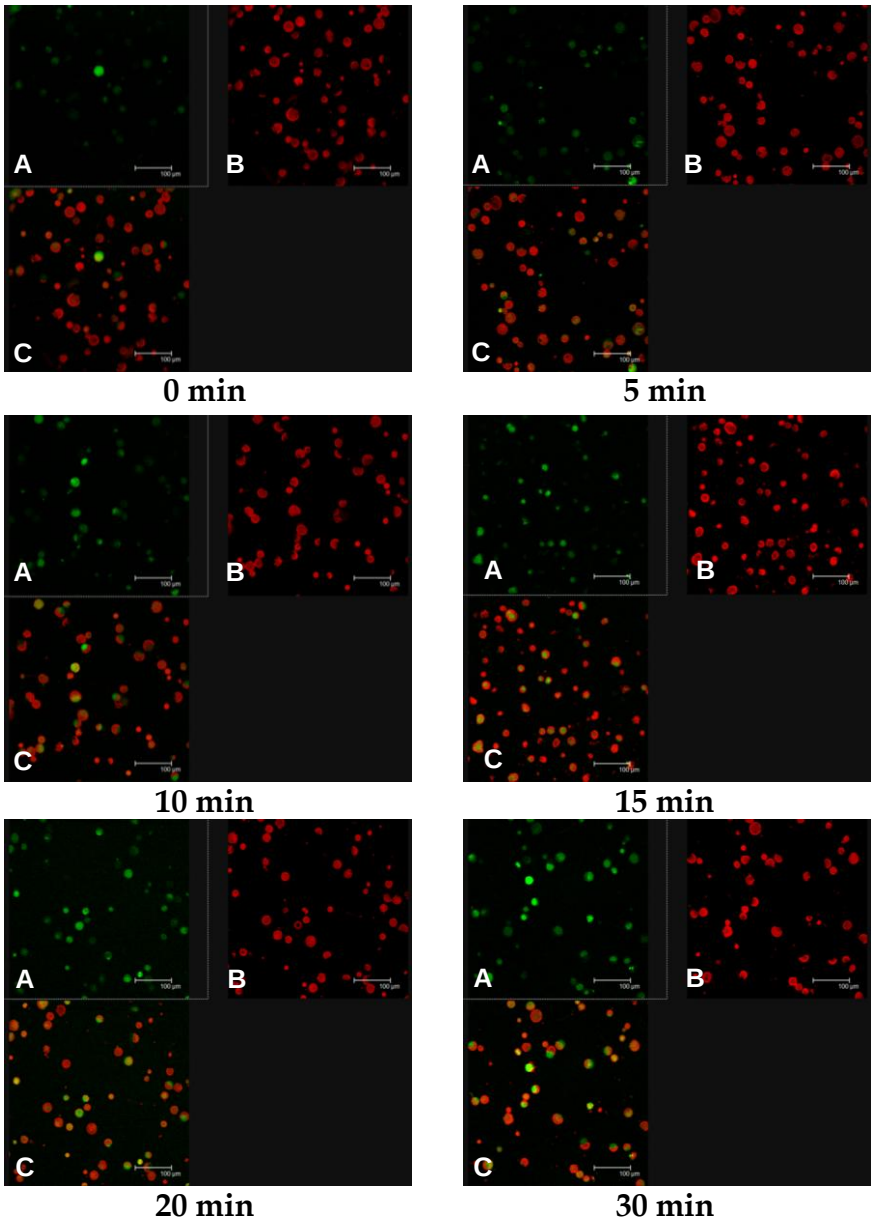

Figure 6.1. The pattern of NO production by SNP, in response to light treatments of protoplasts. The fluorescence intensity as well as the number of fluorescing protoplasts was increased with time. Protoplasts were observed for DAF-fluorescence (A), or chlorophyll auto-fluorescence (B) or both (C). See section 3.9 of Materials and Methods for details. Experiments were repeated at least three times with similar results. Bar represents 100 μm.

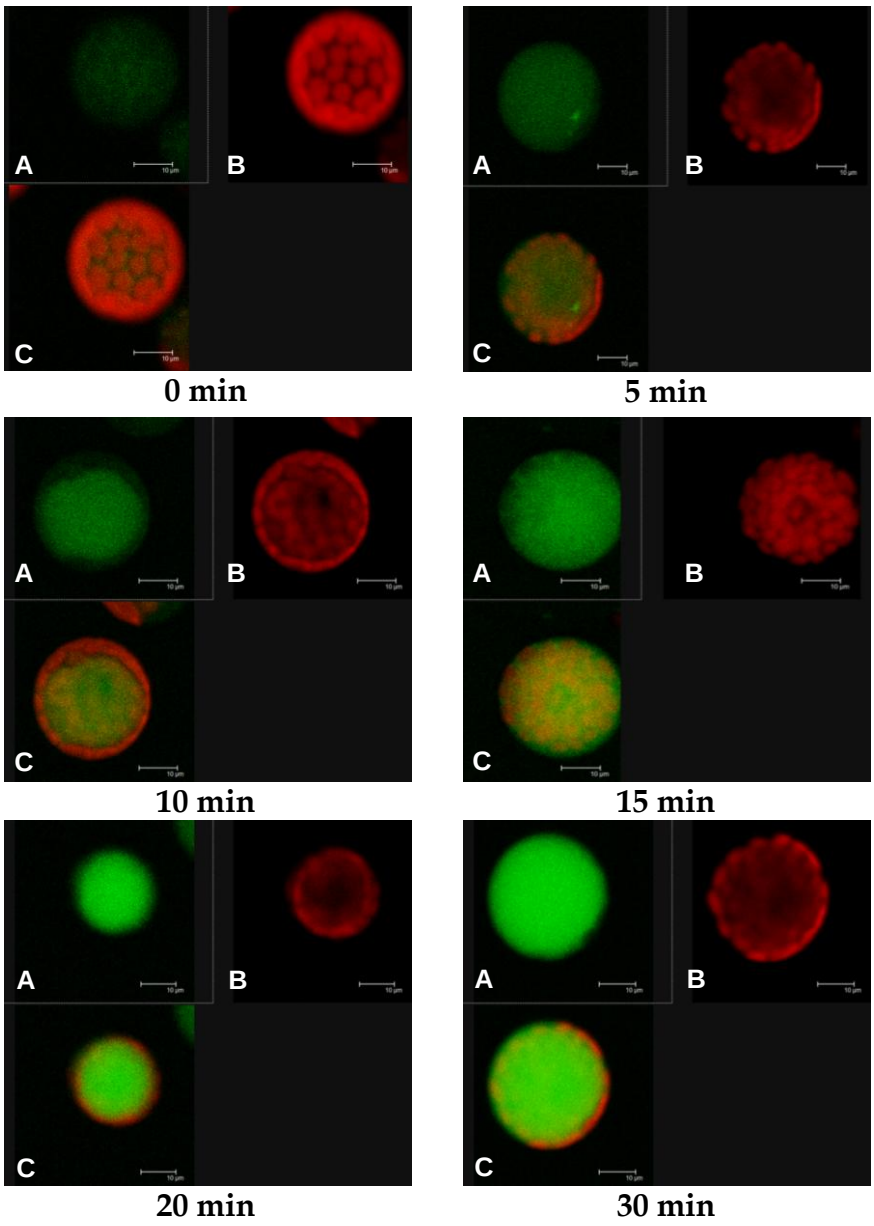

Figure 6.2. The pattern of NO production in SNP treated mesophyll protoplasts of pea during pre-illumination, as indicated by DAF-2DA fluorescence. Protoplasts were observed for DAF-fluorescence (A), or chlorophyll auto-fluorescence (B) or both (C). See section 3.9 of Materials and Methods for details. Experiments were repeated at least three times with similar results. Bar represents 10 μm.

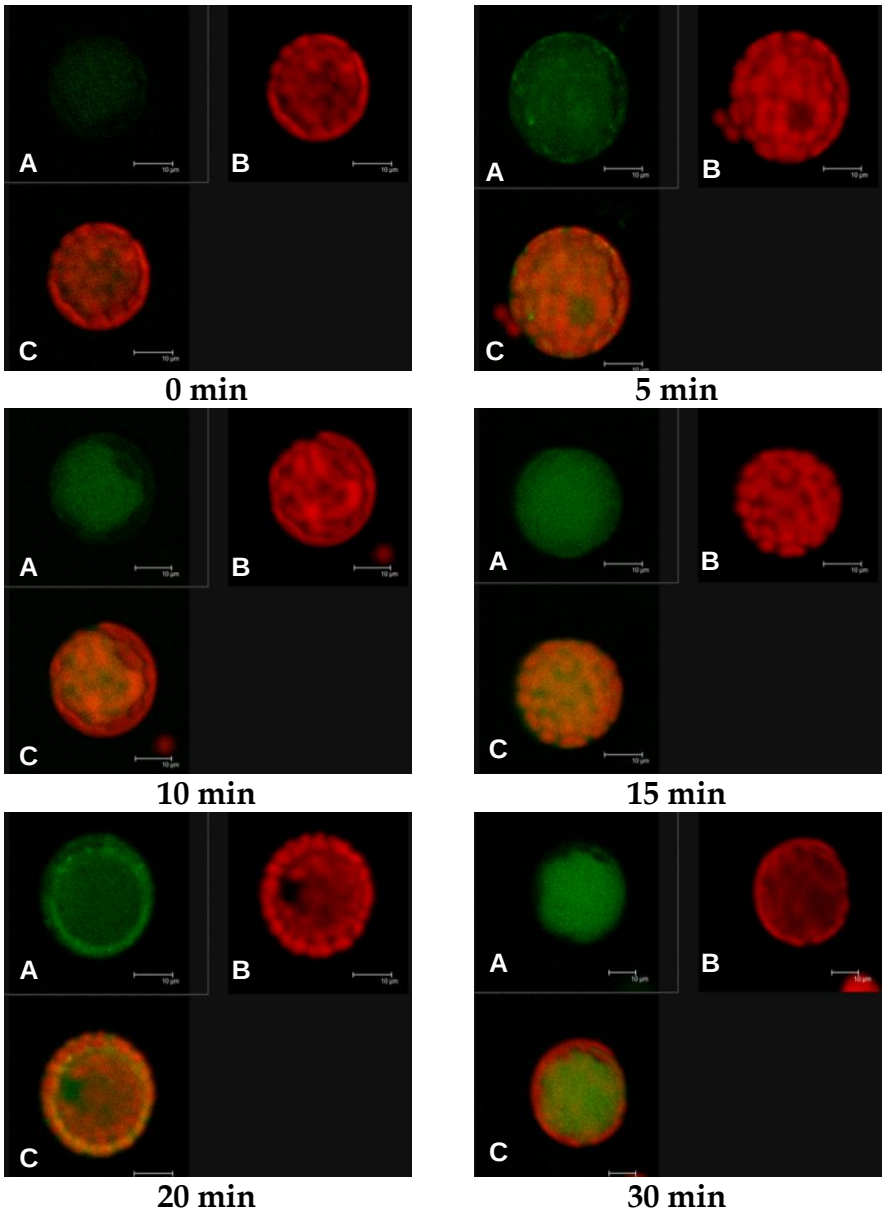

Figure 6.3. The pattern of NO production in SNP treated mesophyll protoplasts of pea during dark incubation, as indicated by DAF-2DA fluorescence. Protoplasts were observed for DAF-fluorescence (A), or chlorophyll auto-fluorescence (B) or both (C). See section 3.9 of Materials and Methods for details. Experiments were repeated at least three times with similar results. Bar represents 10 μm.

6.2.2. Time course analysis of NO effects on photosynthesis

For the time scan experiments, protoplasts were pre-illuminated/kept in dark for different durations (ranging from 0-20 min) in the absence or presence of SNP. The pre-illumination was carried at two different but low/moderate light intensities (50 and 150 µE m^{-2} s^{-1}), to facilitate the NO release. After the specified time points, the pre-illumination was stopped and the protoplasts were exposed to 700 µE m^{-2} s^{-1} light for the photosynthetic readings.

The rate of the photosynthesis did not change much (≤10%) over the time, up to 20 min, in the absence of SNP (Figure 6.4). In contrast, when protoplasts were treated with SNP during pre-illumination, their photosynthetic performance was severely decreased with time. The rate of photosynthetic O_2 evolution decreased by about 40% after 5 min and about 90% by 20 min of SNP treatment. Protoplasts pre-treated with SNP in dark showed the same pattern like control protoplasts, without much change. Pre-illumination with weak light (50 µE m^{-2} s^{-1}) was almost as effective as the light of 150 µE m^{-2} s^{-1}, indicating that SNP may not require high light intensities to release NO and decrease photosynthesis (Figure 6.4).

6.2.3. Effect of NO on photochemical activities of mesophyll protoplasts

A major question that needed to be answered was whether NO affects the photosynthetic carbon fixation or photochemical activities, or both. So, we tried to distinguish the effect of SNP on photochemical activities of intact protoplasts by monitoring three different photochemical reactions: BQ-dependent O_2 evolution (PSII-mediated), NO_2^- dependent O_2 evolution (mediated by PSI and PSII) and

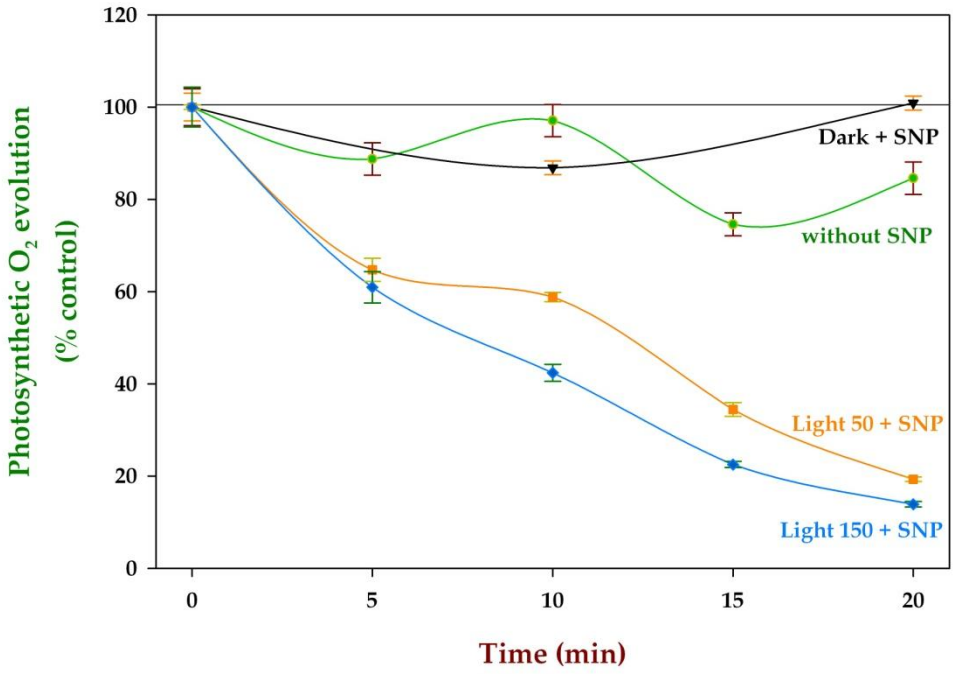

Figure 6.4. Pattern of changes in photosynthesis, with time in mesophyll protoplasts of pea, treated with or without 100 μM SNP. The protoplasts were pre-incubated with SNP either in dark or under of light 50 (Light 50) and 150 (Light 150) μE m^{-2} s^{-1} for different times. Aliquots were examined at specified time points for their rate of O_2 evolution. The rate of photosynthesis in the absence of SNP (control) at the beginning, i.e. zero time was 132 μmol O_2 mg^{-1} Chl h^{-1}. The photosynthetic rates within 5 min of illumination were considered.

HCO_3^- dependent O_2 evolution (reflects carbon assimilation capacity). During the measurements of PSII activity or whole chain (PSII + PSI) activity, the assay medium contained 2.5 mM glycolaldehyde (inhibitor of CO_2 fixation), to ensure that the observed O_2 evolution was due to photochemical activity and not due to carbon fixation.

The exposure of protoplasts to SNP caused a marked inhibition of $NaNO_2$ dependent O_2 evolution much more than that of BQ dependent O_2 evolution (Table 6.1). Treatment with SNP caused 45% inhibition in the rate of HCO_3^- dependent O_2 evolution, whereas the inhibition was 25% and 50% with BQ and NO_2^- respectively, in presence of SNP.

6.2.4. *In vivo* fast transients of chlorophyll a fluorescence in SNP treated protoplasts

The polyphasic rise of Chl *a* fluorescence transients in mesophyll protoplasts of pea after exposure to NO were studied at different time points (Figure 6.5). The protoplasts were pre-illuminated (50 µE m^{-2} s^{-1}) with or without SNP, for different durations (0-30 min). As a control, protoplasts were dark incubated for the same time points. After stipulated time intervals, samples were dark adapted and then OJIP transients were determined using Handy PEA (Hansatech Instruments, UK).

Figure 6.5 shows the typical Chl *a* fluorescence fast OJIP-transients, recorded from mesophyll protoplasts of pea. These kinetics of protoplasts were quite similar to kinetics of leaves, showing three distinct phases of the fluorescence rise from F_0 to F_P (~F_M). SNP treatment resulted in distinct changes in the phases of the OJIP

Table 6.1. Sensitivity of photochemical reactions of protoplasts to SNP treatment. The rates of oxygen evolution when electrons are transferred from H_2O to NO_2 (representing PSII and PSI activity), or when electrons are transferred from H_2O to BQ (indicates PSII activity, excluding PSI) are shown in comparison with the rates of HCO_3^- dependent O_2 evolution (indicating carbon assimilation). The protoplasts were pre-incubated with SNP for 5 min and then the photosynthetic rates within 5 min of illumination were considered.

	Photosynthetic O_2 evolution (μmol mg^{-1} Chl h^{-1})		
	no SNP	SNP (100 μM)	% inhibition
Control	146.0 ± 3.2	80.3 ± 3.7	45 %
Glycolaldehyde (2.5 mM)	0	0	-
Glycolaldehyde + BQ* (1 mM)	263.7 ± 8.6	197.3 ± 6.4	25 %
Glycolaldehyde + $NaNO_2$**(10 mM)	16.4 ± 0.4	8.2 ± 0.3	50 %

* Dependent on PS II alone

** Dependent on Ps II and PS I

Figure 6.5. Original traces of Chl *a* fluorescence (OJIP) recorded in mesophyll protoplasts of pea treated with 100 µM SNP in low light, for different time points. The OJIP transients were induced by a PPFD of 3000 µE m^{-2} s^{-1} with a HandyPEA (Hansatech). Fluorescence intensity is normalized to the value at the Fo. Before measurements protoplasts were dark adapted. These readings are means from three independent experiments done on a particular day and experiments were repeated at least on two different days with similar results.

transients and the typical shape of the Chl *a* fluorescence induction curves. The results demonstrated marked quenching of fluorescence during OJIP transients in SNP treated protoplasts (Figure 6.5). With increasing time of NO exposure, the fluorescence yield at J phase decreased only slightly, whereas phase I and P showed drastic decrease in fluorescence yield (Figure 6.6). Such decrease in F_M indicates a decrease in the reduced state of PQ pool and there by reduced electron transfer to PS I.

6.2.5. Effect of SNP on the maximal quantum efficiency (Fv/Fm)

The Fv/Fm values indicate the photochemical efficiency of PS II, which is a good indicator of photosynthetic performance. The control protoplasts showed an Fv/Fm value of 0.755. When protoplasts were dark incubated with SNP up to 20 min, there was not much change in their Fv/Fm values (Figure 6.7). However, when protoplasts were pre-illuminated in the presence of SNP, there was a marked decrease in the quantum efficiency (Fv/Fm) values with increasing time.

6.2.6. Effect of SNP on the structural and functional parameters derived from the JIP test

To further evaluate the effect of NO on the behavior of primary photochemistry of PS II, we analyzed the OJIP fluorescence transients depicted in Figure 6.5 using JIP test. The JIP test deduces the structural and functional parameters quantifying the photosynthetic behavior of the samples. Figure 6.8 shows the radar plot of the parameters derived from JIP test. The parameters of the control sample (untreated protoplasts) were taken as the reference values (=1) and the relative changes due to

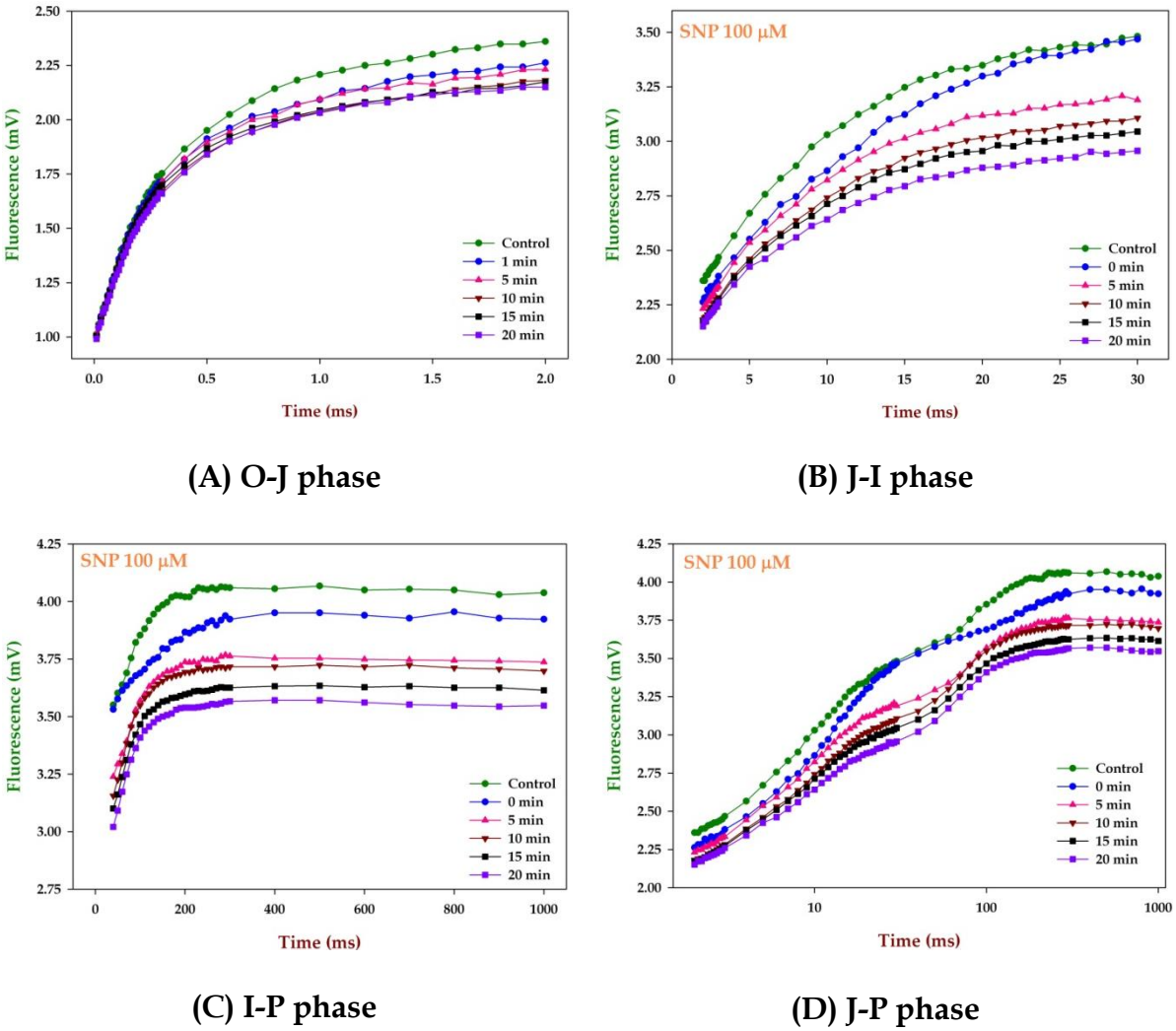

(A) O-J phase **(B) J-I phase**

(C) I-P phase **(D) J-P phase**

Figure 6.6. The OJIP fluorescence kinetics of the mesophyll protoplasts of pea, pre-illuminated with SNP for different time points. (A) O-J phase (B) J-I phase (C) I–P phase and (D) J-P phase. Normalization at F_0 (stand for fluorescence yield at 20 µs) was done. These readings are means from three independent experiments done on a particular day and experiments were repeated at least on two different days with similar results.

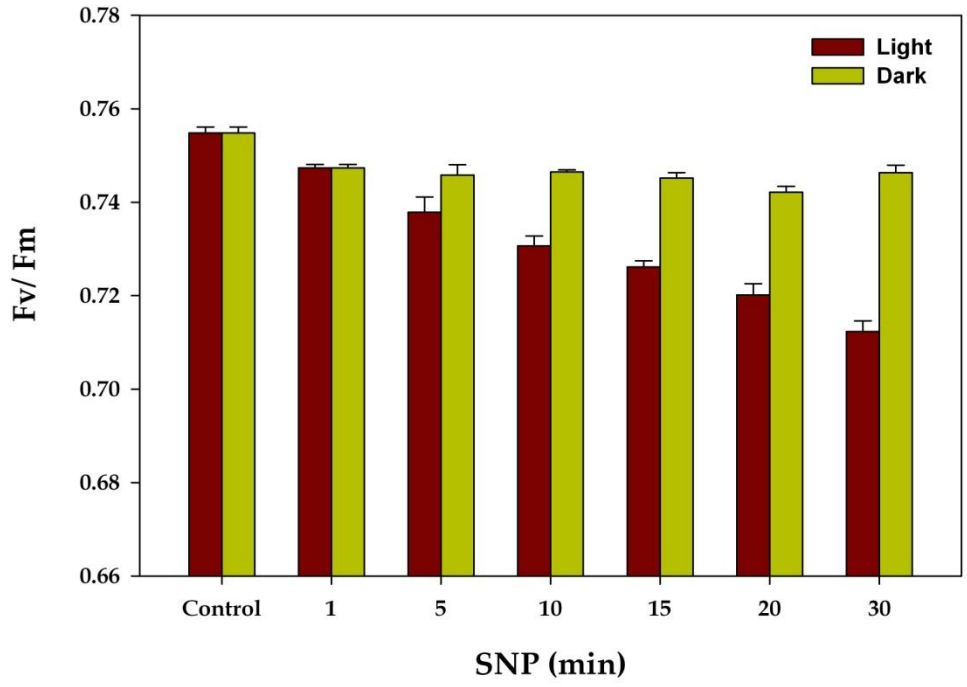

Figure 6.7. Changes in the quantum yield of photosynthetic electron transport (Fv/Fm) in mesophyll protoplasts of pea treated with 100 μM SNP either in light (50 μE m^{-2} s^{-1}) or dark for different time points. All the samples were dark adapted before taking the readings. Each value is a mean ± SE of three independent experiments, done with at least two samples for each measurement on a particular day.

SNP treatments in light were represented.

Our results show that the specific fluxes; absorption (ABS), trapping (TRo) and electron transport (ETo) per active PS II reaction centre did not show any change with SNP treatment. On other hand, the dissipation (DIo/RC) increased with increase in time of SNP treatment (Figure 6.8). The overall performance of PS II, assessed by performance indices [$PI_{(abs)}$ and $PI_{(csm)}$] showed marked decrease with time in protoplasts pre-illuminated with SNP (Figure 6.8). The contribution of RC/ABS (efficiency of light absorption) was very marginal in the PI decrease, as evident with the marginal decrease of RC/ABS in the radar plot.

The derived parameters can be visualized by means of dynamic energy pipeline leaf model of the photosynthetic apparatus, which deals with the phenomenological energy fluxes per cross-section (Figure 6.9). In the control protoplasts all the reaction centers were active (indicated as open circles). With the increase in time of NO exposure, the active reaction centers were converted to inactive reaction centers (indicated as closed circles), as evident with the decrease of RC/CSm (density of active PS II reaction centers) values. A decrease in the electron transport per cross section (ETo/CS) (note the decrease in size of blue arrow), ABS/CSm (yellow colored arrow) and TRo/CSm (cyan colored arrow) was observed after the treatment with SNP with time (Figures 6.8 and 6.9). A summary of changes in fluorescence parameters derived from the JIP test is given in a table (Table 6.2).

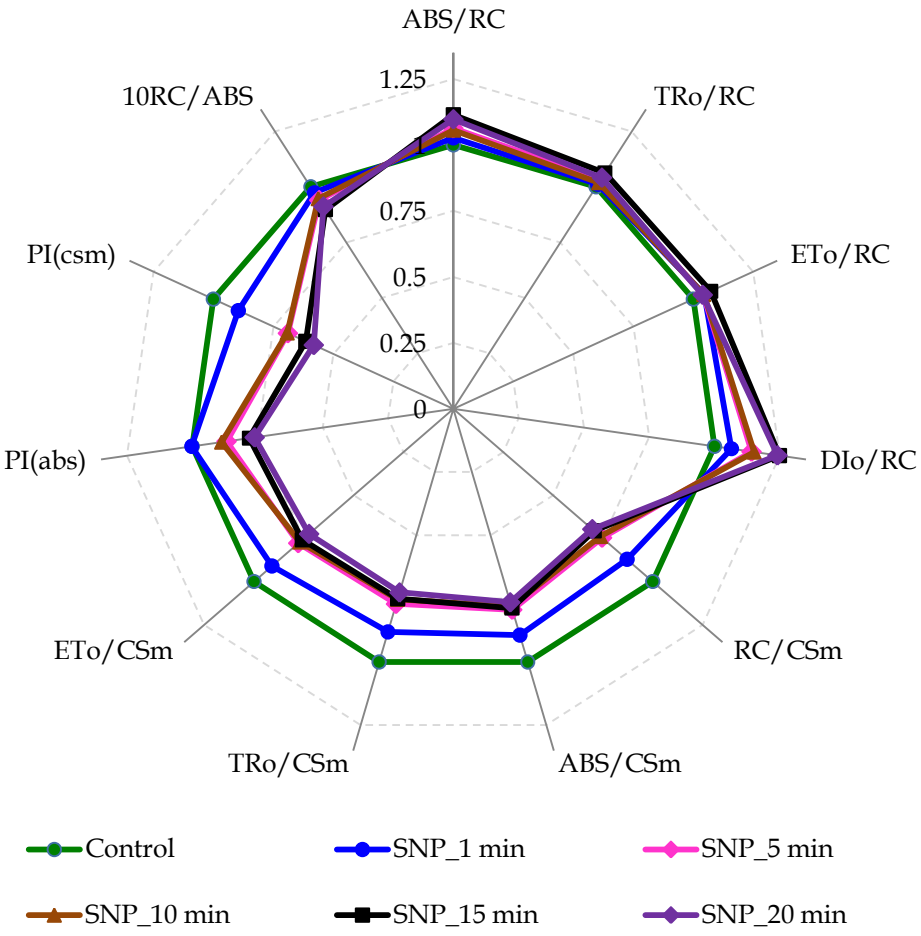

Figure 6.8. Radar plot of specific fluxes (ABS/RC, TRo/RC, ETo/RC), phenomenological fluxes (ABS/CS, TRo/CS, ETo/CS) and the performance indices, derived by the JIP-test from OJIP transients of Figure 6.5. The values are calculated relative to the control (without SNP), taken as 1. For description of the flux parameters, see Table 3.4 in Materials and Methods.

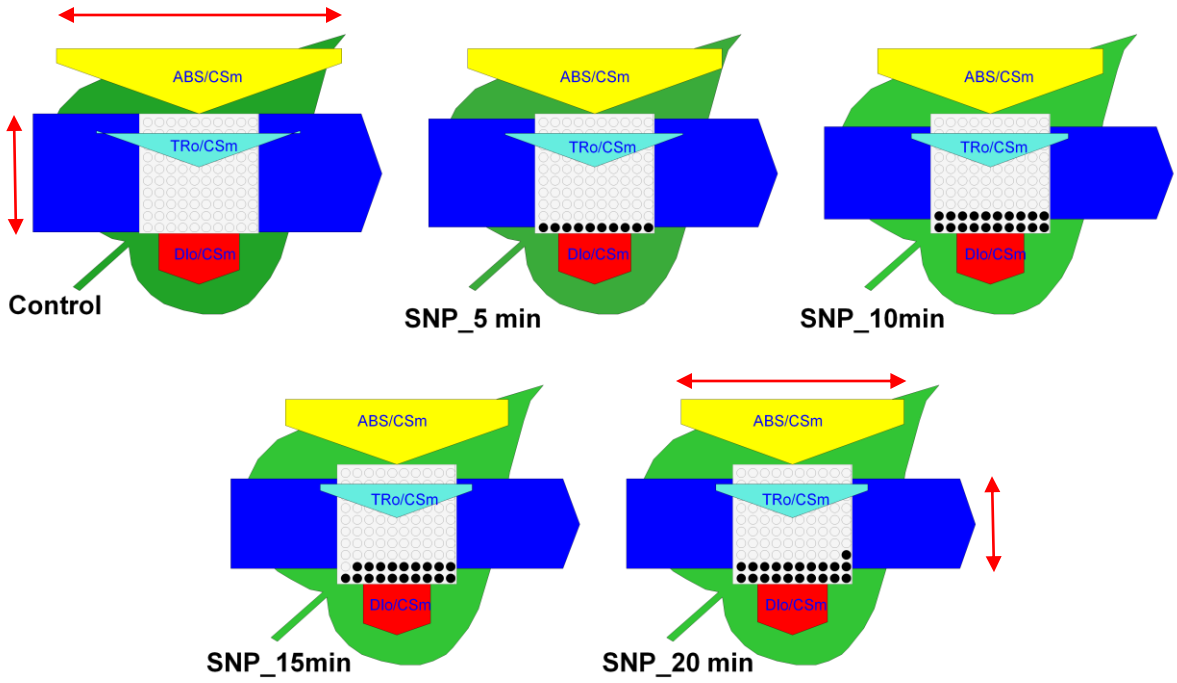

Figure 6.9. Energy pipeline models of phenomenological fluxes (per cross-section, CSm) in protoplasts exposed to 100 μM SNP for various time points. The decrease in absorption (yellow), trapping (cyan) and electron transport (blue), can be seen as changes in width of each arrow (red arrow= scale). Active reaction centers are shown as open circles and inactive reactive centers are shown as closed circles.

Table 6.2. Summary of chlorophyll fluorescence parameters derived by JIP test from the OJIP transients of the mesophyll protoplasts of pea, pre-incubated with or without SNP in light (50 μE m^{-2} s^{-1}) at 0 and 20 min. The data summarized here represents the Figures 6.8 and 6.9.

		Control	**20 min pre-incubation**
Fluorescence Parameter		**No SNP**	**100 μM SNP**
Quantum efficiency of Ps II	Fv/Fm	0.755 ± 0.001	0.712 ± 0.002
Specific fluxes per active reaction center (RC)	ABS/RC	2.79 ± 0.01	3.03 ± 0.03
	TRo/RC	2.01 ± 0.01	2.07 ± 0.03
	ETo/RC	1.17 ± 0.01	1.20 ± 0.02
	DIo/RC	0.78 ± 0.01	0.96 ± 0.00
Phenomenological fluxes per cross section (CSm)	ABS/CSm	738 ± 13	517 ± 8
	TRo/CSm	2058 ± 41	1564 ± 24
	ETo/CSm	1483 ± 31	1067 ± 17
Density of active PS II RC	RC/ CSm	866 ± 13	621 ± 8
Efficiency of light absorption	RC/ABS	3.59 ± 0.02	3.30 ± 0.03
Photosynthetic performance indices	$PI_{(abs)}$	13.00 ± 0.29	9.97 ± 0.52
	$PI_{(csm)}$	26717 ± 386	15553 ± 634

6.3. DISCUSSION

The previous Chapter (No. 5) described that elevated levels of NO could inhibit photosynthesis in mesophyll protoplasts of pea. As per the previous reports, NO could bind to several sites in PS II and inhibit electron transfer (Schansker et al., 2002; Takahashi and Yamasaki, 2002; Wodala et al., 2008). The experiments carried out on isolated chloroplasts, thylakoids and intact leaves using different NO donors reported contradictory results (Review: Hayat et al., 2010). The effects of NO on mesophyll protoplasts photosynthesis however were not investigated so far. The results from this chapter based on the studies on photosynthetic electron transport and non-invasive chlorophyll *a* fluorescence measurements, clarify the situation, and suggests that both PS II and PS I are possible targets of NO action.

6.3.1. The release of NO on exposure to SNP of mesophyll protoplasts

Previous studies suggested that SNP solution is photosensitive and the presence of light is essential for the release of NO from SNP (Wang et al., 2002; Floryszak-Wieczorek et al., 2006). Our studies, using confocal laser scanning microscopy, indicated clearly that NO production occurred when protoplasts were incubated with SNP in light, where as the dark treated protoplasts showed only very small increase in fluorescence (Figure 6.1 to 6.3).

Among the cellular compartments, cytosol showed an early increase in fluorescence, but the NO accumulation was quite pronounced in the vicinity of chloroplasts. Several earlier studies showed NO production in the vicinity of chloroplasts in response to different stress conditions, using NO sensitive

diaminofluorescein probes (Foissner et al., 2000; Gould et al., 2003; Arnaud et al., 2006). Along with these reports, our results complement the view that chloroplasts are one of the possible sources of NO (Jasid et al., 2006; Gas et al., 2009).

6.3.2. NO affects the photochemical reactions of protoplasts

Under several kinds of environmental stress, PSII is the major target of oxidative damage in plants (Aro et al., 2005; Nishiyama et al., 2006). As per our results (Figure 6.4 and Table 6.1), exposure to SNP restricted the electron transport through both PS II and I. This is perhaps the first report on the extreme sensitivity to NO of both photosystems.

The interpretation of SNP mediated effects should be considered with caution, because SNP may also release CN^- apart from NO^+ in light (Feelish, 1998), and CN^- can inhibit photosynthesis at various levels (Wishnick and Lane, 1969; Forti and Gerola, 1977). However, accumulation of CN^- requires considerable time, as significant CN^- levels in treated samples were detected only after 5 h incubation with 5 mM SNP (Bethke et al., 2006; Ederli et al., 2006). Our experiments used only 0.1 mM SNP, and the exposure was always <20 min (Figure 6.4 and Table 6.1). We are therefore confident that SNP effect is due to mostly by NO, as the NO scavenger cPTIO, could reverse completely the inhibition of photosynthesis by SNP (see Figure 5.2 in Chapter 5). Our results also support the use of cPTIO in NO related studies (Ederli et al., 2006; Zhao et al., 2009; Ma et al., 2010).

NO and molecules such as fluoride anions, compete with bicarbonate and can bind reversibly to the nonheme iron (II) (Goussias et al., 2002). Experiments

with isolated thylakoids indicated that NO binding could slow down the rate of electron transfer, particularly between Q_A and Q_B (Diner and Petrouleas, 1990). Other studies have proven that NO can reversibly inhibit electron transfer by binding to several sites in PSII such as the Y_D-Tyr residue of the D2 protein (Sanakis et al., 1997), and the manganese (Mn) cluster of the water-oxidizing complex (Schansker et al., 2002).

6.3.3. NO affects the Chl *a* fluorescence parameters photochemical efficiency and functional parameters of PS II of protoplasts

The mesophyll protoplasts normally exhibited a typical polyphasic rise of fluorescence induction (OJIP transients) (Figure 6.5), similar to that described previously for plants, green algae and cyanobacteria (Sunil et al., 2008; Antal et al., 2009). The SNP treatment caused marked changes not only in the rates of photochemical O_2 evolution (Table 6.1), but also changed PS II photochemistry, as evident with the decreased intensity of fluorescence at J, I and P phases in the OJIP transient with increase in time of NO exposure (Figure 6.5).

The slight decrease in fluorescence at O-J phase with SNP treatment in the present work (Figure 6.6A), may be a reflection of the reduction of the PS II acceptor side i.e. reduction of primary quinone acceptor Q_A to Q_A^- (Schansker et al., 2005). The J-I phase represents PQ pool and showed that there is a reduced electron flow in the electron transport chain (from Q_A to Q_B to Q_B^{2-}) with SNP treatment (Figure 6.6 B). The I-P phase represents the ferredoxin pool size of final electron acceptors on the reducing side of PS I (Tsimilli-Michael and Strasser, 2008). As shown in the

Figure 6.6C, the pool size declined considerably with increasing NO exposure. Thus our result support the suggestion that partial inhibition of PS II by NO is due to impaired steady-state electron transport *in vivo* (Wodala et al., 2008).

The Fv/Fm values, being the result of photochemical quenching, are sensitive indicators of efficiency of PS II performance (Mehta et al., 2010). Our results demonstrate that the elevation of internal NO (by SNP) decreased the Fv/Fm values of protoplasts (Figure 6.7). Such inhibition was not observed in the protoplasts treated in dark. Previous fluorescence studies provided contradictory results on changes induced by NO. In isolated chloroplasts, NO didn't affect Fv/Fm; while in intact leaves, NO decreased its values considerably (Takahashi and Yamasaki, 2002; Yang et al., 2004; Wodala et al., 2008). The part of the discrepancy may be due to different NO donors and experimental conditions. The decrease in Fv/Fm values with SNP treatment is corroborated further by the sensitivity of photochemical reactions to NO (Table 6.1). Taken together, these data provide strong *in vivo* evidence that a partial inhibition of PSII by NO is indeed the cause of impaired steady-state electron transport *in vivo*.

The JIP test quantifies the stepwise flow of energy through PSII (Strasser and Strasser, 1995; Tsimilli-Michael and Strasser 2008). The changes in the functional parameters due to NO treatment as observed by radar plots showed that there was a significant increase in the energy dissipation (DI_0/RC) (Figure 6.8), which depicts that NO caused the impairment of electron transport and increased the energy dissipation non-photochemically, mostly as heat (Strasser et al., 2000). The decrease

in electron transport (ETo) per excited cross section as observed in dynamic leaf models (Figure 6.9) suggests that the elevated NO levels with in the cell resulted in increased numbers of inactive RCs in PSII (Strasser et al., 2004).

Performance index (PI) is a very sensitive index for stress and is used widely to compare the whole primary photochemical reactions (Strasser et al. 2000). The PI is the combined measurement of the density of RC, maximum energy flux reaching PS II reaction centers and the electron transport (Chen and Chang, 2009; Oukarroum et al., 2009). The decrease in ETo/CSm and increase in DIo/CSm in SNP treated protoplasts led to a marked decrease in performance indices like $PI_{(abs)}$ and $PI_{(csm)}$ (Figure 6.8), which suggests that the overall performance of PSII photosynthetic machinery in these protoplasts decreased with NO treatment.

In conclusion, elevated levels of NO decreased the efficiency of photochemical reactions (both PS II and PS I). In addition, NO was shown to decrease the photosynthetic performance indices and increased the dissipation per RC due to inactivation of reaction center complexes with prolonged exposure of NO. Taken together, these findings provide further evidence on the inhibitory effect of NO on photosynthetic efficiency in plants.

6.4. CONCLUSIONS

1. The amount of NO produced from SNP in light treated protoplasts was much more than that of dark pretreated samples and such elevated levels of NO possibly led to further inhibition of photosynthesis with time.

2. The increased amount of NO in the cell caused marked inhibition of photochemical reactions. Both PS II and PS I electron transport were sensitive. Taken together with the results in Chapter 5, we suggest that NO exerts a direct effect on photochemical activities.
3. Elevated NO decreased the fluorescence yield during the OJIP transients with time, and these fluorescence kinetics also pointed the inhibition of electron flow at oxidizing side of PS II.
4. Elevation of NO decreased the maximal quantum efficiency of SNP treated protoplasts, particularly electron transport at the acceptor side of the PS II, reflecting the changes in the efficiency of the photochemical reactions, which is an indicator of photosynthetic performance.
5. NO decreased the photosynthetic performance of protoplasts as indicated by the parameter PI_{abs} and increased the non-photochemical energy dissipation (DIo/RC). A marked decrease in the absorption (ABS) and electron transport (ETo) per cross section suggested inactivation of reaction center complexes with prolonged exposure of SNP.

*****

Chapter 7

Analysis and identification of homozygous *Arabidopsis thaliana* lines over-expressing the genes of glutathione metabolism

Chapter 7

Analysis and identification of homozygous *Arabidopsis thaliana* lines over-expressing the genes of glutathione metabolism

7.1. INTRODUCTION

Environmental stress is the major limiting factor in plant productivity. Plants exposed to environmental stress show diminished photosynthetic metabolism and increased photorespiration, and dissipation of excitation energy, particularly at photosystem II. Although these processes are protective, they still lead to increased formation of ROS, such as superoxide, singlet O_2, H_2O_2 and NO (Ort and Baker, 2002; Asada, 2006). The levels of these radicals are kept minimal by combined efforts of antioxidants (ascorbate and glutathione) and the associated antioxidant enzymes (Dietz et al., 2003; Ball et al., 2004; Foyer and Noctor, 2005).

Glutathione (GSH) is a sulfur containing tripeptide (Glu-Cys-Gly) and is a major non-protein thiol in many organisms, including plants. Besides ascorbate, GSH is considered to be an important intracellular antioxidant metabolite in plants and occurs predominantly in reduced form (GSH). Both Asc and GSH are localized in most of the cell compartments like chloroplasts, mitochondria, cytosol and peroxisomes. Besides the total level of Asc and GSH in the cell, the ratio between reduced and oxidized forms of these molecules play an important role in the activation of various defense mechanisms.

Being crucial for redox homeostasis, both GSH and ascorbate are implicated in stress signaling and regulation of numerous developmental processes (Miller et

al., 2007; Rouhier et al., 2008; Murata et al., 2010; Foyer and Noctor, 2011). Besides these non-enymatic antioxidants, there are several enzymatic antioxidants like GR, SOD, CAT, APX, play significant role in during plant defense. GR is a crucial enzyme of the ASH-GSH cycle to sustain the reduced status of GSH and protect against ROS impart stress tolerance to plants (Mullineaux et al., 1994; Ding et al., 2009). GSH is also an important pool for sulfur storage and the regulation of sulfur metabolism (Kopriva and Rennenberg, 2004; Herschbach et al., 2010).

The over-expression studies and the characterization of a number of *Arabidopsis* mutants during recent years highlighted the important role of glutathione metabolism for tolerance towards environmental stress (Foyer and Noctor, 2009; Liedschulte et al., 2010; Mhamdi et al., 2010; Noctor et al., 2011). Several mutants, *cadmium-sensitive mutan*t (*cad2*, Cobbett et al., 1998), *regulator of APX2-1* (*rax1*, Ball et al., 2004), and *phytoalexin-deficient2* (*pad2*, Parisy et al., 2007), all containing mutations in the gene *GSH1* (encoding γ-glutamylcysteine synthetase, the first enzyme of GSH biosynthesis) reaffirmed the significance of GSH biosynthesis during stress conditions. These mutants showed 20–50% of total glutathione compared to wild-type plants and grew normally with no apparent difference from the wild-type phenotype. However, these plants had significantly increased sensitivity to stress conditions.

In the present study, we have characterized the lines of *Arabidopsis thaliana* plants over-expressing *E. coli* γECS (equivalent of higher plant *GSH1*) in cytosol or chloroplast (hereafter labeled as, **"ggscyt"** and **"ggschp"**) or GR in cytosol (**GRcyt**).

These lines were developed through floral dip method using Agrobacterium based transformation, in the laboratory of Prof. Lise Jouanin (INRA, Versailles, France). The experiments were initiated with T1 seeds of 15 lines of GRcyt and 10 lines each of ggscyt and gshchp (*see Table 3.1,* Materials and Methods). The characterization was done on the basis of metabolite assays and transcript analysis of *GSH1* and *GR* genes. Further analysis was continued to isolate homozygous T4 lines, using kanamycin selection for segregation.

7.2. RESULTS

7.2.1. Biochemical and molecular characterization of *Arabidopsis* tranformants

The T1 seeds were sown on soil to get the T2 plants and they were grown, in controlled environment growth chambers at 25 °C in short days (8h), at an irradiance of 200 μE m^{-2} s^{-1}.

7.2.1.1. Characterization of ggschp plants

After 4 weeks, leaf samples (100 mg FW, 1-2 leaves) were collected from the plants and rapidly frozen in liquid nitrogen. Among the 10 lines of ggschp plants (*see Table 3.1* Material and Methods); four lines (ggschp2, 3, 4 and 6) showed substantially higher (2-3 fold) total glutathione (GSH+GSSG) than wild type control plants, while the lines 1 and 5 showed about 1.5 fold increase. All other lines had levels similar to wild type. The six lines, which showed at least 1.5, fold higher GSH content were used for further assays and selection.

Samples were collected from 3 individual plants of each line and were subjected to GSH assay. Three plants derived from line 2 (named 2A, 2B, 2C) and

one plant from line 6 (named 6A) had about 2-fold higher GSH than that of wild type plants and lines 3B, 4B, and 4C had up to 1.5-fold GSH (Figure 7.1). All the plants from line 1 and 5 showed GSH levels similar to wild type plants.

***Expression of GSH1 transcript in ggschp plants*:**

Total RNA was isolated from the leaves of 4 weeks-old plants. Reverse transcriptase polymerase chain reaction (RT-PCR) was carried out to confirm the expression and level of the transformed bacterial γECS (*GSH1*) transcript. The plants from all the three lines of ggschp2 exhibited high levels of expression of the *GSH1* transcript. Thus the patterns of the GSH assay in the selected T2 lines were quite consistent with the expression patterns of *GSH1* transcript (Figure 7.2). *Actin2* transcript was used as a loading control.

7.2.1.2. Characterization of ggscyt plants

Among the 10 lines of ggscyt, seven lines (1, 3, 4, 5, 8, 9 and10) had 2-4 fold higher total GSH levels, that that of wild type plants. The highest levels of GSH were in line 1 and 3 (3.5 to 4 fold). and all other lines showed about 2-3-fold increase in total GSH content (lines 4, 5, 8, 9 and 10).

The ggscyt lines that showed higher GSH levels were subjected to another round of GSH assay from 3 individual plants per line. Two plants derived from line 1 (named 1A, 1B) and one plant each from lines 3, 9 (3B and 9C) had about 3 to 5-fold GSH when compared to wild type plants. The plants 3A, 3C and the three plants from each line of 4, 5, 8, 9A, 9B, 10A, 10B had 2-3 fold glutathione (Figure 7.3).

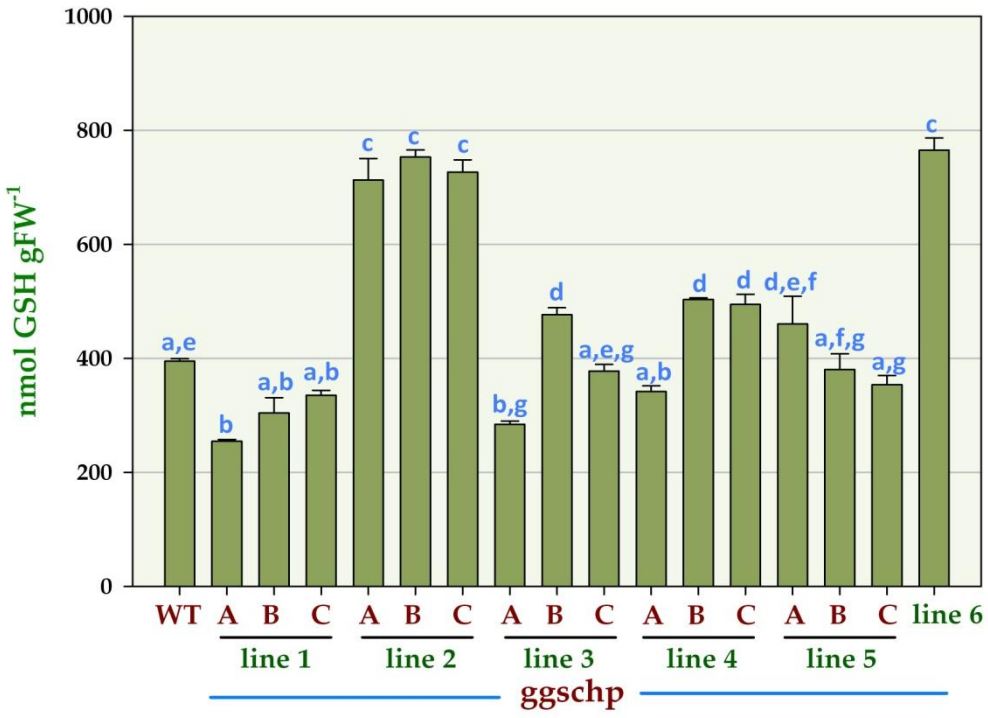

Figure 7.1. The foliar GSH content in the leaves of T2 lines of transformed *Arabidopsis* expressing *GSH1* (transcript encoding *E. coli* γECS) in chloroplast; The alphabets represent the individual plants with in the corresponding line and the numbers represent the identity of line (read as ggschp). Data are means ± SD of three independent assays. Different letters represent values that are statistically different (Student-Newman-Keuls ANOVA test, $P < 0.05$).

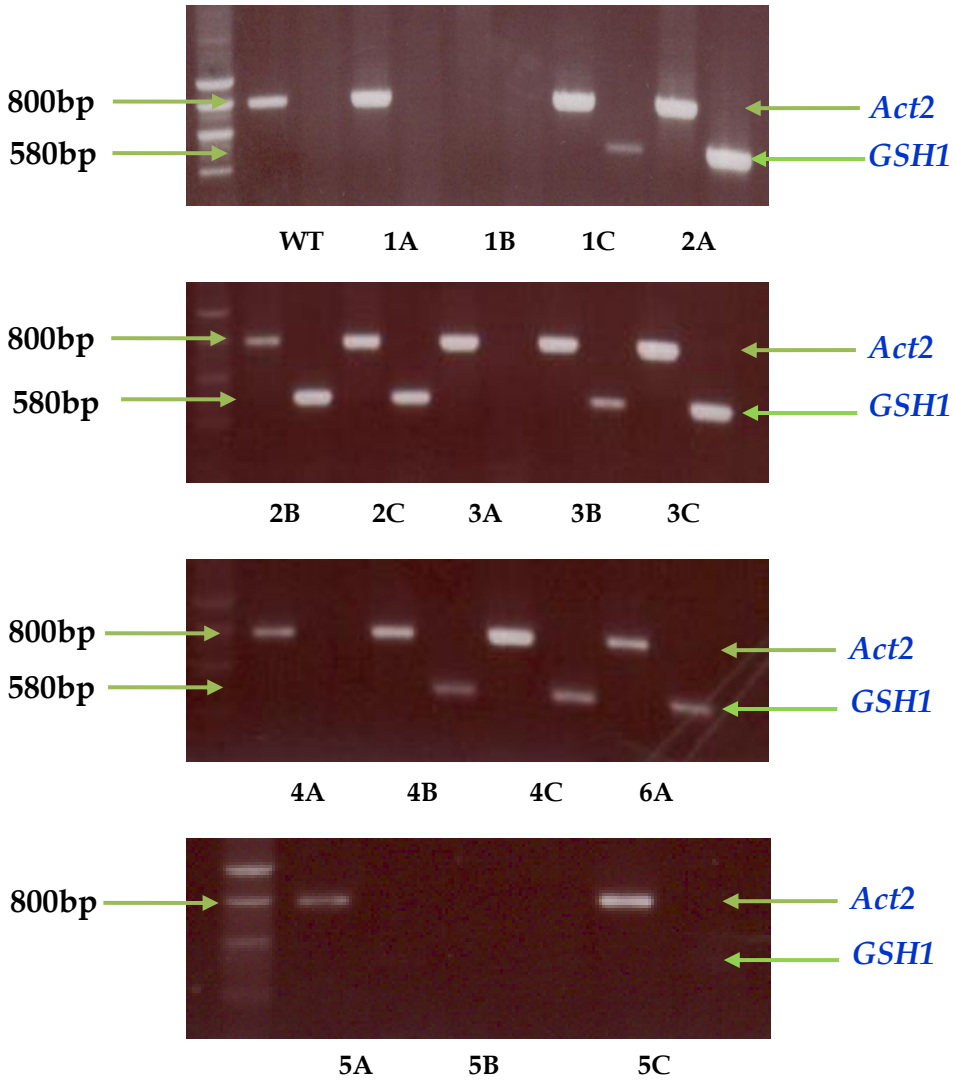

Figure 7.2. RT-PCR expression profile of *GSH1* (transcript encoding *E. coli* γECS) in the transgenic T2 lines, over-expressing the gene in chloroplasts. *Actin2* was used as internal control. The numbers represent the identity of line (read as ggschp). The lane on extreme left represents the smart ladder (Eurogentec, 200-10000bp).

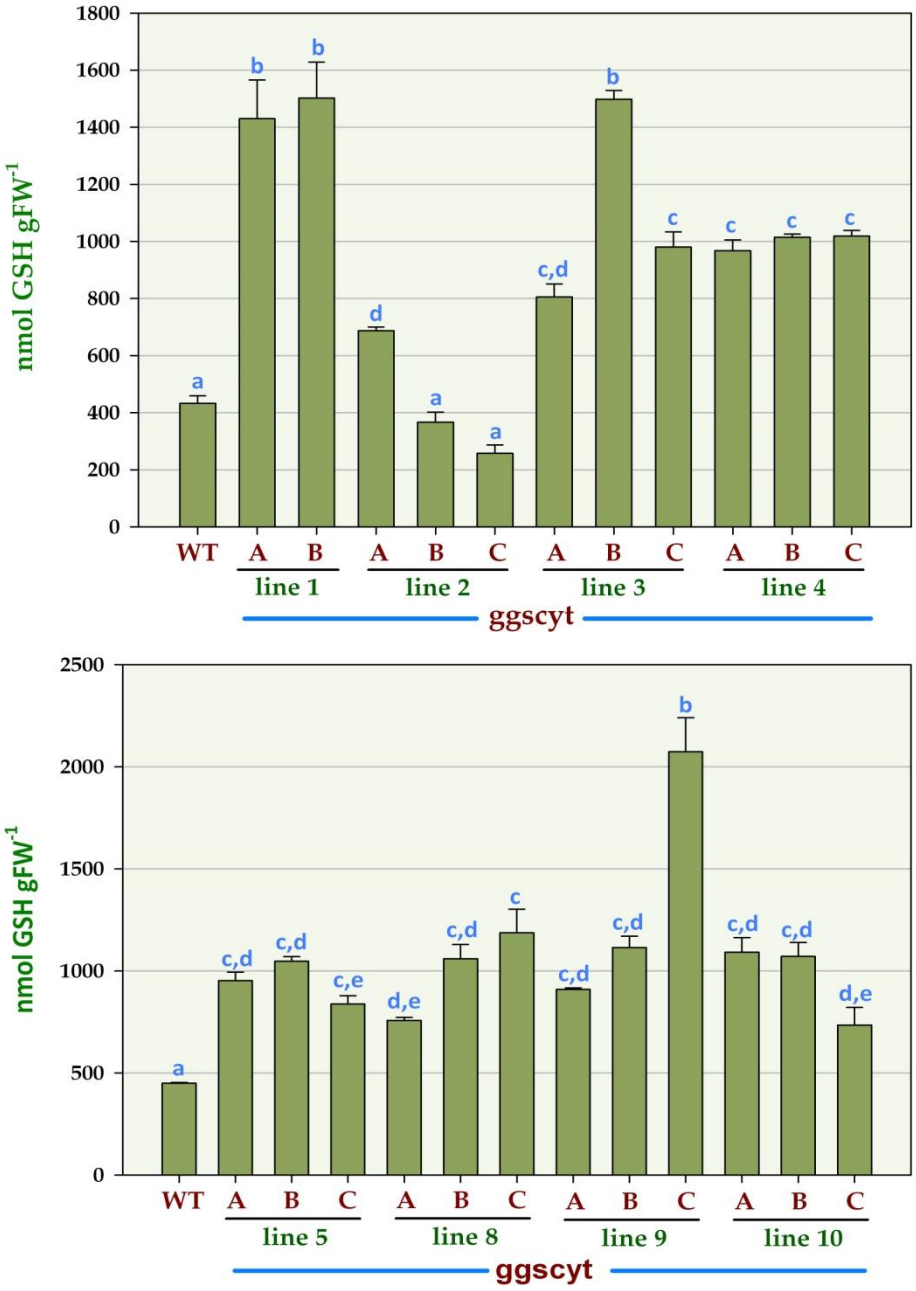

Figure 7.3. The foliar GSH content in the leaves of T2 lines of transformed *Arabidopsis* expressing *GSH1* (transcript encoding *E. coli* γECS) in cytosol; The alphabets represent the individual plants with in the corresponding line and the numbers represent the identity of line (read as ggscyt). Data are means ± SD of three independent assays. Different letters represent values that are statistically different (Student-Newman-Keuls ANOVA test, $P < 0.05$).

***Expression of GSH1 transcript in ggscyt plants*:**

The plants from lines of ggscyt1, 3, 4, 5, 8 and 10 exhibited higher levels of expression corresponding to the introduced *E.coli GSH1* gene (Figure 7.4). The expression patterns obtained by RT-PCR were well complimented with the results obtained from biochemical analysis. For example, the absence of expression of *GSH1* transcript in plants 2B and 2C plants were similar to the wild type and were quite similar to the respective total GSH levels (Figure 7.3).

7.2.1.3. Characterization of GRcyt plants

Out of the 14 GRcyt independent lines, four lines had about 3-4 fold GR activity (1, 2, 5 and 12) than that of wild type plants. Line 12 showed maximum GR activity (4056 nmol NADPH gFW^{-1} min^{-1}). All other lines (lines 4, 7, 8, 9, 11, 13, 14, 15 and 16) showed foliar GR activity similar to the wild type plants.

Individual plants from the lines that showed higher GR activity (line 1, 2, 5 and 12) were subjected to another round of GR assay. Differential activities were observed from the plants derived from lines 1, 2 and 5; whereas all three plants from line 12 had higher GR activities. Plants GRcyt2A and 5A activity is similar to wild type activity. Highest activity (about 8 fold) was observed in plant GRcyt1A and GRcyt12C showed about 5-fold increase in the GR activity (Figure 7.5).

***Expression of GR transcript in GRcyt plants*:**

The plants from the lines of GRcyt1 and GRcyt12 exhibited good levels of expression corresponding to the introduced *E.coli GRcyt* gene, whereas lines from GRcyt2 and GRcyt5 showed differential expression (Figure 7.6). Highest fold of

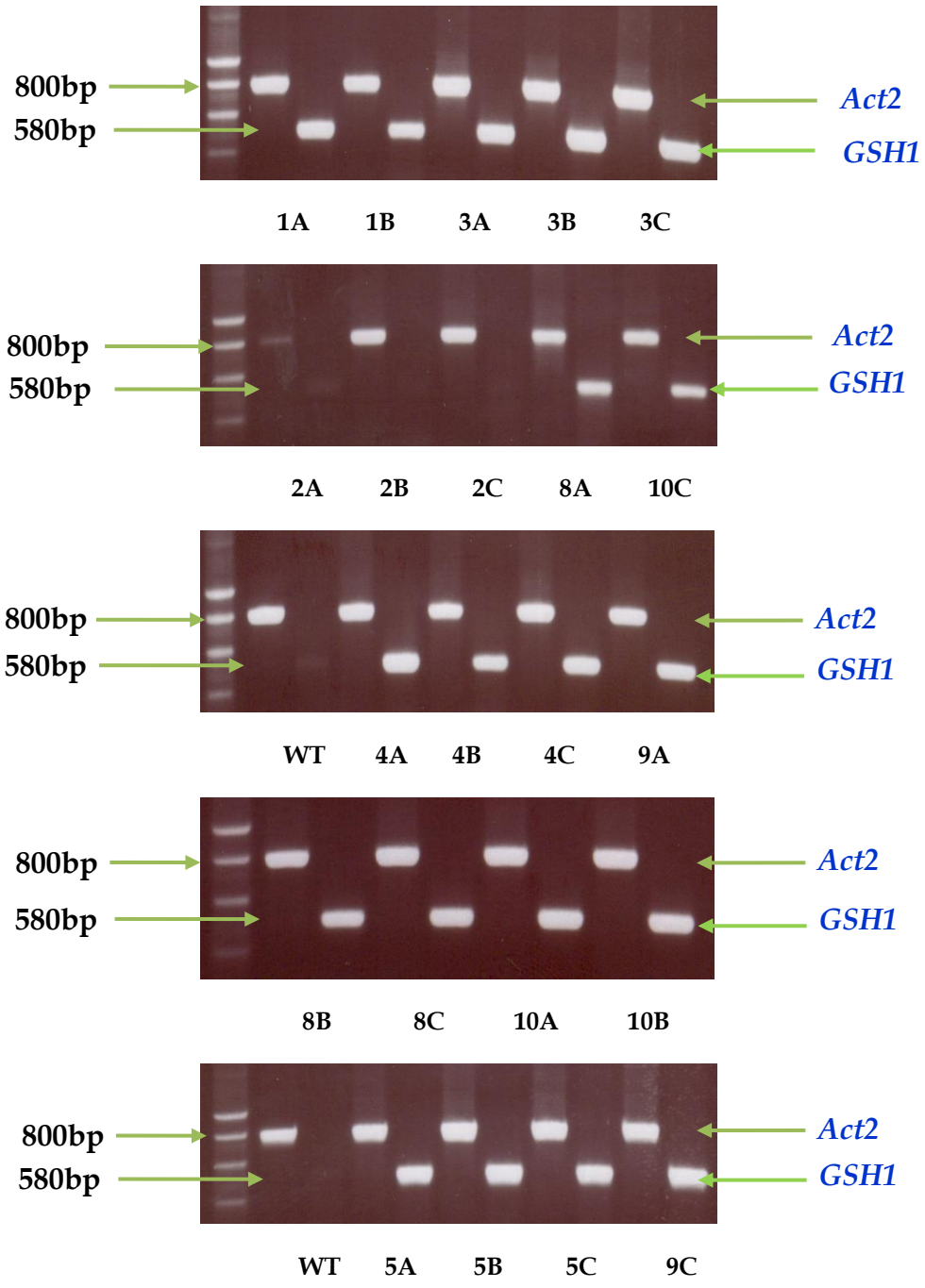

Figure 7.4. RT-PCR expression profile of *GSH1* (transcript encoding *E. coli* γECS) in the transgenic T2 lines, over-expressing γECS in cytosol. *Actin2* was used as internal control. The numbers represent the identity of line (read as ggscyt). The lane on extreme left represents the smart ladder (Eurogentec, 200-10000bp).

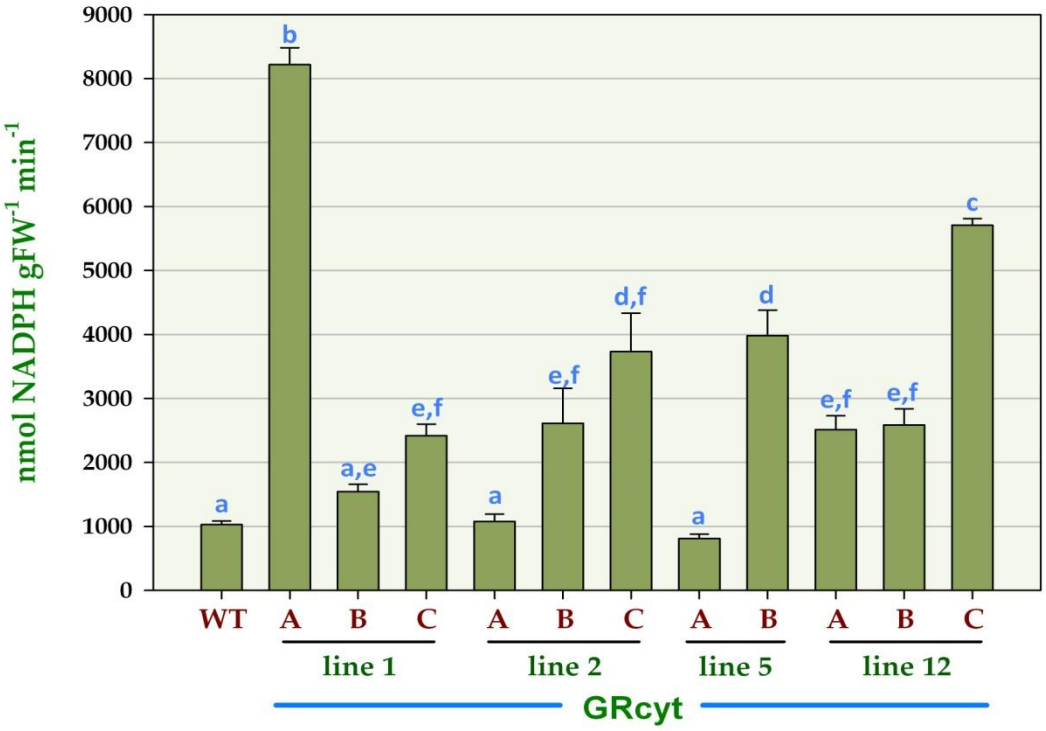

Figure 7.5. The foliar GR activity in the leaves of T2 lines of transformed *Arabidopsis* expressing *E.coli* GR gene in cytosol. The alphabets represent the individual plants with in the corresponding line and the numbers represent the identity of line (read as GRcyt); Data are means ± SD of three independent assays. Different letters represent values that are statistically different (Student-Newman-Keuls ANOVA test, $P < 0.05$).

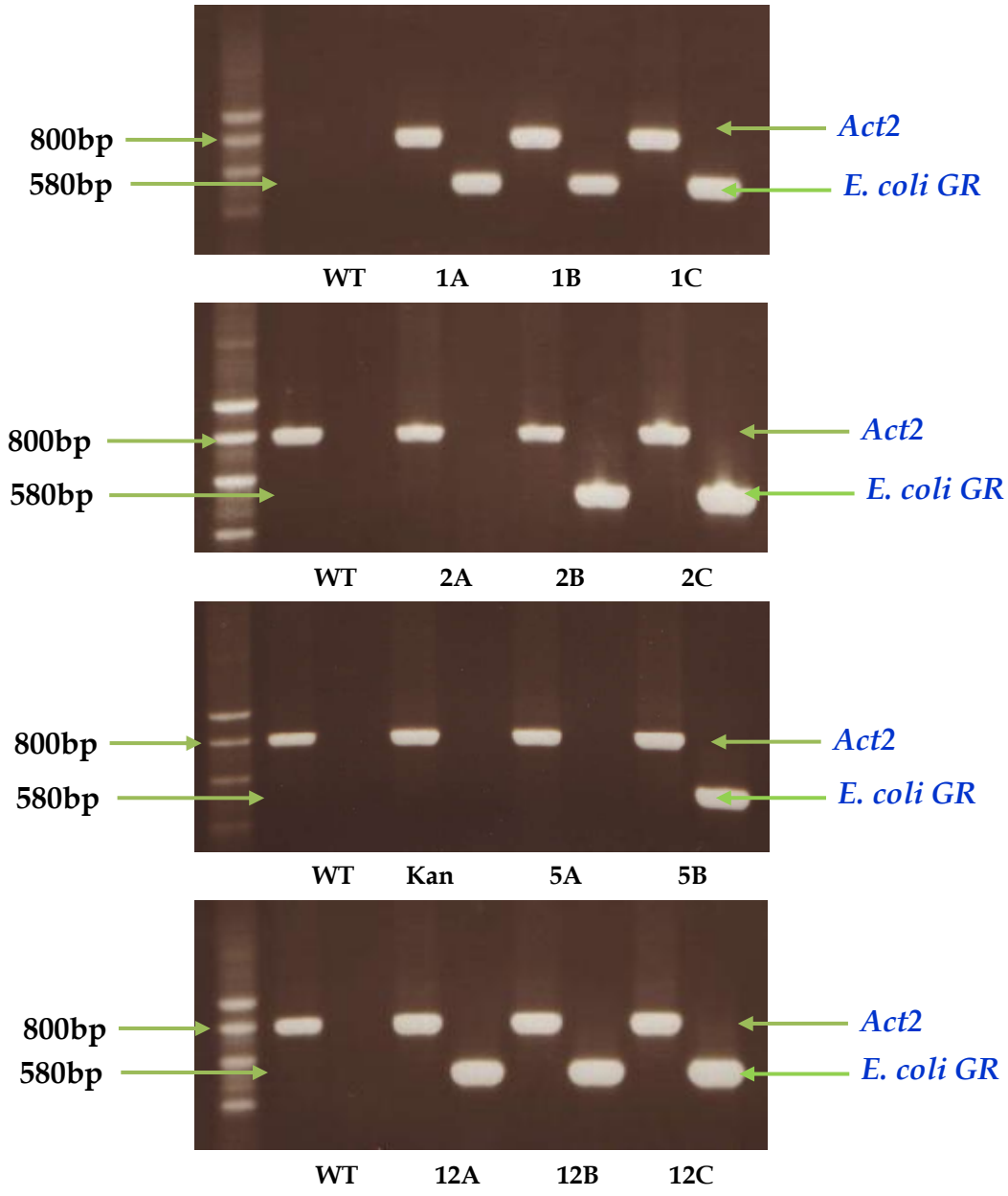

Figure 7.6. RT-PCR expression profile of GR (transcript encoding *E. coli* GR) in the transgenic T2 plants, over-expressing GR in cytosol. *Actin2* was used as internal control. WT= wild type; Kan= plant with empty vector and the numbers represent the identity of line (read as GRcyt). The line on extreme left represents the smart ladder (Eurogentec, 200-10000bp).

expression was observed in GRcyt2C and GRcyt12C. The expression patterns and the band intensities obtained by RT-PCR were in agreement with the enzyme activities obtained from the biochemical analysis (Figure 7.5). In plants over-expressing GR, plants 2A and 5A showed no expression of GR transcript and the GR activity of these plants were similar to the activities of wild type plants.

7.2.2. Selection and identification of homozygous T4 lines

The progeny obtained from T1 transgenic plants were named as T2. T2 plants were checked for integration of foreign gene by counting ratio of the number of tolerant plants to the number of non-tolerant plants on selection medium with kanamycin. The non-transgenic segregants were bleached and stunted (kanamycin sensitive, Kan^S), where as the transgenics plants were green and healthy (kanamysin resistant, Kan^R). According to Mendel's law, the copy number of T-DNA can be determined based on the segregation pattern. If a T1-generation plant carries a single copy of the T-DNA, the phenotype of the T2 offspring will show a clear 3:1 segregation ratio. If a T1-generation plant carries two copies of T-DNA, the segregation ratio of the phenotype of the T2 offspring will be between 3:1 to 15:1, depending on whether the two copies of T-DNA are linked or not, and on the locations of the T-DNA.

7.2.2.1. Identification of homozygous lines in T2 generation

Table 7.1 suggests that plants ggscyt3A and GRcyt2C were homozygous for the transgene. Plants ggscyt1B, 5B, 10A and GRcyt1B were likely to have only one copy of the transgene whereas ggschp6A, ggscyt4A, 8B and GRcyt12C may contain more

than one copy. In plants over-expressing *GRcyt*, out of the 4 selected lines, two lines (GRcyt2C and 12C) showed 100% resistance to kanamycin in T2 generation, whereas line GRcyt1B showed 75% resistance to kanamycin. The plants from the line GRcyt5B showed complete susceptibility to kanamycin, but they showed elevated GR activity in T2 generation. The green and healthy plants (Kan^R) were counted and then transferred to soil for further growth and seed harvest (Table 7.1).

7.2.2.2. Identification of homozygous lines in T3 generation

The seeds from the kanamycin resistant T2 generation seedlings were collected and bulked. About 100 seeds per each transgenic line were grown on kanamycin. The percentage of the healthy (green) seedlings was used to identify homozygous lines (Table 7.2–Table 7.4). If the geminated seedlings from one single line are all healthy, that line is homozygous for the transgene.

Table 7.2 suggests that all the ggschp lines showed a rough 3:1 phenotype ratio. And none of the lines showed homozygous condition which means that all the lines were in hemizygous condition.

In T3 generation, all the plants derived from line 2C and 12C showed 100% resistance to kanamycin, which means these two lines are homozygous, as expected, but line 1B showed differential sensitivity to kanamycin (Table 7.3). So, for subsequent analysis with sodium nitroprusside (SNP) treatments, we have selected plants from line GRcyt2C and 12C.

Out of the six lines we selected for further analysis, two lines from T2 generation (ggscyt3A and 4A) showed 100% homozygocity, while other lines showe

Table 7.1. Kanamycin selection of selected *Arabidopsis* plants (T2 lines) over-expressing γECS in chloroplast or cytosol or GRcyt, which showed higher total GSH/GR activity and strong expression of the bacterial transcript in RT-PCR

	Total seeds	**germinated**	**Kan^R**	**Kan^S**	**Ratio**	**Possible no of inserts***
Col-0	110	101	0	101		Control
ggschp2C	110	110	41	69	0.6/1	-
ggschp6A	111	111	97	14	6.9/1	2
ggscyt1B	113	111	80	31	2.6/1	1
ggscyt3A	110	110	110	0	-	Homozygous
ggscyt4A	111	110	109	1	110/1	3 or 4
ggscyt5B	113	112	84	28	3.0/1	1
ggscyt8B	111	111	104	7	14.9/1	2
ggscyt10A	111	110	72	38	1.9/1	1
GRcyt1B	109	109	74	35	2.1/1	1
GRcyt2C	110	110	110	0	-	Homozygous
GRcyt5B	112	112	2	110	0.02/1	-
GRcyt12C	112	112	111	1	111/1	3 or 4

Kan^R= Kanamycin resistant (Transformed green seedlings)

Kan^S= Kanamycin sensitive (untransformed, bleached and stunted)

* Insert number is the copy number of transgene deduced by genetic segregation of tolerant to kananycin in T2 transgenic plants

Table 7.2. Kanamycin selection of selected Arabidopsis plants over-expressing γECS gene in chloroplasts (ggschp), for homozygote screening in T3 generation

	Total seeds	**germinated**	**Kan^R**	**Kan^S**	**% germination***
Col-0	110	101	0	101	0%
ggschp2C_1	116	115	82	33	71%
ggschp2C_2	117	114	84	30	74%
ggschp6A_1	116	114	83	31	73%
ggschp6A_2	113	113	85	28	75%

* % germination = (Kan^R/total germinated seeds)* 100

Table 7.3. Kanamycin selection of selected GRcyt overexpressing *Arabidopsis* plants for homozygote screening in T3 generation

	Total seeds	**germinated**	**Kan^R**	**Kan^S**	**% germination**
GRcyt1B_1	117	117	58	58	50%
GRcyt1B_2	118	116	9	107	8%
GRcyt1B_3	115	115	1	114	1%
GRcyt1B_4	116	116	74	42	64%
GRcyt2C_1	115	111	111	0	100%
GRcyt2C_2	117	115	115	0	100%
GRcyt5B_1	115	115	2	113	1%
GRcyt12C_1	115	114	114	0	100%
GRcyt12C_2	119	118	118	0	100%
GRcyt12C_3	116	116	116	0	100%

* % germination = (Kan^R/total germinated seeds)* 100

Table 7.4. Kanamycin selection of selected *Arabidopsis* plants over-expressing γECS gene in cytosol (ggscyt), for homozygote screening in T3 generation

	Total Seeds	**germinated**	**Kan^R**	**Kan^S**	**% germination**
Col-0	110	110	0	110	0%
ggscyt1B_1	120	119	54	65	46%
ggscyt1B_2	113	113	67	46	59%
ggscyt1B_3	120	119	88	31	74%
ggscyt1B_4	119	118	91	27	77%
ggscyt3A_1	118	118	118	0	100%
ggscyt3A_2	116	115	115	0	100%
ggscyt3A_3	116	114	112	2	99%
ggscyt4A_1	120	120	120	0	100%
ggscyt4A_2	118	117	117	0	100%
ggscyt4A_3	119	119	119	0	100%
ggscyt4A_4	114	113	113	0	100%
ggscyt4A_5	120	118	118	0	100%
ggscyt4A_6	116	115	115	0	100%
ggscyt5B_1	116	115	115	0	100%
ggscyt5B_2	120	120	120	0	100%
ggscyt5B_3	118	117	117	0	100%
ggscyt5B_4	117	116	110	6	95%
ggscyt8B_1	116	116	116	0	100%
ggscyt8B_2	116	116	116	0	100%
ggscyt8B_3	118	118	87	31	74%
ggscyt10A_1	115	115	87	28	76%
ggscyt10A_2	122	122	83	39	68%
ggscyt10A_3	119	119	80	39	68%
ggscyt10A_4	116	115	115	0	100%
ggscyt10A_5	118	117	117	0	100%
ggscyt10A_6	121	120	111	9	92%

* % germination = (Kan^R/total germinated seeds)* 100

heterozygous condition (ggscyt1B, 5B, 8B and 10A) (Table 7.1). In T3 generation, all the plants derived from ggscyt3A and 4A showed 100% germination on kanamycin indicating the homozygous condition of the transgene (Table 7.4). Plants generated from lines 5B, 8B and 10A showed typical Mendelian segregation patterns of heterozygous plants (3:1 ratio).

7.2.3. GR activities and GR expression in selected T2, T3 and T4 lines of GRcyt over-expressing plants

The two homozygous lines of GRcyt, from T2, T3 and T4 generations were analyzed for total leaf GR capacity. Figure 7.7 shows that GRcyt2C and GRcyt12C plant lines didn't varied their capacity for the total foliar GR activity over the generations. These results were supporting the results of the kanamycin selection, where these plant lines showed homozygous condition in both T2 and T3 generations. Consisting with this notion, enzyme assays showed higher GR activities in T4 generation too. The T4 population of GRcyt2C and 12C were produced from the T3 plants homozygous for the *GR* gene. The T4 lines were genotyped to check the presence of the *GR* gene by polymerase chain reaction (PCR) amplification using GR specific primers. PCR analysis confirmed the presence of the transgene in both the GRcyt lines, where as WT and empty vector plants didn't show any amplification (Figure 7.8).

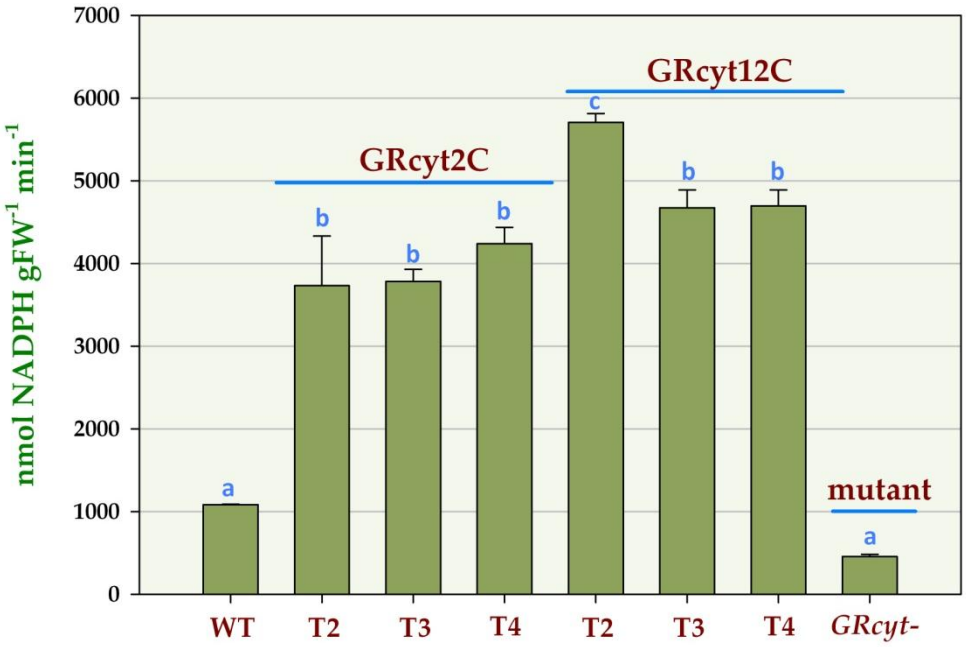

Figure 7.7. GR activity from the individual samples of kanamycin selected lines. each sample consists one rosette from 1 plant. T2, T3 and T4 represent the generation of plants used in the study. Data are means ± SD of three independent assays. Different letters represent values that are statistically different (Student-Newman-Keuls ANOVA test, $P < 0.05$).

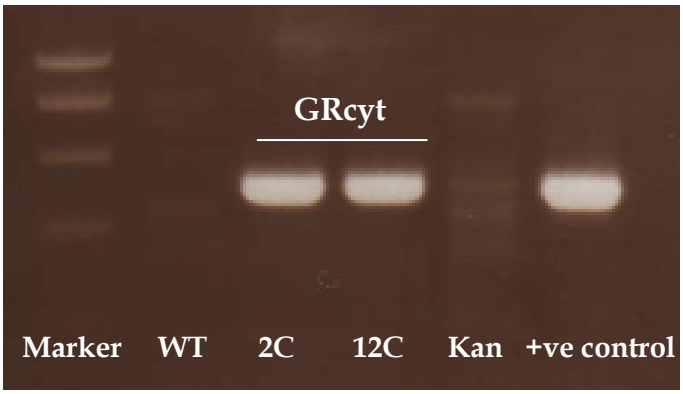

Figure 7.8. Genotyping of GRcyt lines in T4 lines. See materials and methods for PCR cycling conditions. WT= Wild type, Kan= plant with empty vector were used as –ve controls, +ve control = The F1 plant from a cross between GRcyt over-expressor x *cat2* mutant.

7.3. DISCUSSION

7.3.1. Enhanced levels of total glutathione and GSH transcripts in transgenic plants

Transgenic *Arabidopsis* plants carrying bacterial γECS targeted to either chloroplasts or cytosol resulted in the enhancement of total GSH in leaves, up to 2-4 fold over wild type plants. These results are consistent with earlier studies using expression of *E.coli* γECS gene targeted to the poplar chloroplast/cytosol of poplar or tobacco, resulting in increased (up to four-fold) leaf GSH (Noctor et al., 1996; Arisi et al., 1997; Herschbach et al., 2010). The combined expression of γECS and GSH-S resulted in further increase in GSH (Creissen et al., 1999). Conversely, poplar transformants, over-expressing *E. coli* GSH-S (GS) in cytosol, did not show much increase in foliar GSH content (Strohm et al., 1995). The individual plants from the lines that showed higher total GSH content, on subsequent analysis revealed differential GSH content (Figures 7.1 and 7.3) and the reason may be due to the copy number/co-suppression of the native GSH gene. The elevations of total GSH content in transformants are in quite agreement with corresponding increases in *GSH1* transcript levels (Figure 7.2 and 7.4).

Our results suggest that increased activity of GSH in the cytosol is able to sustain the homeostatic restrictions (like feedback regulation) on GSH synthesis (Arisi et al., 1997; Noctor et al., 1998). Such relatively high levels of GSH in the tissues of the plants can protect the cells from oxidative stress damage, as GSH is a major component of the active oxygen scavenging system of the cell (Queval et al.,

2009; Noctor et al., 2011).

7.3.2. Enhanced levels of glutathione reductase in transgenic plants

Arabidopsis plants over-expressing bacterial GR targeted to the cytosol resulted in much higher activities of GR up to 3-4 fold (over the wild type plants). Such pattern of increased GR activity in *Arabidopsis* leaves due to the expression of bacterial GR in the cytosol (Figure 7.5) is quite similar to the earlier reports on *GR* expression in tobacco, poplar, brassica and cotton (Aono et al., 1993; Foyer et al., 1995; Pilon-Smit et al., 2000; Mahan et al., 2009).

However, when three lines obtained from the plants that showed higher GR activity were subjected to another round of GR assay, we found a variability of enzyme activity among the plants (Figure 7.5). The exact reason for this variability is not clear. It is tempting to speculate that an interaction may occur between the bacterial and the native *GR* gene coding for similar enzymes and may result in the variable GR activities (Foyer et al., 1991).

7.3.3. Selection of homozygous T4 lines of GSH and GR over-expressing plants

In order to identify the homozygous lines of the *Arabidopsis* transgenics, based on kanamycin resistance, which is a common selective marker for selection (Toepfer et al., 1988). Seeds obtained from the transgenic plant lines (>2-fold increase in the GSH content/GR activity) were germinated on kanamycin containing medium. Segregation analysis revealed that in T2 and T3 generations, plants ggscyt3A, 4A, GRcyt2C and 12C were homozygous and other plants expressing *GSH1* and *GR* genes showed varied segregation based on the ratio of Kan^R/Kan^S (Table 7.1-7.4).

The verification of T4 lines of *Arabidopsis* plants by PCR confirmed the successful integration of the bacterial *GR* gene into the cytosol of *Arabidopsis* plants (Figure 7.8). Consistent with this observation, the GRcyt2C and GRcyt12C plants showed enhanced GR activity levels (4 to 6-fold over control) in T2, T3 and T4 generations (Figure 7.7).

In conclusion, we have characterized several *Arabidopsis* lines transformed with bacterial γECS gene targeted to either chloroplast/cytosol, and bacterial GR gene targeted to cytosol, from T1 to T4 generations. Together with mutants, homozygous lines would be an excellent system to examine the consequences of disturbed red-ox components over plant metabolism (Maughan and Foyer, 2006; Hanke et al., 2009). Therefore, two homozygous lines (GRcyt2C and GRcyt12C) from T2 and T3 generations were identified to have enhanced levels of GR, which could be used further. Chapter 8 describes the details of the interactions with NO of the selected homozygous T4 lines, in relation to their GSH levels, GR activities and transcripts of several enzymes.

7.4. CONCLUSIONS

1. The GSH content, GR activity and transcript expression of *GSH1* or *GR* were determined in 35 lines of T2 *Arabidopsis thaliana* plants over-expressing the *GSH1* in chloroplasts or cytosol and *GR* in cytosol. From the results, 2 lines in ggschp, 6 lines in ggscyt and 4 lines from GRcyt were identified to have enhanced levels of total GSH or foliar GR activity.
2. Kanamycin based selection of T1 lines in subsequent T2 and T3 generations

revealed that two lines each from ggscyt and GRcyt were homozygous for the respective transgenes.

3. Genotyping of T4 plants selected on kanamycin demonstrated the successful integration of the transgene. Biochemical characteristics of these selected plants revealed that both the T4 lines of GR over-expressors in cytosol didn't have much variation in their foliar GR activities over the generations.
4. The two homozygous lines of GRcyt plants, viz GRcyt2C and GRcyt12, were used further (described in Chapter 8) to analyze the interaction of NO signaling with glutathione metabolism via pharmacological approach.

*****

Chapter 8

Interaction of NO signaling with glutathione metabolism in transgenics and mutant plants of *Arabidopsis thaliana*

Chapter 8

Interaction of NO signaling with glutathione metabolism in transgenics and mutant plants of *Arabidopsis thaliana*

8.1. INTRODUCTION

Nitric oxide (NO) is recognized as a novel biological messenger in plants as well as in animals and is receiving increased attention. An increase in NO levels is associated with a several biochemical and physiological processes in plants, extending from development to responses to its abiotic and biotic stresses (Besson-Bard et al., 2008; Wilson et al., 2008; Leitner et al., 2009; Baudouin, 2011). There can be dual role of NO as a potent oxidant and effective antioxidant in plants.

At the molecular level, NO has been shown to regulate the expression of genes. Treating *Arabidopsis* plants or cell cultures with NO gas or NO donors (such as SNP) was shown to modulate the expression of many genes (Parani et al. 2004; Grun et al., 2006; Besson-Bard et al., 2009a). A significant proportion of these genes (~30%) were putatively related to defense and stress responses, cellular transport, signal transduction, metabolism and photosynthesis (Palmieri et al., 2008; Besson-Bard et al., 2009b; Moreau et al., 2010).

NO has been implicated in modulation of antioxidant metabolite levels/ redox status and antioxidant enzyme responses, particularly under stress (Neill et al., 2008). Glutathione (GSH) is a key player in determining intracellular thiol status in response to oxidative stress. The maintenance of high ratios of reduced glutathione against the oxidized form helps in cellular redox homeostasis under

stress (Ding et al., 2009; Foyer and Noctor, 2011). Evidences has emerged that the GSH biosynthetic pathway is stimulated in response to NO in both animal and plant cells (Gegg et al., 2003; Innocenti et al., 2007; Yap et al., 2010). In the cell environment, NO can react with reduced thiols to form S-nitrosothiols (RSNO) facilitating the process of S-nitrosylation of proteins, peptides, and amino acids (Valderrama et al., 2007). The reaction of NO with glutathione forms S-nitrosoglutathione (GSNO), which is assumed to function both as an intracellular and intercellular NO carrier. The enzyme GSNO reductase (GSNOR) catalyzes the reduction of GSNO and can regulate bioactive NO signal during plant–pathogen interaction and thermal stress (Diaz et al., 2003; Rusterucci et al. 2007; Lee et al. 2008).

Glutathione reductase (GR) is essential in re-generation of glutathione in its reduced state, thus maintaining the optimal redox status of the cell. GR is encoded by two genes in *Arabidopsis* (GR1 and GR2), first one is predicted to encode a cytosolic enzyme and the second one encodes a dual-targeted chloroplast/mitochondrial enzyme. The transgenic plant lines with variable capacity for cytosolic glutathione reductase (GRcyt) have been useful to examine the influence of glutathione status on the cell signaling and metabolism in plants (Maughan and Foyer, 2006; Mhamdi et al., 2010). Indeed, several studies have demonstrated that enhanced chloroplastic GR activity in transgenic plants results in increased protection against oxidative stress (Foyer et al., 1995; Pilon-Smit et al., 2000; Kornyeyev et al., 2003). In contrast, a decrease in GR activity in tobacco plants leads to an increased sensitivity to oxidative stress (Ding et al.,

2009). In GRcyt insertion mutants, oxidation of glutathione occurs independently of increased ROS availability, while GR over-expressors have an increased capacity for glutathione reduction. These lines offer an excellent system to analyze the influence of NO and glutathione in cell signaling.

The present work is an attempt to check the pattern of NO interaction with glutathione metabolism in *Arabidopsis* transgenics using the homozygous T4 lines, over-expressing *Escherichia coli* genes of GR in cytosol. Transgenic *Arabidopsis* plants were grown hydroponically and the sodium nitroprusside (SNP, a NO donor) treatments were used to raise the NO levels in the plant tissue. The transcript changes of the genes (related to glutathione metabolism and few known stress markers) in response to NO was followed using quantitative RT-PCR.

8.2. RESULTS

The transgenic *Arabidopsis* plant lines expressing the *E. coli* gene for GR that was targeted to the cytosol were characterized (Chapter 7) and the two lines which were homozygous for the transgene in T4 generation were selected and used in the present Chapter.

8.2.1. Levels of foliar GR activity, total glutathione and ascorbate in GRcyt plants

The transgenic GR over-expressing plants showed 5-6 fold increase in the total GR activity, compared to WT plants (Figure 8.1). The pattern of such response was similar when plants were grown either hydroponically (Figure 8.1) or on soil (Figure 7.8). These data confirm the efficiency of transformation to over-

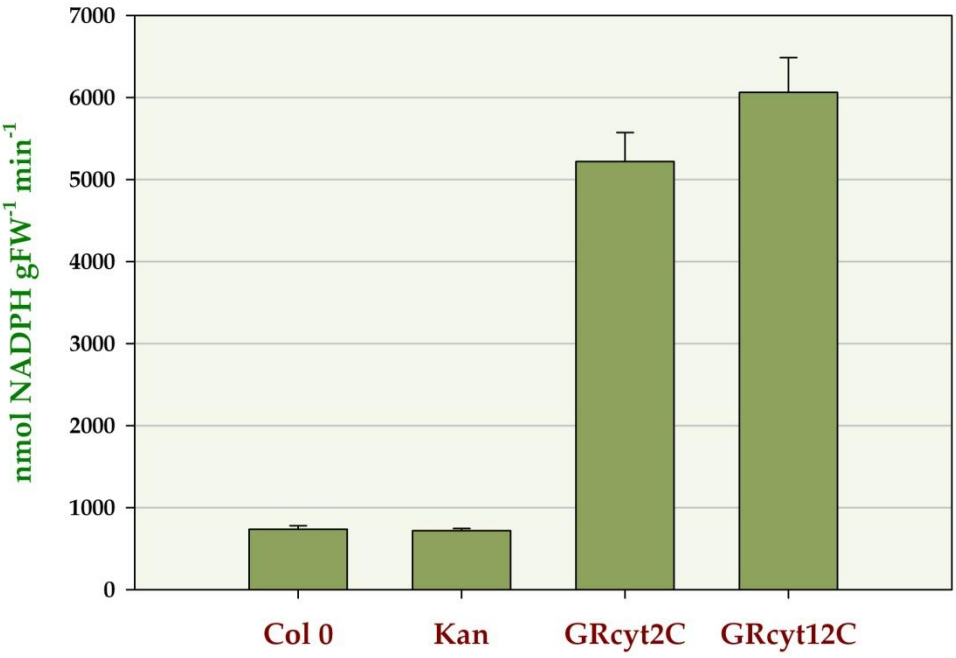

Figure 8.1. Changes in the foliar GR activity in the leaves of homozygous T4 lines of *Arabidopsis* plants. Col 0: wild type Columbia-0 plants; GRcyt: over-expressing *E. coli* GR in cytosol (two lines GRcyt2C and GRcyt12C); Kan: plant with empty vector; Data are means ± SD of three independent reactions.

express GR in leaves of *Arabidopsis*.

Despite the elevated GR levels, the total glutathione content of the leaves in the transgenic plants was similar to wild type (WT) (Figure 8.2A). As expected, the *cad2* mutant showed much less (about 30% of WT) glutathione; whereas the GR insertion mutant (*GRcyt-*) had enhanced levels of total glutathione (Figure 8.2A). The transgenic plants didn't show any perturbation in the total ascorbate levels. All the plants: WT, plants with empty vector (Kan), *cad2*, *GRcyt-* and the high cytosolic-GR expressors (GRcyt2C and GRcyt12C) had similar levels of foliar ascorbate (Figure 8.2B).

8.2.2. Phenotypic appearance of plants treated with SNP

Various degrees of wilting were observed after SNP treatment. After 3 h of SNP treatment, the leaves of WT, mutant and over-expressors showed wilting. However, the GRcyt2C and 12C plants showed a 80% recovery by 12 h of SNP treatment, which is in contrast to continued wilting of WT and empty vector vector plants (Figure 8.3). The mutant plants (*cad2* and *GRcyt*) showed slight recovery in wilting.

8.2.3. Responses to SNP of selected transcripts related to antioxidant metabolism in wild type (WT) plants

The expression patterns of selected transcripts were investigated by qRT PCR at different time periods in *Arabidopsis* after the SNP treatment. The analysis included those of glutathione metabolism and a few other key stress inducible genes. The first set of the qRT-PCR reaction includes all the selected 10 transcripts and SNP treated samples collected at two time points (0 h and 12 h).

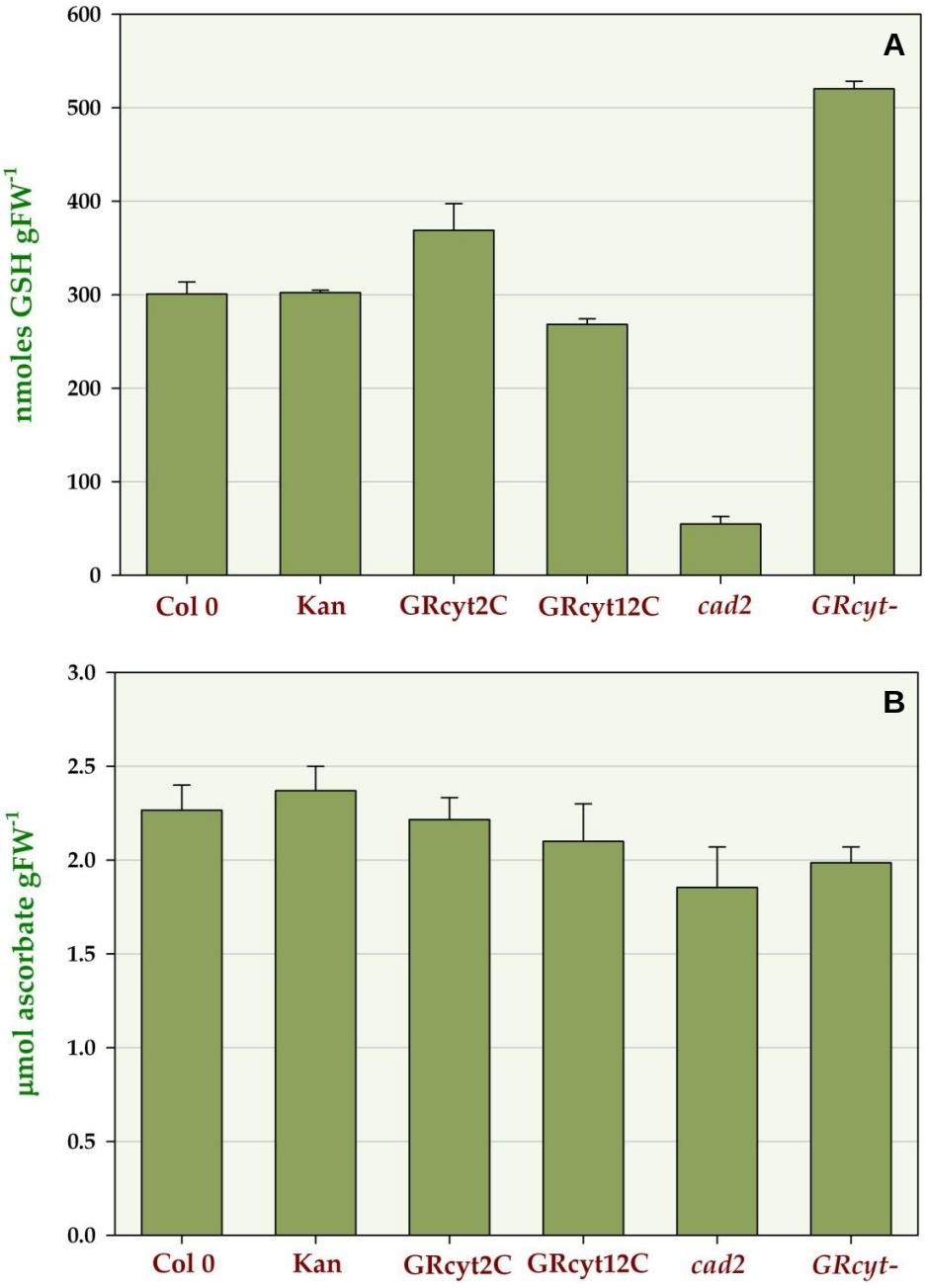

Figure 8.2. Changes in the (A) total GSH content, (B) total ascorbate content, in the leaves of homozygous T4 lines of *Arabidopsis* plants. Col 0: wild type Columbia-0 plants; GRcyt: over-expressing *E. coli* GR in cytosol (two lines GRcyt2C and GRcyt12C); Kan: plant with empty vector; *cad2:* cadmium sensitive glutathione mutant and *GRcyt-*: insertion mutant to down-regulate the levels of GR in cytosol. Data are means ± SD of three independent reactions.

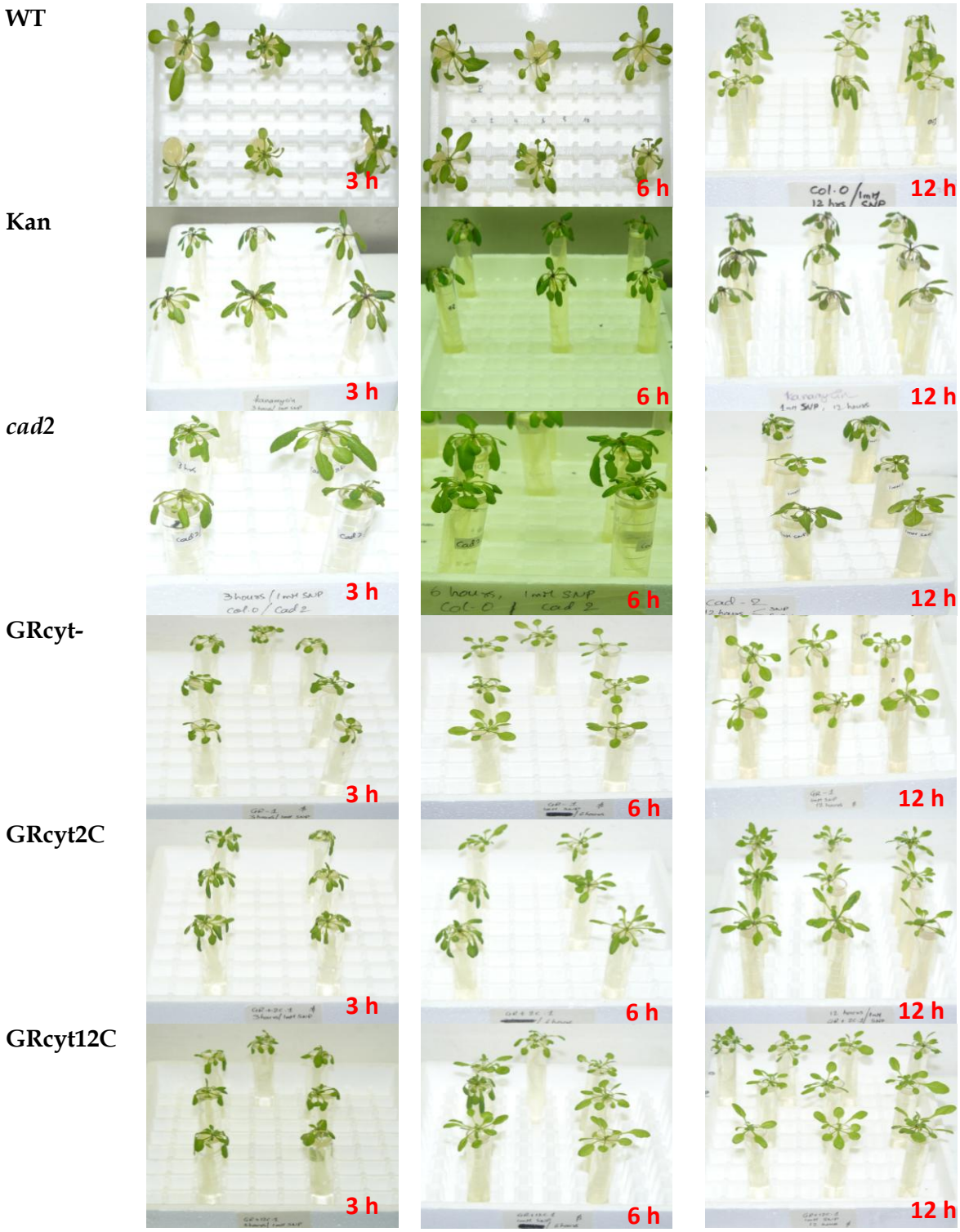

Figure 8.3. Response of four weeks-old homozygous T4 lines of *Arabidopsis* plants to SNP treatment. Col 0: wild type Columbia-0 plants; Kan: plant with empty vector; *cad2:* cadmium sensitive glutathione mutant and *GRcyt-*: insertion mutant to down regulate the levels of GR in cytosol; GRcyt: over-expressing *E. coli* GR in cytosol (two lines GRcyt2C and GRcyt12C). Photographs were taken at 3 or 6 or 12 h after treatment with SNP. Further details are described in Materials and Methods.

The levels of transcripts were double normalized, first with reference to *Actin2* transcript and then with transcript levels at 0 h SNP treatment.

The expression of *GSTu24* (gene encoding glutathione S- transferase), *AOX1a* (gene encoding alternative oxidase) and *cAPX* (gene encoding cytosolic ascorbate peroxidase) were increased by 13-30 fold after 12 h SNP treatment, whereas *PR5* pathogenesis related protein), *GST6* (glutathione s-transferase6) and *ACO* (ACC oxidase; involved in ethylene biosynthesis) transcripts showed about 3-4 fold increase after 12 h treatment. The transcripts encoding the glutathione biosynthetic enzymes γECS (*GSH1*, transcript encoding γ-glutamylcysteine synthetase) and GSH-S (*GSH2*, transcript encoding glutathione synthetase) showed about 2-4 fold increase with 12 h SNP treatment. The GR encoding genes (*GRcyt*, transcript for cytosolic GR and *GRcm*, dual targeted plastidic/mitochondrial isoform) also showed about 2-8 fold increase (Figure 8.4).

Further analysis of the selected transcripts (*GSTu24*, *AOX1a*, *cAPX* and *GRcyt*) at specified time points (3, 6 and 12 h) showed differential expression patterns in response to SNP treatments (Figure 8.5). *GSTu24* transcript expression was markedly increased (124 fold) up to 6 h of treatment, and then declined to a lower level. The *AOX1a* levels increased by 28 fold at 3 h of treatment and then decreased to 21 fold later. The transcripts *cAPX* and *GRcyt* increased 4 to 9 fold over control plants until 12 h (Figure 8.5).

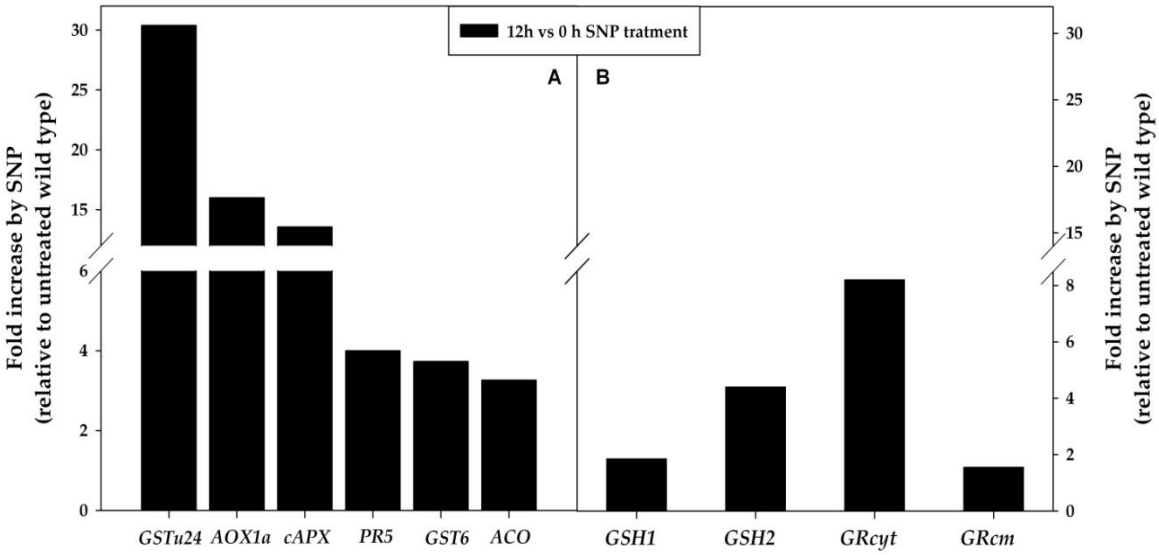

Figure 8.4. SNP treatment enhanced the expression of transcripts related to (A) stress; (B) glutathione metabolism in wild type *Arabidopsis* plants. The transcript abundance 12 h after SNP treatment was measured by qRT-PCR and the values shown are relative to *Actin2* and normalized to the untreated wild type (0 h).

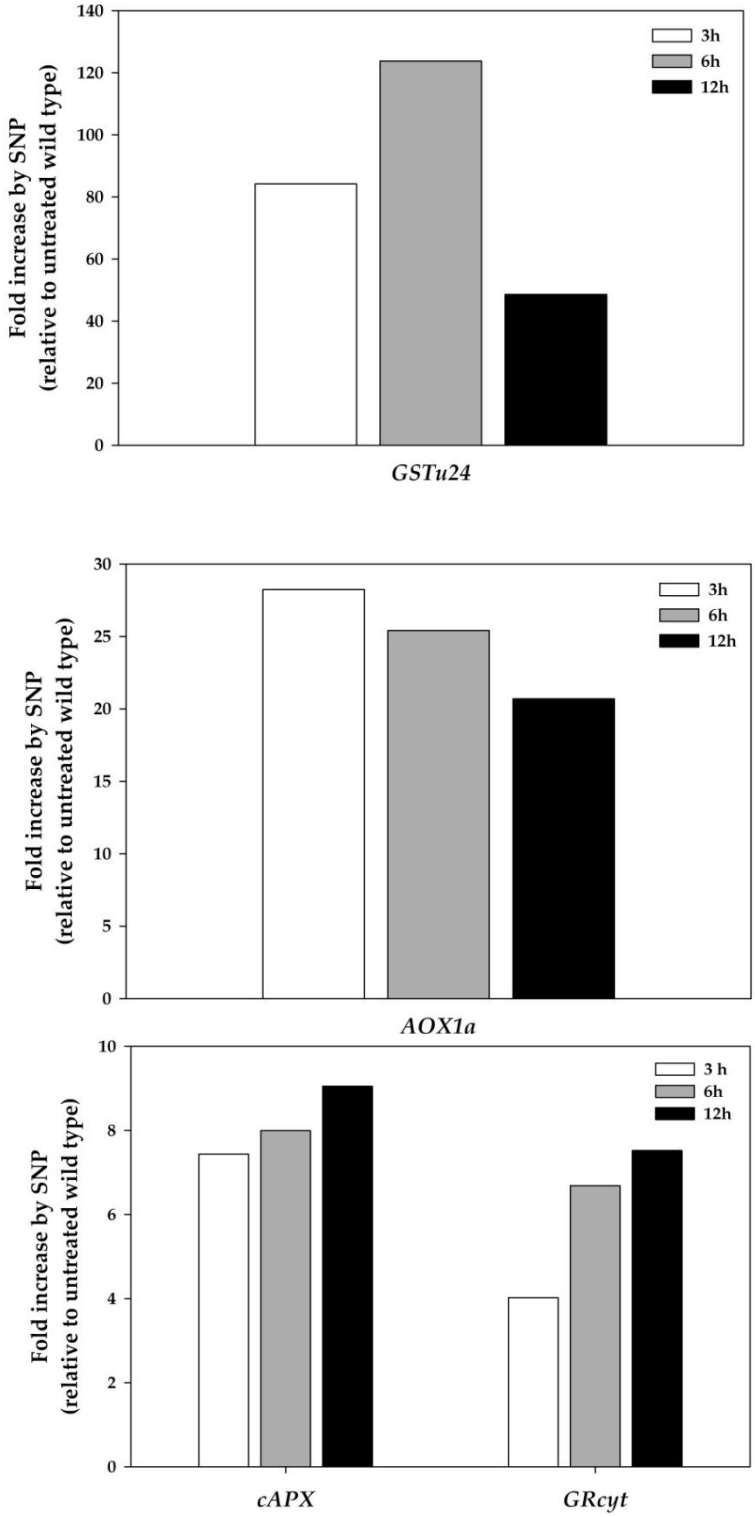

Figure 8.5. SNP treatment enhanced the expression of transcripts *GSTu24*, *AOX1a*, *cAPX* and *GRcyt* in wild type *Arabidopsis* plants. The transcript abundance 12 h after SNP treatment was measured by qRT-PCR and the values shown are relative to *Actin2* and normalized to the untreated wild type (0 h).

8.2.4. Effect of NO on glutathione metabolism in transgenic *Arabidopsis* lines

The *Arabidopsis* lines we used in our study were WT (Col-0), plant with empty vector (Kan), *cad2* mutant, GRcyt over-expressors (GRcyt2C and 12C) and GRcyt mutant (*GRcyt-*). Time course of the SNP treatment was undertaken to monitor the expression of the selected transcripts using quantitative RT-PCR.

When treated with SNP, WT and mutant plants (*cad2* and *GRcyt-*) showed about 2-fold induction of *GSH1* gene after 3 h SNP treatment, which remained at the same level up to 12 h of SNP treatment. In contrast, transgenic plants showed 2-fold and 3.5-fold increase after 3 and 6 h of SNP treatment. However at 12 h after treatment the transcript levels fell down compared to 6 h treatment (Figure 8.6). In WT and GRcyt2C plants, the transcript *GSH2* (*GSH-S*) levels were elevated at 3 h (2-fold) to 12 h (6-fold) of SNP treatment. However, the elevated expression levels (5-fold) were same at 6 and 12 h in *GRcyt-* and GRcyt12C (Figure 8.6).

Expression of *GRcyt* transcript, involved in the glutathione regulation, was quite high in WT and transgenics (showing 5-30 fold increase over the initial levels), but GRcyt mutants, the expression of *GRcyt* was only 4-fold higher at 3 h/6 h, but came down to the levels seen at 0 time after 12 h SNP treatment. The WT and *cad2* mutants showed heavy accumulation of the *GRcyt* transcript (about 25-fold increase after 6 h, but by 12 h, the levels fell down to about 15 to 20-fold increase (Figure 8.6). The changes in *GRcm* transcript were not as pronounced in those of *GRcyt*. The changes were in the range of 2- to 4-fold by 3, and 12 h then the fold increase reduced to 1-fold by 12 h treatment in mutant an

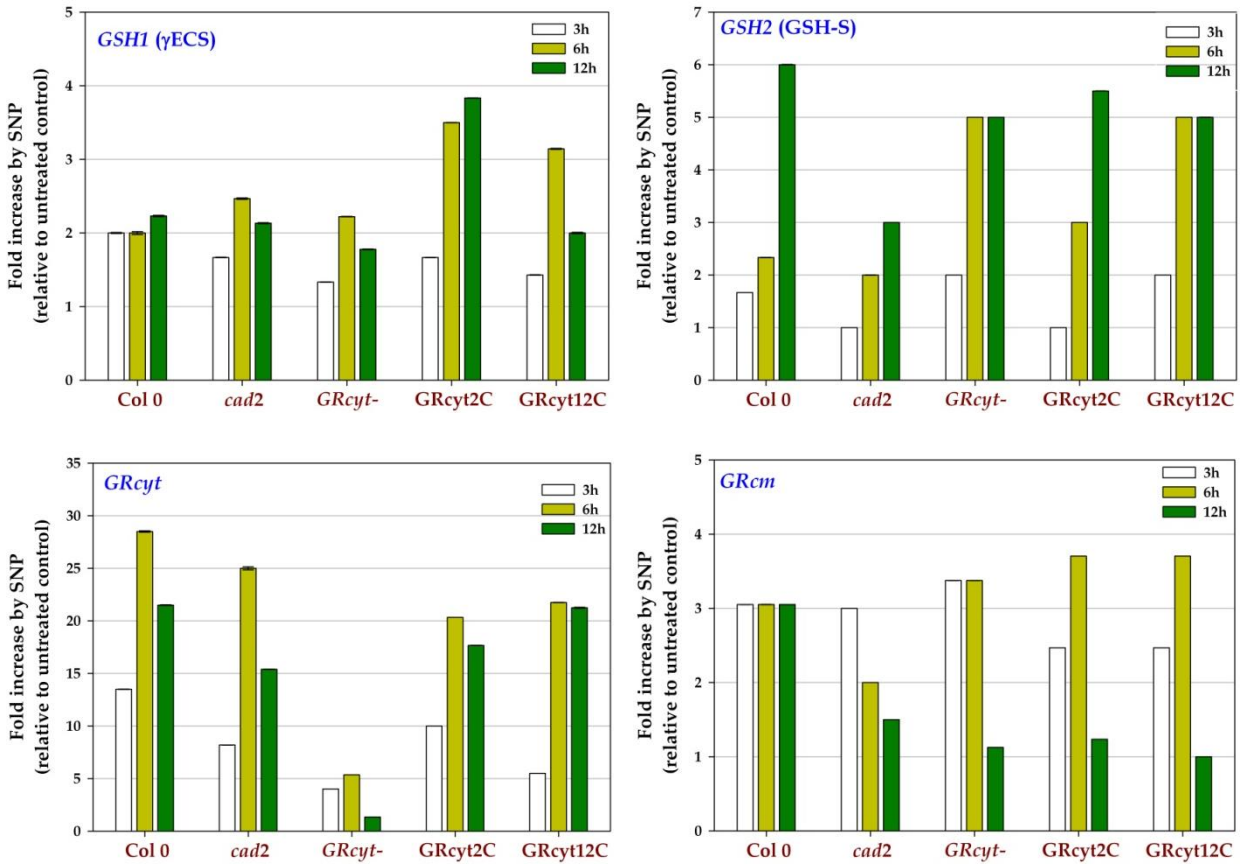

Figure 8.6. Changes in expression values of transcripts related to glutathione metabolism, in *Arabidopsis* plants, after variable periods of treatment with SNP. Col 0: wild type Columbia-0 plants; *cad2:* cadmium sensitive glutathione mutant and *GRcyt*-: insertion mutant to down regulate the levels of GR in cytosol; GRcyt: transgenic plants over-expressing *E. coli* GR in cytosol (two lines GRcyt2C and GRcyt12C). The transcript abundance after SNP treatment was measured by qRT-PCR and the values shown are relative to *Actin2* and normalized to the untreated control plants (0 h). Error bars that are not apparent are contained within the bars.

and transgenic plants (Figure 8.6).

Transcript levels of the other stress responsive genes, *GSTu24*, *AOX1a* and *cAPX* also increased in WT, mutant and trangenics, in response to SNP. However, the stimulation of the expression of *GSTu24* transcript, in mutants' *cad2* and *GRcyt-* (46-fold) at 3 h was less than that in WT plants (150-fold). The transgenics showed increased expression of the transcript with time by SNP treatment (Figure 8.7).

There was significant increase (25 to 150-fold) in the expression of *AOX1a* transcript in the WT, *GRcyt-* and transgenics, by 6 h SNP treatment and then the expression reduced significantly by 12 h treatment. However the expression of this gene was much less in *cad2* plants compared to WT, *GRcyt-* and transgenics (Figure 8.7). The expression of *cAPX* during SNP treatment of the WT, mutants and transgenic plants showed significant induction in the transcript. The expression of transcript *cAPX* increased by 10-30 fold in both the over-expressing plants, with time until 12 h of SNP treatment. In contrast, the *GRcyt-* mutant plant showed a significant decrease in expression by 12 h treatment, whereas there was no change in expression in WT plants (Figure 8.7).

8.3. DISCUSSION

Being a major non-protein thiol in plants, glutathione plays a crucial role in redox homeostasis and has been implicated in stress signaling and regulation (Reichheld et al., 2007; Foyer and Noctor, 2011). Although the involvement of NO in several key regulatory mechanisms in plant cell has already been established, the interaction of NO with e glutathione biosynthesis and regulation

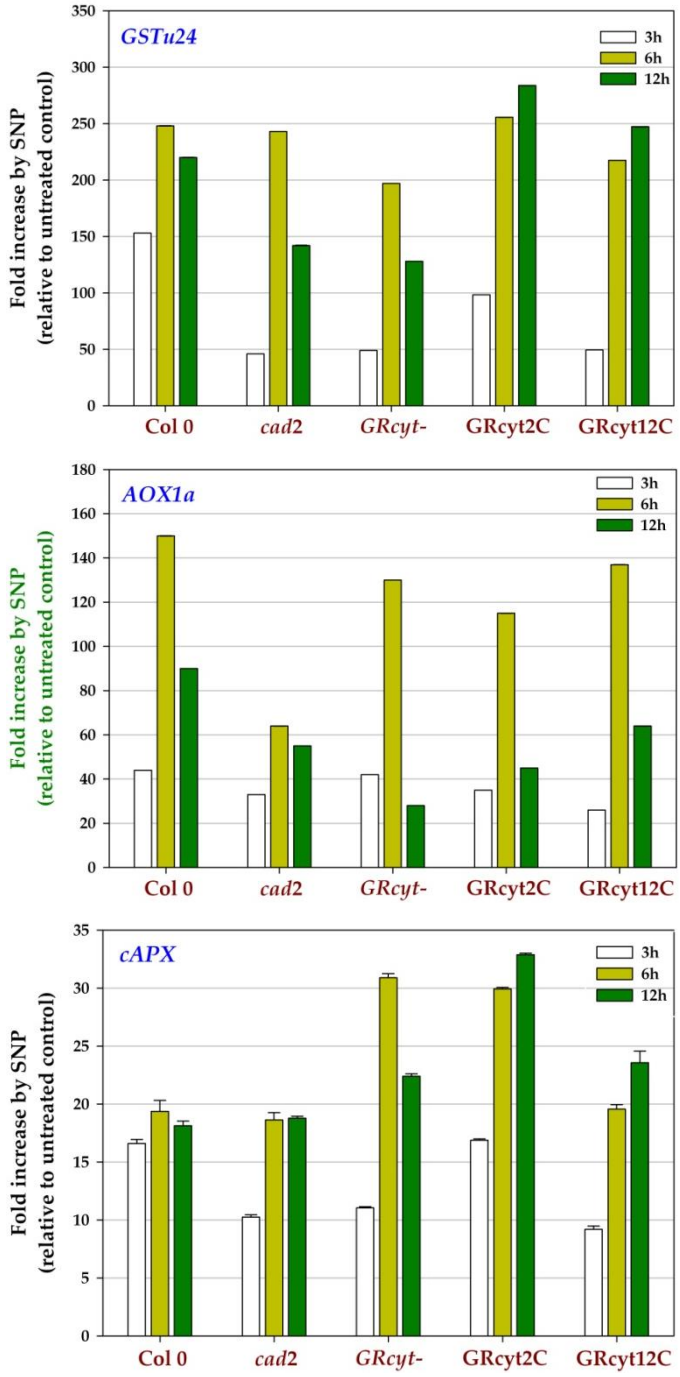

Figure 8.7. Changes in expression values of oxidative stress marker transcripts in *Arabidopsis* plants after variable periods of treatment with SNP. The abbreviations of plants were defined previously in the caption of Figure 8.6. The transcript abundance after SNP treatment was measured by qRT-PCR and the values shown are relative to *Actin2* and normalized to the untreated wild type (0 h). Error bars that are not apparent are contained within the bars.

has not completely elucidated. We, therefore, used transgenic *Arabidopsis* plants over-expressing bacterial glutathione reductase in the cytosol (GRcyt), to dissect the interaction of NO signaling with glutathione metabolism. The results were compared with the responses of related mutants, *cad2* and *GRcyt-*, which contain reduced levels (~30% of WT levels) of glutathione and glutathione reductase respectively.

8.3.1. Consequence of GR over-expression on key antioxidants in *Arabidopsis* plants

The homozygous lines of *Arabidopsis* plants carrying bacterial GR in cytosol resulted in enhanced levels of GR in leaves (Figure 8.1). However, such elevated GR activity of transgenic plants did not translate in to any noticeable effect on the total glutathione content (Figure. 8.2A) or total ascorbate pool of the leaves (Figure 8.2B). Our results are quite similar to the earlier reports, where the tobacco and poplar plants over-expressing *E. coli* GR gene in cytosol did not influence either the glutathione or ascorbate content (Foyer et al., 1991, 1995; Broadbent et al., 1995). In contrast, over-expression of either bacterial or plant *GR* in the chloroplast, led to increase in the foliar GSH levels by up to 50% in poplar, tobacco or potato (Foyer et al., 1995; Creissen et al., 1999; Eltayeb et al., 2010). Similarly, the ascorbate content was also increased in tobacco or cotton plants over-expressing bacterial *GR* in the chloroplast (Foyer et al., 1995; Kornyeyev et al. 2005). The reasons for such differences in literature need to be further studied.

8.3.2. Responses to NO of glutathione synthesis and reduction in GR over-expressors

An enhanced GR levels in cytosol of lines GRcyt2C and 12C is expected to alter the expression of genes involved in defense reactions. Quantitative analysis of appropriate marker transcripts could provide specific information on such possibility. Based on the available literature data (Huang et al., 2002; Grun et al., 2006; Zago et al., 2006), transcripts known to be strongly induced by intracellular NO and by other stresses were chosen for qRT-PCR analysis. Generation of NO was done by supplementing the nutrient solution with SNP, widely used as NO donor (Polverari et al., 2003; Murgia et al., 2004; Ahlfors et al., 2009).

Our results suggest that elevated levels of GR in the transgenics can help to protect plants against NO stress. The transgenic plants showed enhanced resistance to NO treatment in terms of recovery of wilting, while the WT plants continued to wilt (Figure 8.3). These results are in agreement with previous studies, where the over-expression of GR in poplar and tobacco caused a significant increase in their tolerance to oxidative stress (Broadbent et al., 1995; Foyer et al., 1995; Ding et al., 2009).

Long stress periods may involve signaling effects that facilitate the acclimation processes. For example, H_2O_2 generated in the chloroplast during high light stress can act as both a local and systemic signal to elicit defensive or acclimatory responses (Karpinski et al., 2003; Fryer et al., 2003; Mullineaux et al., 2006). We observed that with time, there was an increase in the expression levels of the transcripts *cAPX*, *AOX1a* and *GSTu24* (Figure 8.5), which are widely

known to be involved in plant protection and signaling under various stress conditions (de Pinto et al., 2006; Koussevitzky et al., 2008). Thus, it is reasonable to speculate that NO induced expression of *AOX1a* and *GSTu24* transcripts may be a reflection of the onset of acclimation processes.

The SNP treatment resulted in differential levels of expression of all the selected transcripts (Figures 8.6 and 8.7). Both the over-expressor plants showed similar pattern of increased induction of *GSH1*, *GRcyt* and cAPX with time. These results emphasize the importance of antioxidant enzymes in combating stress conditions. Previous experiments using microarray and cDNA-AFLP approaches have shown that NO-responsive genes include glutathione- and redox related enzymes such as ascorbate peroxidase and alternative oxidase (Huang et al., 2002; Parani et al., 2004; Palmieri et al., 2008). Complimenting well with the above notion, our experiments also showed increased expression of these transcripts with NO treatment.

The expression patterns of the transcripts *GSH2*, *GRcm*, *GSTu24* and *AOX1a* were similar in WT and GR over-expressors (Figure 8.6 and 8.7). The *GSTu24* is among several GSTs induced by herbicide and xenobiotic treatment (Mezzari et al., 2005; Wagner et al., 2002) and induction of this gene could be linked to conjugation of secondary metabolites or stress-induced catabolites. *AOX1a* is another stress marker in plants, as it bypasses the excess electrons generated in mitochondria during stress conditions. The induction of this gene is coupled to plant defense, in many cases (Chivasa and Carr 1998; Huang et al., 2002; Ederli et al., 2006). Similarly the *cAPX* gene is known for its active

involvement in ROS scavenging (Karpinski et al., 1997; Murgia et al., 2004). Consistent with the above notions of the important role in plant defence during different stresses, the levels of *AOX1a* and *cAPX* showed a marked increase with NO treatment during our experiments (Figure 8.7).

In summary, the improved protection, against elevated NO, in GR over-expressing plants could be explained by synergistic effects of GR and other antioxidant enzymes or metabolites that participate in scavenging of free radicals. Further biochemical and molecular analysis can provide new insights into the role of antioxidants and their interaction with NO.

8.4. CONCLUSIONS

1. The levels of major antioxidants in transgenic plants over-expressing GR in cytosol did not alter much, as indicated by the levels of total GSH and the total ascorbate, to those in wild type plants.
2. The treatment with NO caused severe wilting in all the plants, but the transgenic plants recovered from wilting subsequently, indicating that the enhanced levels of GR had a protective role against NO.
3. The qRT-PCR analysis showed increased expression of *GSH1* gene in transgenic T4 lines, when compared to WT. As *GSH1* is the principal component of glutathione biosynthesis, our results suggest that during stress conditions, enhanced GR levels may sustain in glutathione biosynthesis.
4. High expression of *AOX1a* gene, as observed during our experiments, indicate that *AOX1a* could be one of the stress markers.

5. The expression patterns of the transcripts *GSTu24*, *GRcyt* and *cAPX* imply that there parallel defense mechanisms are activated to scavenge the free radicals generated during stress conditions. In summary, plants are equipped with a network of defense mechanisms and exhibit multiple strategies to counter act the stress conditions.

*****

Chapter 9

General Discussion

Chapter 9

General Discussion

The interactions between chloroplasts and mitochondria are known to be mediated by metabolites related to redox shuttles, besides, ROS and nitric oxide (NO) as signals (Raghavendra and Padmasree 2003; Matsuo and Obokata, 2006; Nunes-Nesi et al., 2008). Being readily diffusible, NO and ROS reach a variety of intracellular and extracellular targets and regulate many key cellular responses in plants (Neil et al., 2002). The present investigation is an attempt to study the effects of NO on the patterns of photosynthesis and respiration and in relation to the interaction with glutathione metabolism. The experimental systems were mesophyll protoplasts of pea (to study the organelle interaction) and *Arabidopsis* leaves (to study the interaction of NO with glutathione metabolism). The intracellular NO was raised by pre-incubation with SNP of the experimental systems.

In the first part of our study, we ascertained the functional ability of protoplasts, as compared to leaves. Plant protoplasts provide a unique homogenous suspension of single cell system. With proper precautions, plant protoplasts have been used for a range of experiments including physiological, proteomic and genomic studies (Davey et al., 2005; Yoo et al., 2007; Faraco et al., 2011). However, the isolation procedure involves short, but physiologically stressful steps. We have therefore used for the first time the fast Chl *a* fluorescence transient (OJIP) analysis, for monitoring and assessing the functional photochemical performance of

mesophyll protoplasts at different stages of isolation from pea (*Pisum sativum*) leaves.

The oxygenic photosynthetic organisms show polyphasic rise in Chl a fluorescence with time, consisting of a sequence of phases denoted as OJIP (Strasser et al 2000). Any perturbation in chloroplast structure and function would alter these fluorescence transients (Strasser et al., 2004). The isolation procedure, particularly the digestion step, which involved a period of illumination, suppressed the fluorescence amplitude with time, possibly due to non-photochemical quenching (Figure 4.5B). Such type of light effect on the OJIP transients were earlier reported (Schansker et al., 2006). However, the centrifugation steps didn't alter the OJIP transients and subsequent transfer of protoplasts to iso-osmotic medium resulted in a remarkable recovery of the initial kinetics. The OJIP transients of protoplasts at this stage showed only marginal differences with the transients of the source leaves and demonstrate the similar photosynthetic performance of isolated mesophyll protoplasts to that of intact leaves (Figure 4.6C). In summary, the isolated mesophyll protoplasts maintained their integrity and photosynthetic status very well, as indicated by their high rates of oxygen evolution in light (Figure 4.3). Our results demonstrate that, the Chl *a* fluorescence OJIP transients could be used as a quick non-invasive test to assess the functional integrity and physiological performance of the protoplasts. The protoplasts isolated by our procedure were quite good in terms of basic Chl a fluorescence transients. These protoplasts can

therefore be very useful for studies on not only metabolic processes such as photosynthesis, but also for studies involving cellular signaling.

In the second part of the study, we attempted to assess the role of NO and ROS as biochemical signals between chloroplasts and mitochondria, using mesophyll protoplasts of pea. At present the role of NO and ROS in different aspects of plant metabolism, particularly in signal transduction during abiotic, biotic and defense responses is studied extensively, but is still under debate (Miller et al., 2010; Moreau et al., 2010). Further, the work on the responses of photosynthetic metabolism to the accumulation of NO is quite limited.

When protoplasts were pre-incubated with SNP (to release NO) for 5 min, the protoplasts showed severe inhibition in the CO_2 dependent O_2 evolution in a concentration, time and light dependent manner (Figure 5.1 and 6.4). The possibility of effect of CN^- (by product of SNP) on photosynthesis was cross-checked using cPTIO (specific NO scavenger). The inhibition of photosynthesis by SNP was reversed remarkably by cPTIO, indicating that the inhibition by SNP was mostly due to NO (Figure 5.2). These results support the use of cPTIO in NO related studies (Zhao et al., 2009; Ma et al., 2010). In contrast to photosynthesis, NO didn't exhibit any significant effect on the rate of respiration, indicating that chloroplasts are one of the early targets for NO in cell. Our results are in agreement with the results of Lum et al. (2005) and Jasid et al. (2006).

In contrast to the effect of NO, the exposure of mesophyll protoplasts to H_2O_2 resulted in a significant inhibition of respiration, while the extent of inhibition

was marginal on photosynthesis (Figure 5.3). It is intriguing that the chloroplasts generate considerable levels of ROS, but do not show any effect of external H_2O_2. It is possible that chloroplasts have an efficient ROS scavenging system (Apel and Hirt, 2004). Increasing the concentration of H_2O_2 markedly elevated the inhibition of photosynthesis by 50% and respiration by 85%. Our results suggest that severe inhibition of respiratory metabolism will lead to strong inhibition in photosynthesis. These results endorse the concept of strong dependence of chloroplasts on mitochondria (Raghavendra and Padmasree, 2003). Pre-illumination of protoplasts with H_2O_2 in low light, initially resulted in decrease of respiration but then dramatically increased with the time of treatment (Figure 5.4), which could be partly an effect of light enhanced dark respiration (LEDR). LEDR has been demonstrated earlier in protoplasts and leaves (Reddy et al., 1991; Atkin et al., 1998). We conclude that mitochondria could be one of the primary targets for ROS in plant cell.

The mitochondrial inhibitors, antimycin A and SHAM showed only a marginal effect on respiratory O_2 uptake but decreased rate of photosynthetic O_2 evolution, in a concentration dependent manner (Figures 5.5 and 5.6). A decrease of <15% in the rate of respiration caused an inhibition of 50% in photosynthesis in the presence of antimycin A. Our results reaffirm that mitochondrial metabolism (both COX and AOX pathway) is not only beneficial but also crucial for optimal functioning of photosynthesis (Padmasree and Raghavendra, 1999; Yoshida et al., 2006).

Previous reports suggested that the exchange of metabolites between the organelles is the basis of inter-organellar interactions. In the present work, we tried to assess the roles of NO and ROS during the cross talk between chloroplast and mitochondria. However, our experiments did not find any strong evidence for the role of NO during such interactions, as the sensitivity of photosynthesis to mitochondrial inhibitors was only marginally affected in presence of SNP (Table 5.1). In contrast, H_2O_2 appeared to decrease the sensitivity of photosynthesis to mitochondrial inhibitors, particularly SHAM. In presence of mitochondrial inhibitors protoplasts showed about 50% inhibition in photosynthesis, whereas the presence of H_2O_2 decreased this inhibition to 30% (Table 5.3). These results suggest that H_2O_2 perhaps act as stress signal and mediate the cross talk between chloroplasts and mitochondria. In case of NO, further studies need to be done to clearly elucidate its role during interactions.

Confocal imaging of protoplasts treated with SNP showed time and light dependent increase of NO in the vicinity of chloroplast in protoplasts. The kinetics of DAF-2DA (NO specific fluorescent probe) fluorescence showed elevated levels of NO in protoplast treated with SNP in light over dark (Figures 6.1. to 6.3). Together with previous reports, our results support the concept that chloroplasts are one of the possible sources of NO in cells (Jasid et al., 2006; Gas et al., 2009).

Since we have observed the severe inhibition of photosynthesis by NO in our previous study, we tried to elucidate the possible targets of NO in the photosynthetic electron transport using chlorophyll a fluorescence and PS II

photochemistry in elevated NO conditions. Previous reports using thylakoids and intact leaves, suggested that NO could bind to several sites in photosynthetic electron transport and inhibit photosynthesis (Takahashi and Yamasaki, 2002; Wodala et al., 2008). Several reports suggest that the PS II is the major target of oxidative damage in plants and is very sensitive to environmental changes (Aro et al., 2005). Examining the two components of photosynthetic electron transport; whole chain (NO_2^- dependent) and PS II (BQ dependent) in presence of SNP, revealed that there was reduced rate of electron transport, indicating NO could affect electron transport, both PS II and PS I (Table 6.1). Our results support the study by Wodala et al. (2008) that the partial inhibition of PS II by NO might be due to impaired electron transport.

The Chl *a* fluorescence fast transient (OJIP) analysis showed that intensity of fluorescence in the OJIP transient decreased with SNP treatment in time dependent manner, when compared to control (Figures 6.5 and 6.6). This can be attributed to an inhibition in the electron flow due the decrease in PQ and ferridoxin pools (Tsimilli-Michael and Strasser, 2008). The pool size of the electron acceptors declined considerable with increasing NO exposure to the protoplasts. These results are concurrent with the results obtained using EPR and fluorescence studies demonstrating NO can reversibly bind to several sites in PS II (Sanakis et al., 1997; Schansker et al., 2002). Our results also showed that SNP decreased the Fv/Fm values (represents photochemical efficiency of PS II) in protoplasts(Figure 6.7), which indicated that NO increased the proportion of closed PS II reaction centers

due to the action of NO on electron transport at the acceptor side of PS II (Wodala et al., 2008). NO decreased the photosynthetic performance index [PI $_{(abs)}$], active reaction centers (RC/CSm) and increased the energy dissipation at reaction center (DIo/RC) (Figure 6.8, 6.9 and Table 6.2), due to the inactivation of reaction center complexes with prolonged NO exposure. Based on our results we could suggest that NO affected the efficiency of photochemical reactions and CO_2 fixation of protoplasts.

Plant cells accumulate ROS and NO in response to a wide variety of stresses, which in turn lead to typical signaling pathways (Neil et al., 2002). NO has been implicated in modulation of antioxidant metabolite levels/redox status and antioxidant enzyme responses, particularly under stress (Besson-Bard et al., 2008). Glutathione (GSH) and glutathione reductase (GR) are key players in maintaining an optimal redox status of the cell. Evidences have emerged that GSH biosynthesis is stimulated in response to NO in animal and plant cells (Innocenti et al., 2007; Yap et al., 2010). In the present work we attempted to check the interaction of NO signaling with glutathione metabolism in *Arabidopsis* transgenics. Initially we characterized the *Arabidopsis* lines over-expressing bacterial genes *GSH1* (gene encoding γECS) in chloroplast and cytosol and *GR* in cytosol.

The GSH content, GR activity and the expression of the corresponding transcripts were determined in 35 lines of T2 *Arabidopsis thaliana* plants over-expressing the bacterial *GSH1* in chloroplasts or cytosol and *GR* in cytosol. From the results, 2 lines in ggschp (*GSH1* expression in chloroplasts), 6 lines in ggscyt (*GSH1*

expression in cytosol) and 4 lines from GRcyt (*GR* expression in cytosol) were identified to have enhanced levels of total glutathione or foliar GR activity (Figures 7.1; 7.3 and 7.5). Transgenic *Arabidopsis* plants carrying bacterial genes (*GSH1* and *GR*) resulted in the enhancement of total GSH content or GR activity in the leaves, up to 2-6 fold over wild type plants (Figures 7.1, 7.3 and 7.5). The elevation of GSH content or GR activities in the transgenics are complimenting well with the corresponding transcript levels (Figures 7.2, 7.4 and 7.6). Our results are complimenting well with the previous reports using the expression of same constructs targeted to chloroplasts/cytosol of poplar, tobacco or cotton (Aono et al., 1993; Noctor et al., 1998; Mahan et al., 2009; Herschbach et al., 2010). Such relatively high levels of GSH or GR activities in the tissues of the plants can protect the cells from oxidative stress damage, as GSH is a major component of the active oxygen scavenging system of the cell (Queval et al., 2009; Noctor et al., 2011).

Kanamycin selection of the selected T1 lines in subsequent T2 and T3 generation identified two lines each from ggscyt and GRcyt to be homozygous for the respective transgenes (Tables 7.1 to 7.4). Genotyping of the homozygous T4 lines of GRcyt2C and 12C confirmed the integration of transgene in to the genome of *Arabisopsis* and showed enhanced levels of GR activity over the generations (Figures 7.7 and 7.8). These lines were further used to analyze the interaction of NO with glutathione metabolism.

Although, the involvement of NO in several key regulatory mechanisms in plant cells has been established, the interaction of NO with the glutathione

metabolism has not been completely elucidated. The over-oxpression of bacterial *GR* in the cytosol of *Arabidopsis* plants did not alter the antioxidant metabolism in plants (Figures 8.1 and 8.2). A similar result was earlier reported in tobacco plants over-expressing *GR* gene in cytosol (Foyer et al., 1991; Broadbent et al., 1995).

Time scan of the experiments was carried out with transgenic plants treated with/without SNP to observe any phenotypic and transcript changes. Elevated levels of NO caused severe wilting in plants but the transgenic plants recovered subsequently from wilting (Figure 8.3). Our results show that enhanced levels of GR in plants had a protective role during NO stress.

Quantitative analysis (by qRT-PCR) of selected transcripts (related to glutathione metabolism) can provide useful information on the perception and response of oxidative stress. The transcripts related to glutathione metabolism and other key stress inducible genes, were therefore studied. Their qRT-PCR analysis showed increased expression of *GSH1*, *GRcyt* and cAPX in transgenics over wild type and mutants (Figure 8.6 and 8.7). Our results re-emphasize the importance of these antioxidant enzymes in combating stress conditions (Murgia et al., 2004; Ding et al., 2009; Ivanova et al., 2011). Similarly, long stress periods may cause signaling effects that allow eliciting defensive or acclimatory responses (Fryer et al., 2003; Mullineaux et al., 2006). The induced expression of *cAPX, GSTu24* and *AOX1a* with time during our experiments, complimented well with the above notion.

The high expression of *AOX1a* gene during our experiments supports several other reports, stating *AOX1a* as one of the important stress marker (Huang et al.,

2002; Ederli et al., 2006). The expression patterns of the transcripts *GSTu24* and *cAPX* may be a reflection of the onset of acclimation processes. Our results imparts that apart from GSH, ascorbate and GR, there are several other defense mechanisms that may activate and participate during counter action of plants against stress conditions (de Pinto et al., 2006; Koussevitzky et al., 2008).

Our results emphasize that the NO could directly affect the photosynthesis, whereas H_2O_2 could modulate the interactions between mitochondria and chloroplasts. We could characterize over-expression of glutathione metabolism genes and identify homozygous T4 lines, which can be used to elucidate the interaction of NO with glutathione in cellular signaling. Further work is necessary to dissect the role of NO during such interactions. Recent availability of the mutants with altered capacity of NO production, such as *AtNOA1, NIA1 and NIA2* offer additional models to examine and understand the roles of NO in not only interactions but also in various cellular metabolisms.

*****

Chapter 10

Literature cited

Chapter 10

Literature cited

Abat JK, Mattoo AK and Deswal R (2008) S-nitrosylated proteins of a medicinal CAM plant Kalanchoe pinnata—ribulose-1, 5-bisphosphate carboxylase/oxygenase activity targeted for inhibition. FEBS J **275:** 2862–2872

Ahlfors R, Brosch M, Kollist H and Kangasjrvi J (2009) Nitric oxide modulates ozone-induced cell death, hormone biosynthesis and gene expression in Arabidopsis thaliana. Plant J **58:** 1– 12

Alderton WK, Cooper CE and Knowles RG. 2001. Nitric oxide synthases: structure, function and inhibition. Biochem J **357:** 593–615

Allen JF (1993) Control of gene expression by redox potential and the requirement for chloroplast and mitochondrial genomes. J Theor Biol **165:** 609-631

Antal TK, Matorin DN, Ilyash LV, Volgusheva AA, Osipov V, Konyuhov IV, Krendeleva TE and Rubin AB (2009) Probing of photosynthetic reactions in four phytoplanktonic algae with a PEA fluorometer. Photosynth Res **102:** 67–76

Aono M, Kubo A, Saji H, Tanaka K and Kondo N (1993) Enhanced tolerance to photooxidative stress of transgenic Nicotiana tabacum with high chloroplastic glutathione reductase activity. Plant Cell Physiol **34:** 129–135

Apel K and Hirt H (2004) Reactive oxygen species: metabolism, oxidative stress, and signal transduction. Annu Rev Plant Biol **55:** 373–399

Arisi ACM, Noctor G, Foyer C, Jouanin L (1997) Modifications of thiol contents in poplars (Populus tremula × P. alba) overexpressing enzymes involved in glutathione synthesis. Planta **203:** 362–372

Arnaud N, Murgia I, Boucherez J, Briat JF, Cellier F and Gaymard F (2006) An iron-induced nitric oxide burst precedes ubiquitin-dependent protein degradation for Arabidopsis AtFer1 ferritin gene expression. J Biol Chem **281:** 23579–23588

Arnon DI (1949) Copper enzymes in isolated chloroplasts. Polyphenol oxidase in *Beta vulgaris*. Plant Physiol **24:** 1-15

Aro EM, Suorsa M, Rokka A, Allahverdiyeva Y, Paakkarinen V, Saleem A, Battchikova N and Rintamaki E (2005) Dynamics of photosystem II: a proteomic approach to thylakoid protein complexes. J Exp Bot **56:** 347–356

Asada K (2006) Production and scavenging of reactive oxygen species in chloroplasts and their functions. Plant Physiol **141:** 391-396

Atkin OK, Evans JR and Siebke K (1998) Relationship between the inhibition of leaf respiration by light and enhancement of leaf dark respiration following light treatment. Aust J Plant Physiol **25:** 437-443

Atkin OK, Millar AH, Gardeström P and Day DA (2000) Photosynthesis, carbohydrate metabolism and respiration in leaves of higher plants. *In* RC Leegood, TD Sharkey, S von Caemmerrer, eds, Photosynthesis: Physiology and Metabolism. Kluwer Academic Publishers, The Netherlands, pp 153-175

Baker NR (2008) Chlorophyll fluorescence: a probe of photosynthesis in vivo. Annu Rev Plant Biol **59:** 89-113

Ball L, Accotto GP, Bechtold U, Creissen G, Funck D, Jimenez A, Kular B, Leyland N,

Mejia-Carranza J, Reynolds H, Karpinski S and Mullineaux PM (2004) Evidence for a direct link between glutathione biosynthesis and stress defense gene expression in Arabidopsis. Plant Cell **16:** 2448–2462

Baudouin E (2011) The language of nitric oxide signalling. Plant Biol. **13:** 233-242

Bauwe H, Hagemann M and Fernie AR (2010) Photorespiration: players, partners and origin. Trends Plant Sci **15:** 330–336

Besson-Bard A, Gravot A, Richaud P, Auroy P, Duc C, Gaymard F, Taconnat L, Renou JP, Pugin A and Wendehenne D (2009a) Nitric oxide contributes to cadmium toxicity in Arabidopsis by promoting cadmium accumulation in roots and by up-regulating genes related to iron uptake. Plant Physiol **149:** 1302–1315

Besson-Bard A, Astier J, Rasul S, Wawer I, Dubreuil-Maurizi C, Jeandroz S and Wendehenne D (2009b) Current view of nitric oxide-responsive genes in plants. Plant Sci **177:** 302–309

Besson-Bard A, Pugin A and Wendehenne D (2008) New insights into nitric oxide signaling in plants. Annu Rev Plant Biol **59**: 21–39

Bethke PC, Libourel IGL and Jones RL (2006) Nitric oxide reduces seed dormancy in Arabidopsis. J Exp Bot **57:** 517–526

Blattner FR, Plunkett G III, Bloch CA, Perna NT, Burland V, Riley M, Collado-Vides J, Glasner JD, Rode CK, Mayrew GF et al., (1997) The compl**et**e genome sequence of *Escherichia coli* K-12. Science **277:** 1453-1474

Blokhina O and Fagerstedt KV (2010) Reactive oxygen species and nitric oxide in plant mitochondria: origin and redundant regulatory systems. Physiologia Plantarum **138:** 447-462

Broadbent P, Creissen GP, Kular B, Wellburn AR and Mullineaux PM (1995) Oxidative stress responses in transgenic tobacco containing altered levels of gluthatione reductase activity. Plant J **8:** 247-255

Buchanan BB and Balmer Y (2005) Redox regulation: a broadening horizon. Annu Rev Plant Biol **56:** 187–220

Cairns NG, Pasternak M, Wachter A, Cobbett CS and Meyer AJ (2006) Maturation of *Arabidopsis* seeds is dependent on glutathione biosynthesis within the embryo. Plant Physiol **141**: 446–455

Chen LS and Cheng L (2009) Photosystem 2 is more tolerant to high temperature in apple (*Malus domestica* Borkh.) leaves than in fruit peel. Photosynthetica **47:** 112-120

Chew O, Whelan J, Millar AH (2003) Molecular definition of the ascorbate-glutathione cycle in Arabidopsis mitochondria reveals dual targeting of antioxidant defenses in plants. J Biol Chem **278:** 46869–46877

Chivasa S and Carr JP (1998) Cyanide restores N gene-mediated resistance to tobacco mosaic virus in transgenic tobacco expressing salicylic acid hydroxylase. Plant Cell **10:** 1489-1498

Clough SJ and Bent AF (1998) Floral dip: a simplified method for ***Agrobacterium*-**mediated transformation of **Arabidopsis thaliana**. Plant J **16:** 735–743

Cobbett CS, May MJ, Howden R, Rolls B (1998) The glutathione-deficient, cadmium-sensitive mutant, cad2-1, of Arabidopsis thaliana is deficient in γ-glutamylcysteine synthetase. Plant J **16:** 73–78

Creissen G, Firmin J, FryerM, Kular B, Leyland N, Reynolds H, Pastori G, Wellburn F, Baker N, Wellburn A, Baker N, Wellburn A and Mullineaux P (1999) Elevated glutathione biosynthetic capacity in the chloroplasts of transgenic tobacco plants paradoxically causes increased oxidative stress. Plant Cell **11:** 1277–1291

Davey MR, Anthony P, Power JB and Lowe KC (2005) Plant protoplasts: Status and biotechnological perspectives. Biotechnol Adv **23**: 131-171

de Pinto MC, Paradiso A, Leonetti P and De Gara L (2006) Hydrogen peroxide, nitric oxide and cytosolic ascorbate peroxidase at the crossroad between defence and cell death. Plant J **48:** 784-795

del Rio LA, Sandalio LM, Corpas FJ, Palma J and, Barroso JB (2006) Reactive oxygen species and reactive nitrogen species in peroxisomes: production, scavenging and role in cell signaling. Plant Physiol **141:** 330–335

Delledonne M, Xia Y, Dixon RA and Lamb C (1998). Nitric Oxide Functions as a signal in plant disease resistance. Nature **394:** 585-588

Devi MT, Vani T, Reddy MM and Raghavendra AS (1992) Rapid isolation of mesophyll and guard cell protoplasts from pea and maize leaves. Indian J Exp Biol **30:** 424-428

Diaz M, Achkor H, Titarenko E and Martinez MC (2003) The gene encoding glutathione dependent formaldehyde dehydrogenase / GSNO reductase is responsive to wounding, jasmonic acid and salicylic acid. FEBS Lett **543:** 136-139

Dietz KJ (2003) Redox control, redox signaling, and redox homeostasis in plant cells. Int Rev Cytol **228:** 141–193

Dinakar CH, Abhaypratap V, Yearla SR, Raghavendra AS, Padmasree K (2010) Importance of ROS and antioxidant system during the beneficial interactions of mitochondrial metabolism with photosynthetic carbon assimilation. Planta **231:** 461-474

Diner BA and Petrouleas V (1990) Formation by NO of nitrosyl adducts of redox components of the photosystem II reaction center. II: Evidence that HCO_3^-/CO_2 binds to the acceptor-side non-heme iron. Biochim Biophys Acta **1015:** 141–149

Ding SH, Lu QT, Zhang Y, Yang ZP, Wen XG, Zhang LX and Lu CM (2009) Enhanced sensitivity to oxidative stress in transgenic tobacco plants with decreased glutathione reductase activity leads to a decrease in ascorbate pool and ascorbate redox state. Plant Mol Biol **69**: 577–592

Durner J, Wendehenne D and Klessig DF (1998). Defense gene induction in tobacco by nitric oxide, cyclic GMP and cyclic ADP-ribose. Proc Nat Sci **95:** 10328-10333

Dutilleul C, Driscoll S, Cornic G, De Paepe R, Foyer CH and Noctor G (2003) Functional mitochondrial complex I is required by tobacco leaves for optimal photosynthetic

performance in photorespiratory conditions and during transients. Plant Physiol **131:** 264–275

Ederli L, Morettini R, Borgogni A, Wasternack C, Miersch O, Reale L, Ferranti F, Tosti N, Pasqualini S (2006) Interaction between nitric oxide and ethylene in the induction of alternative oxidase in ozone-treated tobacco plants. Plant Physiol **142:** 595-608

Edwards EA, Rawsthorne S and Mullineaux PM (1990) Subcellular distribution of multiple forms of glutathione reductase in leaves of pea (*Pisum sativum* L.). Planta **180:** 278–284

Faraco M, Di Sansebastiano GP, Spelt K, Koes RE and Quattrocchio FM (2011) One Protoplast Is Not the Other! Plant Physiol **156:** 474-478

Feelisch M (1998) The use of nitric oxide donors in pharmacological studies. Naunyn Schmiedebergs Arch Pharmacol **358:** 113–122

Fernie AR, Carrari F and Sweetlove LJ (2004) Respiratory metabolism: glycolysis, the TCA cycle and mitochondrial electron transport. Curr Opin Plant Biol **7:** 254-261

Floryszak-Wieczorek J, Milczarek G, Arasimowicz M and Ciszewski A (2006) Do nitric oxide donors mimic endogenous NO-related response in plants? Planta **224**: 1363–1372

Foissner I, Wendehenne D, Langebartels C and Durner J (2000) In vivo imaging of an elicitor-induced nitric oxide burst in tobacco. Plant J **23:** 817–824

Forti G and Gerola P (1977) Inhibition of photosynthesis by azide and cyanide and the role of oxygen in photosynthesis. Plant Physiol **59:** 859–862

Foyer CH and Halliwell B (1976) The presence of glutathione and glutathione reductase in chloroplasts: A proposed role in ascorbic acid metabolism. Planta **133:** 21–25

Foyer CH and Noctor G (2000) Oxygen processing in photosynthesis: regulation and signaling. New Phytol **146:** 359–388

Foyer CH and Noctor G (2003) Redox sensing and signaling associated with reactive oxygen in chloroplasts, peroxisomes and mitochondria. Physiol Plant **119:** 355–364

Foyer CH and Noctor G (2005) Redox homeostasis and antioxidant signaling: a metabolic interface between stress perception and physiological responses. Plant Cell **17**: 1866-1875

Foyer CH and Noctor G (2009) Redox regulation in photosynthetic organisms: signaling, acclimation, and practical implications. Antioxid Redox Signal **11:** 861–905

Foyer CH and Noctor G (2011) Ascorbate and Glutathione: The Heart of the Redox Hub. Plant Physiol **155:** 2-18

Foyer CH, Lelandais M, Galap C and Kunert KJ (1991) Effects of Elevated Cytosolic Glutathione Reductase Activity on the Cellular Glutathione Pool and Photosynthesis in Leaves under Normal and Stress Conditions. Plant Physiol **97:** 863–872

Foyer CH, Lopez-Delgado H, Dat JF and Scott IM (1997) Hydrogen peroxide- and glutathione-associated mechanisms of acclamatory stress tolerance and signalling. Physiol Plant **100:** 241–254

Foyer CH, Rowell J and Walker D (1983) Measurement of the ascorbate content of spinach leaf protoplasts and chloroplasts during illumination. Planta **157:** 239–244

Foyer CH, Souriau N, Perret S, Lelandais M, Kunert KJ, Pruvost C and Jouanin L (1995) Overexpression of glutathione reductase but not glutathione synthetase leads to increases in antioxidant capacity and resistance to photoinhibition in poplar trees. Plant Physiol **109:** 1047–1057

Fryer MJ, Ball L, Oxborough K, Karpinski S, Mullineaux PM and BakerNR (2003) Control of ascorbate peroxidase 2 expression by hydrogen peroxide and leaf water status during excess light stress reveals a functional organisation of Arabidopsis leaves. Plant J **33:** 691–705

Gardestrom P, Igamberdiev AU and Raghavendra AS (2002) Mitochondrial functions in light. In: Foyer CH, Noctor G (eds) Photosynthetic nitrogen assimilation and associated carbon and respiratory metabolism. Kluwer Academic Publishers, The Netherlands, pp 151–172

Gas E, Flores-Pérez, Sauret-Güeto S and Rodríguez-Concepción M (2009) Hunting for plant nitric oxide synthase provides new evidence of a central role for plastids in nitric oxide metabolism. Plant Cell **21:** 18–23

Gegg ME, Beltran B, Salas-Pino S, Bolanos JP, Clark JB, Moncada S and Heales SJ (2003) Differential effect of nitric oxide on glutathione metabolism and mitochondrial function in astrocytes and neurones: Implications for neuroprotection/ neurodegeneration? J Neurochem **86**: 228–237

Gould KS, Lamotte O, Klinger A, Pugin A and Wendehenne D (2003) Nitric oxide production in tobacco leaf cells: A generalized stress response? Plant Cell Environ **26:** 1851–1862

Goussias C, Deligiannakis Y, Sanakis Y, Ioannidis N and Petrouleas V (2002) Probing subtle coordination changes in the iron-quinone complex of photosystem II during charge separation, by the use of NO. Biochemistry **41:** 15212–15223

Govindjee (1995) Sixty three years since Kautsky: Chlorophyll a fluorescence. Aust J Plant Physiol **22**: 131-160

Govindjee (2004) Chlorophyll a fluorescence: a bit of basics and history. *In* GC Papageorgiou, Govindjee, eds, Advances in Photosynthesis and Respiration: Chlorophyll a Fluorescence. A Signature of Photosynthesis. Springer, Dordrecht, The Netherlands, pp 1-42.

Grün S, Lindermayr C, Sell S and Durner J (2006) Nitric oxide and gene regulation in plants. J Exp Bot **57:** 507-516

Halliwell B and Gutteridge JMC (1999) Oxidative stress and antioxidant protection: some special cases. In: Halliwell B, Gutteridge JMC, editors. Free Radicals in Biology and Medicine. 3rd ed. Oxford: Clarendon Press; 530-533

Hanke GT, Holtgrefe S, König N, Strodtkötter I, Voss I and Scheibe R (2009) Use of transgenic plants to uncover strategies for maintenance of redox homeostasis during photosynthesis. Adv Bot Res **52:** 207–251

Harrison SJ, Mott EK, Parsley K, Aspinall S, Gray JC and Cottage A (2006) A rapid and robust method of identifying transformed Arabidopsis thaliana seedlings following floral dip transformation. Plant Methods **2**: 19

Hayat S, Hasan SA, Mori M, Fariduddin Q and Ahmad A (2010) Nitric oxide: chemistry, biosynthesis, and physiological role. In S Hayat, M Mori, J Pichtel, A Ahmad, eds, Nitric Oxide in Plant Physiology. Wiley-VCH Verlag GmbH & Co., KGaA, Weinheim, pp 1–15

Herschbach C, Rizzini L, Mult S, Hartmann T, Busch F, Peuke AD, Kopriva S and Ensminger I (2010) Over-expression of bacterial gamma-glutamylcysteine synthetase (GSH1) in plastids affects photosynthesis, growth and sulphur metabolism in poplar (Populus tremula x Populus alba) dependent on the resulting gamma-glutamylcysteine and glutathione levels. Plant Cell Environ **33:** 1138-51

Hill AC and Bennett JH (1970) Inhibition of apparent photosynthesis by nitrogen oxides. Atmos Environ **4:** 341–348

Hoagland DR and Arnon DI (1950) The water-culture method of growing plants without soil. California Agricultural Experiment Station Circular pp1-39

Huang X, von Rad U and Durner J (2002) Nitric oxide induces transcriptional activation of the nitric oxide-tolerant alternative oxidase in Arabidopsis suspension cells. Planta **215:** 914–923

Igamberdiev AU, Hurry V, Krömer S and Gardeström P (1998) The role of mitochondrial electron transport during photosynthetic induction. A study with barley (Hordeum vulgare) protoplasts incubated with rotenone and oligomycin. Physiol Plant **104:** 431-439

Innocenti G, Pucciariello C, Le Gleuher M, Hopkins J, Stefano M, Delledonne M, Puppo A, Baudouin E and Frendo P (2007) Glutathione synthesis is regulated by nitric oxide in Medicago truncatula roots. Planta **225**: 1597–1602

Ivanova LA, Ronzhina DA, Ivanov LA, Stroukova LV, Peuke AD and Rennenberg H (2011) Over-expression of *gsh1* in the cytosol affects the photosynthetic apparatus and improves the performance of transgenic poplars on heavy metal-contaminated soil. Plant Biol **13:** 649-659

Jasid S, Simontacchi M, Bartoli CG, Puntarulo S (2006) Chloroplasts as a nitric oxide cellular source: effect of reactive nitrogen species on chloroplastic lipids and proteins. Plant Physiol **142:** 1246–1255

Jiménez A, Hernandez JA, del Rio LA and Sevilla F (1997) Evidence for the presence of the ascorbate-glutathione cycle in mitochondria and peroxisomes of pea leaves. Plant Physiol **114:** 275–284

Jones DP (2006) Redefining oxidative stress. Antioxid Redox Signal **8**: 1865–1879

Joshi MK and Mohanty P (1995) Probing photosynthetic performance by chlorophyll fluorescence: Analysis and interpretation of fluorescence parameters. J Sci Ind Res **54**: 155-174

Karpinski S, Escobar C, Karpinska B, Creissen G, Mullineaux PM (1997) Photosynthetic electron transport regulates the expression of cytosolic ascorbate peroxidase genes in Arabidopsis during excess light stress. Plant Cell **9:** 627-640

Karpinski S, Gabrys H, Mateo A, Karpinska B and Mullineaux PM (2003) Light perception in plant disease defence signalling. Curr Opin Plant Biol **6:** 390–396

Kautsky H, Appel W and Amann H (1960) Chlorophyll fluorescence and carbon assimilation. Part XIII. The fluorescence and the photochemistry of plants. Biochem Z **332:** 277–292

Kojima H, Nakatsubo N, Kikuchi K, Kawahara S, Kirino Y, Nagoshi H, Hirata Y and Nagano T (1998) Detection and imaging of nitric oxide with novel fluorescent indicators: diaminofluoresceins. Anal Chem **70:** 2446–2453

Kopriva S and Rennenberg H (2004) Control of sulfate assimilation and glutathione synthesis: interaction with N and C metabolism. J Exp Bot **55**: 1831–1842

Kornyeyev D, Logan BA, Allen RD, and Holaday AS (2005) Field grown cotton plants with elevated activity of chloroplastic glutathione reductase exhibit no significant alteration of diurnal and seasonal patterns of excitation energy partitioning and CO2 fixation. Field Crops Res. **94:** 165-175

Kornyeyev D, Logan BA, Payton P, Allen RD and Holaday AS (2003) Elevated chloroplastic glutathione reductase activities decrease chilling induced photoinhibition by increasing rates of photochemistry but not thermal energy dissipation, in transgenic cotton. Func Plant Biol **30:** 101–110

Koussevitzky S, Suzuki N, Huntington S, Armijo L, Sha W, Cortes D, Shulaev V and Mittler R (2008) ASCORBATE PEROXIDASE 1 plays a key role in the response of Arabidopsis thaliana to stress combination. J Biol Chem **283**: 34197-34203

Krause GH and Weis E (1991) Chlorophyll fluorescence and photosynthesis: the basics. Annu Rev Plant Physiol Plant Mol Biol **42**: 313–349

Lazar D (2006) The polyphasic chlorophyll a fluorescence rise measured under high intensity of exciting light. Funct Plant Biol **33:** 9–30

Lee U, Wie C, Fernandez BO, Feelish M and Vierling E (2008) Modulation of nitrosative stress by S-nitrosoglutathione reductase is critical for thermo-tolerance and plant growth in Arabidopsis. Plant Cell **20**: 786–802

Leitner M, Vandelle E, Gaupels F, Bellin D and Delledonne M (2009) NO signal in the haze: nitric oxide signalling in plant defence. Curr Opin Plant Biol **12:** 451–458

Liedschulte V, Wachter A, Zhigang A and Rausch T (2010) Exploiting plants for glutathione (GSH) production: Uncoupling GSH synthesis from cellular controls results in unprecedented GSH accumulation. J Plant Biotechnol 8: 807-820

Lindermayr C, Saalbach G and Durner J (2005) Proteomic identification of *S*-nitrosylated proteins in Arabidopsis. Plant Physiol **137**: 921-930

Lindermayr C, Sell S, Müller B, Leister D and Durner J (2010) Redox Regulation of the NPR1-TGA1 System of *Arabidopsis thaliana* by Nitric Oxide. Plant Cell **22:** 2894–2907

Lum HK, Lee CH, Chu Butt YK and Lo SCL (2005) Sodium nitroprusside affects the level of photosynthetic enzymes and glucose metabolism in Phaseolus aureus (mung bean). Nitric Oxide **12:** 220–230

Ma WW, Xu WZ, Xu H, Chen YS, He ZY and Ma M (2010) Nitric oxide modulates cadmium influx during cadmium-induced programmed cell death in tobacco BY-2 cells. Planta **232:** 325–335

Mahan JR, Gitz DC, Payton PR and Allen R (2009) Overexpression of glutathione reductase in cotton does not alter emergence rates under temperature stress, Crop Sci. **49:** 272–280

Maruta T, Tanouchi A, Tamoi M, Yabuta Y, Yoshimura K, Ishikawa T and Shigeoka S (2010) Arabidopsis chloroplastic ascorbate peroxidase isoenzymes play a dual role in photoprotection and gene regulation under photooxidative stress. Plant Cell Physiol **51:** 190–200

Matsuo M and Obokata J (2006) Remote control of photosynthetic genes by the mitochondrial respiratory chain. Plant J **47:** 873–882

Maughan S and Foyer CH (2006) Engineering and genetic approaches to modulating the glutathione network in plants. Physiol Plant **126:** 382-397

Maughan SC, Pasternak M, Cairns N, Kiddle G, Brach T, Jarvis R, Haas F, Nieuwland J, Lim B, Müller C, Salcedo-Sora E, Kruse C, Orsel M, Hell R, Miller AJ, Bray P, Foyer CH, Murray JAH, Meyer AJ and Cobbett CS (2010) Plant homologs of the Plasmodium falciparum chloroquinone-resistance transporter, PfCRT, are required for glutathione homeostasis and stress responses. Proc Natl Acad Sci USA **107:** 2331-2336

Maxwell DP, Wang Y and McIntosh L (1999) The alternative oxidase lowers mitochondrial reactive oxygen production in plant cells. Proc Natl Acad Sci USA **96:** 8271-8276

May MJ, Vernoux T, Leaver C, Van Montagu M and Inzé D (1998) Glutathione homeostasis in plants: implications for environmental sensing and plant development. J Exp Bot **49:** 649–667

Mehta P, Jajoo A, Mathur S and Bharti S (2010) Chlorophyll *a* fluorescence study reveling effects of high salt stress on photosystem II in wheat leaves. Plant Physiol Biochem **48:** 16–20

Meyer AJ (2008) The integration of glutathione homeostasis and redox signaling. J Plant Physiol **165:** 1390–1403

Meyer AJ, Brach T, Marty L, Kreye S, Rouhier N, Jacquot JP and Hell R (2007) Redox-sensitive GFP in *Arabidopsis thaliana* is a quantitative biosensor for the redox potential of the cellular glutathione redox buffer. Plant J **52:** 973–986

Mezzari MP, Walters K, Jelinkova M, Shih MC, Just CL and Schnoor JL (2005) Gene expression and microscopic analysis of Arabidopsis exposed to chloroacetanilide herbicides and explosive compounds. A phytoremediation approach. Plant Physiol

138: 858–86

Mhamdi A, Hager J, Chaouch S, Queval G, Han Y, Taconnat L, Saindrenan P, Gouia H, Issakidis-Bourguet E, Renou JP and Noctor G (2010) Arabidopsis GLUTATHIONE REDUCTASE 1 plays a crucial role in leaf responses to intracellular hydrogen peroxide and in ensuring appropriate gene expression through both salicylic acid and jasmonic acid signaling pathways. Plant Physiol **153:** 1144-1160

Michelet L, Zaffagnini M, Marchand C, Collin V, Decottignies P, Tsan P, Lancelin JM, Trost P, Miginiac-Maslow M, Noctor G and Lemaire SD (2005) Glutathionylation of chloroplast thioredoxin-f is a redox signaling mechanism in plants. Proc Natl Acad Sci USA **102**: 16478–16483

Millar AH and Day DA (1996) Nitric oxide inhibits cytochrome oxidase but not alterntive oxidase in plant mitochondria. FEBS Lett **398:** 155-158

Millar AH, Whelan J, Soole KL and Day DA (2011) Organization and regulation of mitochondrial respiration in plants. Annu Rev Plant Biol **62:** 79-104

Miller G, Suzuki N, Ciftci-Yilmaz S and Mittler R (2010) Reactive oxygen species homeostasis and signalling during drought and salinity stresses. Plant Cell Environ **33:** 453–467

Miller G, Suzuki N, Rizhsky L, Hegie A, Koussevitzky S and Mittler R (2007) Double mutants deficient in cytosolic and thylakoid ascorbate peroxidase reveal a complex mode of interaction between reactive oxygen species, plant development, and response to abiotic stresses. Plant Physiol **144:** 1777-1785

Mittler R, Vanderauwera S, Gollery M, Breusegem FV (2004) Reactive oxygen gene network of plants. Trends Plant Sci **9:** 490-498

Mittler R, Vanderauwera S, Suzuki N, Miller G, Tognetti VB, Vandepoele K, Gollery M, Shulaev V and Van Breusegem F (2011) ROS signaling: the new wave? Trends Plant Sci **16:** 300-309

Møller IM (2001) Plant mitochondria and oxidative stress: Electron transport, NADPH turnover, and metabolism of reactive oxygen species. Annu Rev Plant Physiol Plant Mol Biol **52:** 561-591

Moller IM, Jensen PE and Hansson A (2007) Oxidative modifications to cellular components in plants. Annu Rev Plant Biol **58:** 459–481

Moreau M, Lindermayr C, Durner J and Klessig DF (2010) NO synthesis and signalling in plants: where do we stand? Physiol Plant **138:** 372–383

Mubarakshina MM, Ivanov BN, Naydov IA, Hillier W, Badger MR and Krieger-Liszkay A (2010) Production and diffusion of chloroplastic H_2O_2 and its implication to signaling. J Exp Bot **61:** 3577-3587

Mullineaux PM and Rausch T (2005) Glutathione, photosynthesis and the redox regulation of stress-responsive gene expression. Photosynth. Res **86:** 459–474

Mullineaux PM, Creissen G, Broadbent P, Reynolds H, Kular B and Wellburn A (1994) Elucidation of the role of glutathione reductase using transgenic plants. Biochem Soc Trans **22:** 931–936

Mullineaux PM, Karpinski S and Baker NR (2006) Spatial dependence for hydrogen peroxide-directed signalling in light stressed plants. Plant Physiol **141:** 346–350

Murgia I, de Pinto MC, Delledonne M, Soave C and De Gara L (2004) Comparative effects of various nitric oxide donors on ferritin regulation, programmed cell death, and cell redox state in plant cells. J Plant Physiol **161:** 777–783

Navarre DA, Wendehenne D, Durner J, Noad R and Klessig DF (2000) Nitric oxide modulates the activity of tobacco aconitase. Plant Physiol **122:** 573-582

Navrot N, Rouhier N, Gelhaye E and Jaquot JP (2007) Reactive oxygen species generation and antioxidant systems in plant mitochondria. Physiol Plant **129:** 185–195

Neil S, Desikan R, Clarke A, Hurst R and Hancock JT (2002) Hydrogen peroxide and nitric oxide as signalling molecules in plants. J Exp Bot **53:** 1237-1247

Neill S, Barros R, Bright J, Desikan R, Hancock J, Harrison J, Morris P, Ribeiro D and Wilson I (2008) Nitric oxide, stomatal closure, and abiotic stress. J Exp Bot **59**: 165–176

Nishimura M, Douce R and Akazawa T (1985) A Simple Method for Estimating Intactness of Spinach Leaf Protoplasts by Glycolate Oxidase Assay. Plant Physiol **78**: 343-346

Nishiyama Y, Allakhverdiev SI and Murata N (2006) A new paradigm for the action of reactive oxygen species in the photoinhibition of photosystem II. Biochim Biophys Acta **1757:** 742-749

Noctor G (2006) Metabolic signalling in defence and stress: the central roles of soluble redox couples. Plant, Cell and Environment **29:** 409-425

Noctor G and Foyer CH (1998) Ascorbate and glutathione: Keeping active oxygen under control. Annu Rev Plant Physiol Plant Mol Biol 49:249–279.

Noctor G and Foyer CH (1998) Simultaneous measurement of foliar glutathione and amino acids by high-performance liquid chromatography: a comparison with two other methods for assay of glutathione. Anal Biochem **264:** 98–110

Noctor G, Arisi A-CM, Jouanin L and Foyer CH (1998) Manipulation of glutathione and amino acid biosynthesis in the chloroplast. Plant Physiol **118:** 471–482

Noctor G, De Paepe R and Foyer CH (2007) Mitochondrial redox biology and homeostasis in plants. Trends Plant Sci **12:** 125–134

Noctor G, Gomez L, Vanacker H and Foyer CH (2002) Interactions between biosynthesis, compartmentation and transport in the control of glutathione homeostasis and signalling. J Exp Bot **53**: 1283–1304

Noctor G, Queval G, Mhamdi A, Chaouch S and Foyer CH (2011) Glutathione. *In* The Arabidopsis Book. American Society of Plant Biologists, Rockville, MD **9:** 1-32

Noctor G, Strohm M, Jouanin L, Kunert KJ, Foyer CH and Rennenberg H (1996) Synthesis of glutathione in leaves of transgenic poplar (Populus tremula × P. alba) overexpressing γ-glutamylcysteine synthetase. Plant Physiol **112:**1071–1078

Noguchi K and Yoshida K (2008) Interaction between photosynthesis and respiration in illuminated leaves. Mitochondrion **8:** 87-99

Nunes-Nesi A, Sulpice R, Gibon Y and Fernie AR (2008) The enigmatic contribution of mitochondrial function in photosynthesis. J Exp Bot **59:** 1675-1684

Nunes-Nesi A, Sweetlove LJ and Fernie AR (2007) Operation and function of the tricarboxylic acid cycle in the illuminated leaf. Physiol Plant **129**: 45-56

Ort DR and Baker NR (2002) A photoprotective role for O_2 as an alternative electron sink in photosynthesis. Curr Opin Plant Biol **5:** 193–198

Oukarroum A, Schansker G and Strasser RJ (2009) Drought stress effects on photosystem I content and photosystem II thermotolerance analyzed using Chl a fluorescence kinetics in barley varieties differing in their drought tolerance. Physiol Plant **137**: 188–199

Padmasree K and Raghavendra AS (1999) Importance of oxidative electron transport over oxidative phosphorylation in optimizing photosynthesis in mesophyll protoplasts of pea (Pisum sativum L). Physiol Plant **105:** 546-553

Padmasree K and Raghavendra AS (2001) Consequence of restricted mitochondrial oxidative metabolism on photosynthetic carbon assimilation in mesophyll protoplasts: Decrease in light activation of four chloroplastic enzymes. Physiol Plant **112:** 582–588

Padmasree K, Padmavathi L and Raghavendra AS (2002) E**ss**enti**al**ity of mitochondri**al** oxid**a**tive met**a**bo**l**i**s**m for photo**s**ynthe**sis**: optimiz**a**tion of c**a**rbon **ass**imi**la**tion **and** protection **a**g**a**in**s**t photoinhibition. Crit Rev Biochem Mo**l** Bio**l 37**: 71–119

Palmieri MC, Sell S, Huang X, Scherf M, Werner T, Durner J and Lindermayr C (2008) Nitric oxide-responsive genes and promoters in *Arabidopsis thaliana*: a bioinformatics approach. J Exp Bot **59:** 177–186

Parani M, Rudrabhatla S, Myers R, Weirich H, Smith B, Leaman DW and Goldman SL (2004) Microarray analysis of nitric oxide responsive transcripts in *Arabidopsis*. Plant Biotechnol J **2:** 359–366

Parisy V, Poinssot B, Owsianowski L, Buchala A, Glazebrook J, Mauch F (2007) Identification of PAD2 as a γ-glutamylcysteine synthetase highlights the importance of glutathione in disease resistance of Arabidopsis. Plant J **49:** 159–172

Pasternak M, Lim B, Wirtz M, Hell R, Cobbett CS and Meyer AJ (2008) Restricting glutathione biosynthesis to the cytosol is sufficient for normal plant development. Plant J **53:** 999–1012

Pesaresi P, Schneider A, Kleine T and Leister D (2007) Interorganellar communication. Curr Opin Plant Biol **10:** 600-606

Pfannschmidt T, Bräutigam K, Wagner R, Dietzel L, Schröter Y, Steiner S and Nykytenko A (2009) Potential regulation of gene expression in photosynthetic cells by redox and energy state: approaches towards better understanding. Ann Bot **103**: 599–607

Pfannschmidt T, Nilsson A and Allen JF (1999) Photosynthetic control of chloroplast gene expression. Nature **397**: 625–628

Pignocchi C and Foyer CH (2003) Apoplastic ascorbate metabolism and its role in the regulation of cell signalling. Curr Opinion Plant Biol **6**: 379-389

Pilon-Smits EAH, Zhu YL, Sears T and Terry N (2000) Overexpression of glutathione reductase in Brassica juncea: effects on cadmium accumulation and tolerance. Physiol Plant **110:** 455–460

Pitzschke A, Forzani C and Hirt H (2006) Reactive oxygen species signaling in plants. Antioxid Redox Signal **8:** 1757-1764

Polverari A, Molesini B, Pezzotti M, Buonaurio R, Marte M and Delledonne M (2003) Nitric oxide-mediated transcriptional changes in *Arabidopsis thaliana.* Mol Plant-Microbe Interact **16:** 1094–1105

Prakash JSS, Srivastava A, Strasser RJ and Mohanty P (2003) Senescence-induced alternation in the photosystem II functions of *Cucumis sativus* cotyledons: probing of senescence driven alternation of photosystem II by chlorophyll *a* fluorescence induction O-J-I-P transients. Indian J Biochem Biophys **40**:160–168

Priault P, Tcherkez G, Cornic G, De Paepe R, Naik R, Ghashghaie J, Streb P (2006) The lack of mitochondrial complex I in a CMSII mutant of Nicotiana sylvestris increases photorespiration through an increased internal resistance to CO_2 diffusion. J Exp Bot **57:** 3195–3207

Purvis AC (1997) Role of the alternative oxidase in limiting superoxide production by plant mitochondria. Physiol Plant **100:** 165-170

Queval G, Issakidis-Bourguet E, Hoeberichts FA, Vandorpe M, Gakiere B, Vanacker H, Miginiac-Maslow M, Van Breusegem F and Noctor G (2007) Conditional oxidative stress responses in the Arabidopsis photorespiratory mutant *cat2* demonstrate that redox state is a key modulator of daylength-dependent gene expression and define photoperiod as a crucial factor in the regulation of H_2O_2-induced cell death. Plant J **52:** 640–657

Queval G, Thominet D, Vanacker H, Miginiac-Maslow M, Gakière B and Noctor G (2009) H_2O_2-activated up-regulation of glutathione in Arabidopsis involves induction of genes encoding enzymes involved in cysteine synthesis in the chloroplast. Mol Plant **2:** 344-356

Quick WP and Horton P (1984) Studies on the induction of chlorophyll fluorescence in barley protoplast. 11. Resolution of fluorescence quenching by redox state and the transthylakoid pH gradient. Proc R SOC Lond B 220: 371-382

Quick WP and Horton P (1986) Studies on the induction of chlorophyll fluorescence in barley protoplasts. III. Correlation between changes in the level of glycerate 3-phosphate and the pattern of fluorescence quenching. Biochim Biophys Acta **849:** 1-6

Raghavendra AS and Padmasree K (2003) Beneficial interactions of mitochondrial metabolism with photosynthetic carbon assimilation. Trends Plant Sci **8:** 546 −553

Reddy AR, Raghavendra AS (2006) Photooxidative stress. In: KV Madhava Rao, Raghavendra AS, Reddy KJ (eds): Physiology and molecular biology of stress tolerance in plants, Springer, The Netherlands, pp.157-186

Reddy MM, Vani T, Raghavendra AS (1991) Light-enhanced dark respiration in mesophyll protoplasts from leaves of pea. Plant Physiol **96:** 1368-1371

Reichheld JP, Khafif M, Riondet C, Droux M, Bonnard G and Meyer Y (2007) Inactivation of thioredoxin reductases reveals a complex interplay between thioredoxin and glutathione pathways in *Arabidopsis* development. Plant Cell **19:** 1851–1865

Riazunnisa K, Padmavathi L, Scheibe R and Raghavendra AS (2007) Preparation of *Arabidopsis* mesophyll protoplasts with high rates of photosynthesis. Physiol Plant **129**: 679–686

Romero-Puertas MC, Corpas FJ, Sandalio LM, Leterrier M, Rodriguez-Serrano M, del Rio LA, Palma JM (2006) Glutathione reductase from pea leaves: response to abiotic stress and characterization of the peroxisomal isozyme. New Phytol **170:** 43-52

Rouhier N, Lemaire S and Jacquot JP (2008) The role of glutathione in photosynthetic organisms, emerging functions for glutaredoxins and glutathionylation. Annu Rev Plant Biol **59:** 143-166

Rozen S and Skaletsky HJ (2000) Primer3 on the WWW for general users and for biologist programmers. *In* S Krawetz, S Misener, eds, Bioinformatics Methods and Protocols: Methods in Molecular Biology. Humana Press, Totowa, NJ, pp 365-386

Rumer S, Gupta KJ and Kaiser WM (2009) Plant cells oxidize hydroxylamines to NO. J Exp Bot **60:** 2065–2072

Rusterucci C, Espunya MC, Diaz M, Chabannes M and Martinez MC (2007) S-Nitrosoglutathione reductase affords protection against pathogens in Arabidopsis, both locally and systemically. Plant Physiol **143:** 1282–1292

Sanakis Y, Goussias C, Mason RP and Petrouleas V (1997) NO interacts with the tyrosine radical YD_ of photosystem II to form an iminoxyl radical. Biochemistry **36:** 1411–1417

Saradadevi K and Raghavendra AS (1992) Dark respiration protects photosynthesis against photoinhibition in mesophyll protoplasts of pea (*Pisum sativum*). Plant Physiol **99:** 1232-1237

Schansker G, Goussias C, Petrouleas V and Rutherford AW (2002) Reduction of the Mn cluster of the water-oxidizing enzyme by nitric oxide: formation of an S-2 state. Biochemistry **41:** 3057–3064

Schansker G, Tóth SZ and Strasser RJ (2005) Methylviologen and dibromothymoquinone treatments of pea leaves reveal the role of photosystem I in the Chl *a* fluorescence rise OJIP. Biochim Biophys Acta **1706:** 250–261

Schansker G, Tóth SZ and Strasser RJ (2006) Dark recovery of the Chl *a* fluorescence transient (OJIP) after light adaptation: the q*T*-component of non-photochemical quenching is related to an activated photosystem I acceptor side. Biochim Biophys Acta **1757**: 787–797

Scheibe R (2004) Malate valves to balance cellular energy supply. Physiol Plant **120**: 21–26

Schreiber U and Neubauer C (1987) The polyphasic rise of chlorophyll fluorescence upon onset of strong illumination: II. Partial control by the Photosystem II donor side and possible ways of interpretation. Z Naturforsch **42:** 1255-1264

Schreiber U, Hormann H, Neubauer C and Klughammer C (1995) Assessment of photosystem II photochemical quantum yield by chlorophyll fluorescence quenching analysis. Aust J Plant Physiol **22**: 209-220

Sheen J (2001) Signal transduction in maize and *Arabidopsis* mesophyll protoplasts. Plant Physiol **127:** 1466–1475

Smirnoff N and Wheeler GL (2000) Ascorbic acid in plants: Biosynthesis and function. Crit Rev Biochem Mol Biol **35:** 291–314

Srivastava A, Strasser RJ and Govindjee (1995) Polyphasic rise of chlorophyll a fluorescence intensity and quantum yield of photosystem II of herbicide-resistant D1 mutants of Chlamydomonas reinhardtii. Photosynth Res **43:** 131-141

Stirbet A and Govindjee (2011) On the relation between the Kautsky effect (chlorophyll *a* fluorescence induction) and photosystem II: Basics and applications of the OJIP fluorescence transient. J Photochem Photobiol B **104:** 236-57

Stöhr C and Ullrich WR (2002) Generation and possible roles of NO in plant roots and their apoplastic space. J Exp Bot **53:** 2293–2303

Strasser RJ and Govindjee (1992) On the O-J-I-P fluorescence transient in leaves and D1 mutants of Chlamydomonas reinhardtii. In: Murata N (ed) Research in Photosynthesis, Vol II,Kluwer Academic Publishers, Dordrecht. pp 29-32

Strasser RJ, Tsimilli-Michael M and Srivastava A (2004) Analysis of the chlorophyll a fluorescence transient. *In* GC Papageorgiou, Govindjee, eds, Advances in Photosynthesis and Respiration: Chlorophyll a Fluorescence. A Signature of Photosynthesis. Springer, Dordrecht, The Netherlands, pp 321–362

Strasser BJ and Strasser RJ (1995) Measuring fast fluorescence transients to address environmental questions: the JIP-test. *In* P Mathis, eds, Photosynthesis: from light to biosphere. Kluwer Academic Publishers, Dordrecht, pp 977–980

Strasser RJ, Srivastava A, Tsimilli-Michael M (2000) The fluorescence transient as a tool to characterize and screen photosynthetic samples. In: Probing photosynthesis: mechanisms, regulation and adaptation, M. Yunus, U. Pathre, P. Mohanty (eds.), Taylor & Francis, London, GB, Ch. 25: pp. 445-483 (2000)

Strauss AJ, Krüger GHJ, Strasser J and Van Heerdena PDR (2007) The role of low soil temperature in the inhibition of growth and PSII function during dark chilling in soybean genotypes of contrasting tolerance. Physiol Plant **131**: 89–105

Strohm M, Jouanin L, Kunert KJ, Pruvost C, Polle A, Foyer CH and Rennenberg H (1995) Regulation of glutathione synthesis in leaves of transgenic poplar (Populus tremula×P. alba) overexpressing glutathione synthetase. Plant J **7:** 141–145

Sunil B, Riazunnisa K, Sai Krishna T, Schansker G, Strasser RJ, Raghavendra AS, Mohanty P (2008) Application of fast chlorophyll *a* fluorescence transient (OJIP)

analysis to monitor functional integrity of pea (*Pisum sativum*) mesophyll protoplasts during isolation. Indian J Biochem Biophys **45**: 37-43

Sweetlove LJ, Beard KFM, Nunes-Nesi A, Fernie AR and Ratcliffe RG (2010) Not just a circle: flux modes in the plant TCA cycle. Trends Plant Sci **15:** 462–470

Sweetlove LJ, Fait A, Nunes-Nesi A, Williams T and Fernie AR (2007) The mitochondrion: an integration point of cellular metabolism and signaling. Crit Rev Plant Sci **26:** 17-43

Takahashi S and Yamasaki H (2002) Reversible inhibition of photophosphorylation in chloroplasts by nitric oxide. FEBS Lett **512:** 145-148.

Talla SK, Riazunnisa K, Padmavathi L, Sunil B, Rajsheel P and Raghavendra AS (2011) Ascorbic acid is a key participant during the interactions between chloroplasts and mitochondria to optimize photosynthesis and protect against photoinhibition. J Biosci **36:** 163–173

Tanou G, Molassiotis A and Diamantidis G (2009) Hydrogen peroxide- and nitric oxide-induced systemic antioxidant prime-like activity under NaCl-stress and stress-free conditions in citrus plants. J Plant Physiol **166:** 1904–1913

Tcherkez G and Farquhar GD (2005) Carbon isotope effect predictions for enzymes involved in the primary carbon metabolism of plant leaves. Funct Plant Biol **32**: 277-291

Tietze F (1969) Enzymic method for quantitative determination of nanogram amounts of total and oxidized glutathione: applications to mammalian blood and other tisues. Anal Biochem **27:** 502–522

Topfer R, ScheU J and Steinbis HH (1988) Versatile cloning vectors for transient gene expression and direct gene transfer in plants. Nucl Acids Res **16:** 8725

Tóth SZ, Schansker G, Garab G and Strasser RJ (2007) Photosynthetic electron transport activity in heat-treated barley leaves: the role of internal alternative electron donors to photosystem II. Biochim Biophys Acta **1767:** 295–305

Tsimilli-Michael M and Strasser RJ (2008) In vivo assessment of plants'vitality: applications in detecting and evaluating the impact of mycorrhization on host plants. In: Varma A, ed. Mycorrhiza: state of the art, genetics and molecular biology, eco-function, biotechnology, eco-physiology, structure and systematics, 3rd edn. Berlin: Springer, 679–703.

Tzafrir I, Pena-Muralla R, Dickermann A, Berg M, Rogers R, Hutchens S, Sweeney TC, McElver J, Aux G, Patton D, et al (2004) Identification of genes required for embryo development in Arabidopsis. Plant Physiol **135:** 1206–1220

Valderrama R, Corpas FJ, Carreras A, Fernández-Ocaña A, Chaki M, Luque F, Gómez-Rodríguez MV, Colmenero-Varea P, Del Río LA and Barroso JB (2007) Nitrosative stress in plants. FEBS Lett **581**: 453–461

Vandenabeele S, Van Der Kelen K, Dat J, Gadjev I, Boonefaes T, Morsa S, Rottiers P, Slooten L, Van Montagu M, Zabeau M, Inze D and Van Breusegem FA (2003)

comprehensive analysis of hydrogen peroxide-induced gene expression in tobacco. Proc Natl Acad Sci USA **100:** 16113– 16118

Vanderauwera S, Zimmermann P, Rombauts S, Vandenabeele S, Langebartels C, Gruissem W, Inze D and Van Breusegem F (2005) Genome-wide analysis of hydrogen peroxide-regulated gene expression in Arabidopsis reveals a high light-induced transcriptional cluster involved in anthocyanin biosynthesis. Plant Physiol **139:** 806– 821

Veljovic-Jovanovic SD, Pignocchi C, Noctor G and Foyer CH (2001) Low ascorbic acid in the vtc-1 mutant of Arabidopsis is associated with decreased growth and intracellular redistribution of the antioxidant system. Plant Physiol **127:** 426–435

Wachter A, Wolf S, Steiniger H, Bogs J and Rausch T (2005) Differential targeting of GSH1 and GSH2 is achieved by multiple transcription initiation: implications for the compartmentation of glutathione biosynthesis in the Brassicaceae. Plant J **41:** 15-30

Wagner AM and Moore AL (1997) Structure and function of the plant alternative oxidase: its putative role in the oxygen defence mechanism. Biosci Rep **17:** 319-333

Wagner U, Edwards R, Dixon DP and Mauch F (2002) Probing the diversity of the Arabidopsis glutathione *S*-transferase gene family. Plant Mol Biol **49**: 515–532

Walker D (1988) The use of the oxygen electrode and fluorescence probes in simple measurements of photosynthesis. University of Sheffield press, Sheffield, UK

Wang PG, Xian M, Tang X, Wu X, Wen Z, Cai T and Janczuk AJ (2002) Nitric oxide donors: chemical activities and biological applications. Chem Rev **102:** 1091-1134

Wilson ID, Neill SJ and Hancock JT (2008) Nitric oxide synthesis and signaling in plants. Plant Cell Environ **31:** 622-631

Wishnick M and Lane MD (1969) Inhibition of ribulose diphosphate carboxylase by cyanide. J Biol Chem **244:** 55–59

Wodala B, Deák Z, Vass I, Erdei L, Altorjay I and Horváth F (2008) In vivo target sites of nitric oxide in photosynthetic electron transport as studied by chlorophyll fluorescence in pea leaves. Plant Physiol **146:** 1920–1927

Xiang C and Oliver DJ (1998) Glutathione metabolic genes coordinately respond to heavy metals and jasmonic acid in Arabidopsis. Plant Cell **10:**1539-1550

Yang JD, Zhao HL, Zhang TH and Yun JF (2004) Effects of exogenous nitric oxide on photochemical activity of photosystem II in potato leaf tissue under non-stress condition. Acta Bot Sin **46:** 1009–1014

Yap LP, Garcia JV, Han DS and Cadenas E (2010) Role of nitric oxide-mediated glutathionylation in neuronal function: potential regulation of energy utilization. Biochemical J **428**: 1-85

Yoo SD, Cho YH, Sheen J (2007) Arabidopsis mesophyll protoplasts: a versatile cell system for transient gene expression analysis. Nat Protocols **2:** 1565–1572

Yoshida K, Terashima I and Noguchi K (2006) Distinct roles of the cytochrome pathway and alternative oxidase in leaf photosynthesis. Plant Cell Physiol **47:** 22-31

Yoshida K, Terashima I and Noguchi K (2007) Up-regulation of mitochondrial alternative oxidase concomitant with chloroplast over-reduction by excess light. Plant Cell Physiol **48:** 606-614

Zago E, Morsa S, Dat JF, Alard P, Ferrarini A, Inze D, Delledonne M and Van Breusegem F (2006) Nitric oxide- and hydrogen peroxide-responsive gene regulation during cell death induction in tobacco. Plant Physiol **141:** 404-411

Zhao MG, Chen L, Zhang LL, Zhang WH (2009) Nitric reductase-dependent nitric oxide production is involved in cold acclimation and freezing tolerance in Arabidopsis. Plant Physiol **151:** 755-767

Zimmermann P, Hirsch-Hoffmann M, Hennig L and Gruissem W (2004) GENEVESTIGATOR: Arabidopsis microarray database and analysis toolbox. Plant Physiol **136:** 2621–2632

Zottini M, Formentin E, Scattolin M, Carimi F, Lo Schiavo F and Terzi M (2002) Nitric oxide affects plant mitochondrial functionality in vivo. FEBS Lett **515:** 75-78

*****

Annexure

Research publications and papers presented

(First pages of the article are attached)

Research Publications:

1. Talla S, Riazunnisa K, Padmavathi L, **Sunil B**, Rajsheel P, Raghavendra AS (2011) Ascorbic acid is a key participant during the interactions between chloroplasts and mitochondria to optimize photosynthesis and protect against photoinhibition. J Biosci **36:** 163-73
2. **Sunil B**, Riazunnisa K, Sai Krishna T, Schansker G, Strasser RJ, Raghavendra AS, Mohanty P (2008) Application of fast chlorophyll *a* fluorescence transient (OJIP) analysis to monitor functional integrity of pea (*Pisum sativum*) mesophyll protoplasts during isolation. Indian J Biochem Biophys **45**: 37-43
3. **Sunil B**, Raghavendra AS (2005) Recent advances in biochemistry of photosynthetic carbon assimilation. Proc AP Akad Sci **9**: 305-312
4. **Sunil B**, Ramireddy E, Raghavendra AS (2005) Manipulation of photosynthetic carbon metabolism through biotechnology. Proc AP Akad Sci **3**: 237-242

Book chapters/ Symposia proceedings:

1. Riazunnisa K, Padmavathi L, **Sunil B**, Raghavendra AS (2008) Multiple factors mediate the crosstalk between mitochondrial metabolism and photosynthetic carbon assimilation: roles of photorespiratory CO_2 and ascorbate. In JF Allen, E Gantt, JH Golbek, B Osmond, eds, Photosynthesis. Energy from the Sun. Springer Netherlands, pp. 1057-1061
2. **Sunil B**, Raghavendra AS (2006) Genetic manipulation of photosynthesis in higher plants: Progress and Possible applications. In PC Trivedi, eds, Plant Biotechnology: Perspectives and prospects. Pointer Publishers, Jaipur, India, pp. 4-20
3. Padmavathi L, Riazunnisa K, **Sunil B**, Raghavendra AS (2005) Role of Ascorbic acid during interaction between mitochondria and chloroplasts to optimize photosynthesis. In A Van der Est, D Bruce, eds, Photosynthesis: Fundamental Aspects to Global Perspectives. Alliance Communications Group, Lawrence, KS, USA, pp. 928-930

Papers presented at the conferences:

1. **B. Sunil** and Agepati S. Raghavendra. Identification of possible targets of nitric oxide (NO) during modulation of photosynthesis by NO in pea mesophyll protoplasts. International conference on plant science in post genomic era (ICPSPGE-2011); 17th-19th February 2011; Sambalpur University, Orissa, India.
2. **B. Sunil**, Reto J Strasser, Prasanna Mohanty and Agepati S Raghavendra. Possible role of nitric oxide (NO) as biochemical signal during photosynthesis, respiration and their interactions in mesophyll protoplasts of pea (*Pisum sativum*. L). Photosynthesis in the Global Perspective; 27th - 29th November 2008; Indore, India.
3. **B. Sunil**, Guillaume Queval, Graham Noctor and Agepati S. Raghavendra. Metabolic cross talk between chloroplasts & mitochondria: Role of nitric oxide and its interaction with Glutathione metabolism. BioQuest-2008; 15th - 16th March 2008; University of Hyderabad, Hyderabad, India.
4. **B. Sunil**, K. Riazunnisa, L. Padmavathi, and Agepati S Raghavendra. Metabolic cross talk between chloroplasts and mitochondria: role of reactive oxygen species, nitric oxide and ascorbic acid. International Conference on Plant Mitochondria Biology (ICPMB); 28th May - 2nd June 2005; Strasbourg, France.
5. **B. Sunil**, G. Vijay Kumar and Agepati S. Raghavendra. Role of nitric oxide during interaction between photosynthesis and respiration in mesophyll protoplasts of pea (Pisum sativum. L). XVII National Symposium on Photosciences for the Millennium (NASPHOM); 19th-21st February 2005; Sambalpur University, Orissa, India.
6. L. Padmavathi, K. Riazunnisa, **B. Sunil** and Agepati S Raghavendra. Role of Ascorbic acid during interaction between mitochondria and chloroplasts to optimize photosynthesis. 13th International congress of Photosynthesis; 29thAugust - 3rd September 2004; Montreal, Canada.

Ascorbic acid is a key participant during the interactions between chloroplasts and mitochondria to optimize photosynthesis and protect against photoinhibition

SAIKRISHNA TALLA, KHATEEF RIAZUNNISA, LOLLA PADMAVATHI, BOBBA SUNIL, PIDAKALA RAJSHEEL and AGEPATI S RAGHAVENDRA*

Department of Plant Sciences, School of Life Sciences, University of Hyderabad, Hyderabad 500 046, India

**Corresponding author (Fax, +91-40-23010120; Email, asrsl@uohyd.ernet.in; as_raghavendra@yahoo.com)*

The possible role of L-ascorbate (AsA) as a biochemical signal during the interactions between photosynthesis and respiration was examined in leaf discs of *Arabidopsis thaliana*. AsA content was either decreased as in AsA-deficient *vtc1* mutants or increased by treatment with L-galactono-1, 4-lactone (L-GalL, a precursor of AsA; EC 1.3.2.3). In mutants, photosynthesis was extremely sensitive to both antimycin A (inhibitor of the cytochrome *c* oxidase pathway [COX pathway]) and salicylhydroxamic acid (SHAM, inhibitor of the alternative pathway [AOX pathway]), particularly at high light conditions. Mitochondrial inhibitors lowered the ratio of reduced AsA to total AsA, at high light, indicating oxidative stress in leaf discs. Elevation of AsA by L-GalL decreased the sensitivity of photosynthesis at high light to antimycin A or SHAM, sustained photosynthesis at supraoptimal light and relieved the extent of photoinhibition. High ratios of reduced AsA to total AsA in L-GalL-treated leaf discs suggests that L-GalL lowers oxidative stress. The protection by L-GalL of photosynthesis against the mitochondrial inhibitors and photoinhibition was quite pronounced in *vtc1* mutants. Our results suggest that the levels and redox state of AsA modify the pattern of modulation of photosynthesis by mitochondrial metabolism. The extent of the AOX pathway as a percentage of the total respiration in *Arabidopsis* mesophyll protoplasts was much higher in *vtc1* than in wild type. We suggest that the role of AsA becomes pronounced at high light and/or when the AOX pathway is inhibited. While acknowledging the importance of the COX pathway, we hypothesize that AsA and the AOX pathway may complement each other to protect photosynthesis against photoinhibition.

[Talla S, Riazunnisa K, Padmavathi L, Sunil B, Rajsheel P and Raghavendra AS 2011 Ascorbic acid is a key participant during the interactions between chloroplasts and mitochondria to optimize photosynthesis and protect against photoinhibition. *J. Biosci.* **36** 163–173] **DOI** 10.1007/s12038-011-9000-x

1. Introduction

Interorganelle interactions between chloroplasts and mitochondria through cytosol and peroxisomes are essential for the optimization of photosynthesis (Gardeström *et al*. 2002; Padmasree *et al*. 2002; Noctor *et al*. 2007; Nunes-Nesi *et al*. 2008). Such an interaction between chloroplasts and mitochondria is not surprising, but is intriguing. A well-known basis of interorganelle interactions is the exchange of metabolites between them. However, there could be other possible signals, such as reactive oxygen species (ROS), nitric oxide (NO), cytosolic pH and

Keywords. L-Ascorbate; L-galactone-1, 4-lactone; interorganelle interaction; *vtc1* mutant

Abbreviations used: AOX, alternative oxidase; AsA, ascorbate; CCCP, carbonyl cyanide *m*-chlorophenylhydrazone; COX, cytochrome c oxidase; L-GalL, L-galactono-1, 4-lactone; DHA, dehydroascorbate; L-GalLDH, L-galactono-1, 4-lactone dehydrogenase; L-GalLDH, L-galactono-1, 4-lactone dehydrogenase; H_2O_2, hydrogen peroxide; ROS, reactive oxygen species; SHAM, salicylhydroxamic acid

Indian Journal of Biochemistry & Biophysics
Vol. 45, February 2008, pp. 37-43

Application of fast chlorophyll *a* fluorescence transient (OJIP) analysis to monitor functional integrity of pea *(Pisum sativum)* mesophyll protoplasts during isolation

B Sunil[1], K Riazunnisa[1], T Sai Krishna[1], Gert Schansker[2], Reto J Strasser[2], Agepati S Raghavendra[1] and Prasanna Mohanty[1*#]

[1]Department of Plant Sciences, School of Life Sciences, University of Hyderabad, Hyderabad 500 046, India
[2]Bioenergetics Laboratory, University of Geneva, CH-1254, Jussy-Geneva, Switzerland

Received 10 May 2007; revised 28 November 2007

Intact and metabolically very active mesophyll protoplasts were isolated rapidly from pea (*Pisum sativum)* leaves. The functional performance of protoplasts at various stages of their isolation was analyzed by using fast Chl *a* fluorescence OJIP transients and compared with that of intact leaves. The results demonstrated that the OJIP transients could successfully be used to monitor the quality of mesophyll protoplasts at different isolation steps. The protoplasts maintained their integrity and photosynthetic status very well, and their performance was very similar to that of the intact leaves.

Keywords: Chl *a* fluorescence, Functional integrity, Mesophyll protoplasts, O-J-I-P Transients, *Pisum sativum*, Protoplast isolation

Plant protoplasts form unique, single cell and versatile system for use in a variety of biochemical, biophysical and physiological experiments[1]. They find use in tissue culture, plant transformation and in several other fields of modern biotechnology. The protoplasts, which represent cell wall less mesophyll cells have been isolated from a variety of tissues both from monocotyledonous and dicotyledonous plants. The yield and efficiency besides the intactness are important for protoplast isolation.

Application of chlorophyll (Chl *a*) fluorescence fast-transient analysis is a simple and useful non-invasive tool to monitor chloroplast function *in vivo* as well as *in vitro*[2]. The fast OJIP transient and its quantification by the JIP test provide a sensitive and reliable test for the functionality of photosynthetic system and vitality of green tissues[3-6]. The Chl *a* fluorescence transients, both fast and slow are used extensively in studies on various aspects of plant biology from physiology, biotechnology to eco-physiology[1,4,6]. These Chl *a* fluorescence transients have the potential to be exploited in studies on plant protoplasts.

Isolation of intact mesophyll protoplasts from leaves involves short, but physiologically stressful steps, such as enzymatic digestion at acidic *p*H and alternate periods of light and darkness[7]. During such isolation procedure, the bioenergetic organelles of chloroplasts and mitochondria could experience metabolic disturbances. Earlier, we have developed an extremely efficient procedure for isolating intact mesophyll protoplasts from pea *(Pisum sativum)* leaves for studies on photosynthesis and respiration[7,8]. In addition, a fast and reliable procedure for isolation of metabolically active mesophyll protoplasts from model plant *Arabidopsis thaliana* has recently been developed[9].

In this communication, we have used for the first time the fast Chl *a* fluorescence transients for monitoring and assessing the functional photochemical performance of mesophyll protoplasts at different stages of isolation from pea (*Pisum sativum*) leaves. Our results demonstrate the similar photosynthetic performance of isolated mesophyll protoplasts to that of intact leaves.

Materials and Methods

Plant material

Pea (*Pisum sativum* L. cv. Arkel) plants were raised from seeds (procured from Pocha Seeds Co. Ltd, Pune, India) in the green house with average

*Author for correspondence
E-mail: prasanna37@hotmail.com, photosis@rediffmail.com
Fax: 0674 -2550274
Mailing address:
INSA Honorary Scientist, C\o Regional Plant Resource Centre, Nayapalli, Bhubaneswar 751015, Orissa, India

Abbreviations: Chl, chlorophyll; FDA, fluoresceine diacetate; PQ, plastoquinone; PS, photosystem; Q_A, primary quinone electron acceptor of PS II; Q_B, secondary quinone electron acceptor of PSII

Proc. A.P. Akademi of Sciences, Hyderabad
Vol. 9 (4) 2005: 305-312

RECENT ADVANCES IN BIOCHEMISTRY OF PHOTOSYNTHETIC CARBON ASSIMILATION

B. SUNIL and *AGEPATI S. RAGHAVENDRA
Department of Plant Sciences, School of Life Sciences,
University of Hyderabad, Hyderabad 500 046, A.P., India
Fax: +91-40- 23010145; Email: asrsl@uohyd.ernet.in

Abstract

During photosynthesis, photochemical reactions derive assimilatory power (ATP and NADPH) from radiant energy. The assimilatory power is then used for assimilation of carbon or nitrogen or sulfur. This article summarizes some of the advances in our understanding of photosynthetic carbon metabolism through the C_3 or C_4 or C_2 (photorespiration) pathways. Marked interactions of photosynthesis with mitochondrial respiration and N-metabolism are recognized. Dramatic progress has also been achieved in genetic manipulation of several C_3 and C_4 enzymes.

Keywords : C_3, C_4, Calvin cycle, CAM, carbon assimilation, mitochondrial respiration, photorespiration, rubisco.

Introduction

Photosynthesis is composed of two major phases: photochemical reactions and assimilation of carbon (or nitrogen or sulfur). Carbon assimilation by plants and other photosynthetic organisms is a very important event in the global carbon cycle. Plants fix carbon primarily into 3-phosphoglycerate (PGA, a 3-carbon compound) and the process is named as C_3 photosynthesis or C_3 pathway or Calvin cycle. The other two variants of photosynthetic carbon assimilation are C_4 photosynthesis (or C_4 pathway) and Crassulacean acid metabolism (CAM). Among the *ca.* 300 000 higher plants on the earth, almost 90% are C_3 plants, while the CAM and C_4 species constitute about 10% and 3%, respectively (Table 1). Most of the crops (particularly cereals, legumes, and oilseed crops) are of the C_3 type.

This article summarizes the recent advances in our knowledge of photosynthetic carbon assimilation in higher plants. Some of the recent books on this topic are by Raghavendra (1998), Hall and Rao (1999), Yunus *et al.* (2000), Lawlor (2001) and Blankenship (2002).

C_3 photosynthesis or Calvin cycle

During the Calvin Cycle or C_3 pathway, the first stable product of carboxylation is PGA. Detailed description of the path of carbon assimilation in C_3 plants can be found in several excellent reviews (Martin *et al.*, 2000; von Caemmerer and Quick, 2000; Raghavendra, 2003).

Among the recent developments related to Calvin cycle are the extensive reports on: (i) structural biology and mechanisms of RuBP carboxylase/oxygenase (Rubisco), (ii) regulation of other key enzymes and (iii) genetic manipulation of Calvin cycle enzymes. Despite being in

*Corresponding author

Proc. of AP Akademi of Sciences
Vol. 9, No. 3, 2005, pp.237-242

MANIPULATION OF PHOTOSYNTHETIC CARBON METABOLISM THROUGH BIOTECHNOLOGY

B. SUNIL, ESWAR RAMIREDDY and AGEPATI S. RAGHAVENDRA
Department of Plant Sciences, School of Life Sciences, University of Hyderabad, Hyderabad 500 046.

Recent advances in identifying genes and their introduction into target plant opened up a wide opportunity to manipulate photosynthesis in plants. This review describes the genetical manipulation of photosynthetic carbon assimilation and partitioning. There has been stupendous progress in overexpressing or suppressing the key enzymes of not only Calvin cycle but also the C_4 pathway. However, only very few reports are available on the transformation of CAM plants. Introduction of super-Rubisco, keeping the leaves green, synchronization of efficiency in source and sink tissues and introduction of novel CO_2 concentrating mechanisms are a few novel approaches.

Photosynhesis is one of the most important metabolic processes in plants. Crop yields are dependent on the amount of light intercepted by plants and their photosynthetic capacity over a growing season. Breeding and agronomic practices have achieved a remarkable improvement of photosynthetic performance. However, modification of photosynthetic metabolism itself has proved to be a complex task, as these processes involve manipulating suites of genes located in different tissues.

This review focuses on the efforts to manipulate genetically the enzymes of photosynthetic carbon metabolism. In several instances, reviews are cited to limit the length of this article. Modification of photosynthetic electron transport components are aptly described by Gupta *et al.* (2002) and Labate *et al* (2004).

Calvin Cycle

Several efforts to improve photosynthetic carbon fixation focused on modulating the key Calvin cycle enzymes like ribulose-1,5-bisphosphate carboxylase/oxygenase (Rubisco), fructose-1,6-bisphosphatase (FBPase) or sedoheptulose-1,7-bisphosphatase (SBPase) (Spreitzer and Salvucci, 2002; Raines, 2003). The isolation and sequencing of genes coding the Calvin cycle enzymes facilitated the production and study of transgenic plants with reduced levels of these enzymes (Fig. 1).

Antisense technology was used to decrease the amount of Rubisco in tobacco, rice and the C_4 plant *Flaveria bidentis* (Spreitzer and Salvucci, 2002; Parry *et al.*, 2003). Decreased Rubisco content induces photoprotective mechanisms by decreasing the sink for electrons and increases the N-use efficiency (Makino *et al.*, 1997; Schoefs *et al.*, 2001).

Rubisco has to be activated by rubisco activase to become catalytically competent (Portis, 2003). Antisense RNA techniques reduced the Rubisco activase levels and decreased net rates of photosynthesis (Zhang *et al.* 2002). Although the precise mechanism is unclear, there is to manipulate Rubisco activase and thereby Rubisco, for increased photosynthesis.

CHAPTER TWO

Multiple Factors Mediate the Cross Talk Between Mitochondrial Metabolism and Photosynthetic Carbon Assimilation: Roles of Photorespiratory CO_2 and Ascorbate

K. Riazunnisa, L. Padmavathi, B. Sunil, and Agepati S. Raghavendra

Abstract The biochemical basis of interactions between chloroplasts and mitochondria to optimize photosynthesis is examined using pea or Arabidopsis. Mesophyll protoplasts of pea required much less CO_2 for maximal photosynthesis, than their chloroplasts. Such low requirement for CO_2 could be due to an internal carbon source and/or a CO_2 concentrating mechanism in mesophyll protoplasts. The suppression of protoplast photosynthesis by photorespiratory inhibitors (aminooxyacetate, AOA or glycine hydroxamate, GHA) indicated that photorespiration could be a significant source of CO_2 for photosynthesis by mesophyll protoplasts at limiting CO_2 and atmospheric oxygen. Photosynthesis in Asc-deficient *vtc1* mutant of Arabidopsis decreased strongly at high light and was quite sensitive to SHAM. We suggest that recycling of photorespiratory CO_2 and ascorbate can be additional factors involved in the beneficial interactions of mitochondria and chloroplasts.

Keywords Ascorbate, *vtc1* mutant, carbonic anhydrase, interorganelle interactions

Department of Plant Sciences, School of Life Sciences, University of Hyderabad, Hyderabad 500 046, India

J.F. Allen, E. Gantt, J.H. Golbeck, and B. Osmond (eds.), *Photosynthesis. Energy from the Sun: 14th International Congress on Photosynthesis*, 1057–1061.

Introduction

Interorganelle interactions between chloroplasts and mitochondria through cytosol and peroxisomes is essential to optimize photosynthesis (Raghavendra and Padmasree 2003; Nunes-Nesi et al. 2007). Besides rapid exchange of metabolites there could be other signals between chloroplasts, mitochondria and other compartments such as reactive oxygen species (ROS), nitric oxide (NO), cytosolic pH and ascorbate (Asc) (Raghavendra and Padmasree 2003; Noctor et al. 2007).

Photosynthesis by pea mesophyll protoplasts requires <1 mM bicarbonate, in contrast to chloroplasts, which require up to 10 mM bicarbonate for their photosynthesis (Riazunnisa et al. 2006). The low requirement of CO_2 for photosynthesis by protoplasts of pea could be due to a CO_2 concentrating mechanism or high internal CO_2. Asc is the most abundant antioxidant in plant cells and ubiquitous. The Asc-deficient *vtc1* mutants of *Arabidopsis* were sensitive to various stress conditions like high light or SO_2 (Müller-Moulé et al. 2004). The last step of Asc synthesis is catalyzed by L-galactono-1,4-lactone dehydrogenase, located on the inner mitochondrial membrane. Thus, mitochondria are crucial for synthesis of Asc, required for scavenging active oxygen

PLANT BIOTECHNOLOGY
Perspectives and Prospects
Festschrift in honour of Prof. C.P. Malik

2

GENETIC MANIPULATION OF PHOTOSYNTHESIS IN HIGHER PLANTS: PROGRESS AND POSSIBLE APPLICATIONS

B. SUNIL AND AGEPATI S. RAGHAVENDRA

INTRODUCTION

Significant increases in the grain production are required, to meet the demand for food from the growing world population, particularly in relation to crops grown in developing countries. Significant improvements in crop yields during the twentieth century have been achieved through the use of high yielding cultivars and optimized improved agricultural practices. As the suitable land and the available water supplies are extremely limited, the development of high-yielding crop plants with sustained productivity under limiting environmental conditions is essential to achieve the increase in food production.

Photosynthesis is one of the most important metabolic processes in plants. Increasing photosynthetic capacity per unit leaf area has therefore been an important target to achieve an increase in yield potential. Breeding and agronomic practices have already achieved a remarkable improvement of photosynthetic performance. However, modification of photosynthetic metabolism itself has proved to be a complex task, as these processes involve manipulating whole suites of genes located in different tissues. The advances in

Editor
Prof. P.C. Trivedi

Pointer Publishers
Jaipur 302 003 (Raj) India

Article Number: u1345

ROLE OF ASCORBIC ACID DURING INTERACTIONS BETWEEN MITOCHONDRIA AND CHLOROPLASTS TO OPTIMIZE PHOTOSYNTHESIS

L. Padmavathi, K. Riazunnisa, B. Sunil, A. S. Raghavendra. Department of Plant Sciences, School of Life Sciences, University of Hyderabad, Hyderabad 500046, India

Keywords: Ascorbate, Mitochondria, Chloroplasts, Interorgnelle interaction, Photosynthesis

INTRODUCTION

In chloroplasts, ascorbate helps detoxify H_2O_2 produced during the Mehler reaction and is regenerated via the ascorbate-glutathione cycle (Foyer & Haliwell 1976). Ascorbate is thus important for photoprotection of chloroplasts. The *vtc* mutants of *Arabidopsis* (deficient in ascorbate), were sensitive to various stress conditions like high light ozone, SO2, or UV-B radiation (Noctor & Foyer 1998, Müller-Moulé et al 2003).

Mitochondria play an important role in the ascorbate metabolism of the cell. The last step in ascorbate synthesis is catalyzed by L-galactono-1,4-lactone dehydrogenase (GALDH), located on the inner mitochondrial membrane (Smirnoff et al 2001). It is proposed that GALDH can contribute electrons to cytochrome c of the mitochondrial electron transport chain (Bartoli et al 2000). Also, ascorbate pool is greater in high light acclimated plants than those in normal light (Gatzek et al 2002).

Interorganelle interaction between chloroplasts and mitochondria through cytosol and peroxisomes is essential to optimize photosynthesis (Raghavendra & Padmasree 2003). The interaction is facilitated through: metabolite shuttles, energy/redox exchange and recycling of carbon and nitrogen (Gardeström et al 2002, Padmasree et al 2002). Recent work suggests the existence of a signaling network between chloroplasts and mitochondria, that involves ROS and antioxidants (Foyer & Noctor 2003).

Our aim was to examine the role of ascorbate in the interaction between chloroplasts and mitochondria. Experiments were planned to study the effects of modulation of mitochondrial oxidative metabolism on the biosynthesis, redox status and the total pool of ascorbate and on photosynthesis in leaf discs of pea. The ascorbate content was modulated by feeding L-galactono-1,4-lactone (GAL), a precursor of ascorbate, and the consequent effects on photosynthesis and respiration were studied.

MATERIALS AND METHODS

Preparation and treatment of leaf discs. Discs (ca. 0.25 cm^2) were punched from leaves of pea (*Pisum sativum*, var. Arkel) under water. These discs (19 in number) were incubated in 5 cm diameter petri dishes containing water or test compounds. During incubation, the leaf discs were illuminated (unless otherwise mentioned) under a dim light (100 $\mu mol\, m^{-2}\, s^{-1}$) for effective entry of test compounds.

Measurement of photosynthesis and respiration. After a given treatment, the leaf discs were quickly blotted dry and transferred into the leaf disc oxygen electrode chamber (Hansatech Instruments Ltd., King's Lynn, UK). Photosynthetic oxygen evolution or dark oxygen uptake was measured at 25 °C by a computerized system (Padmavathi & Raghavendra 2001).

Extraction and estimation of ascorbate. The procedure of Foyer et al (1983) was followed with slight modifications. Each sample (19 leaf discs), after the said treatment, was frozen in liquid nitrogen and extracted into perchlorate and used for ascorbate estimation (A_{265}) using ascorbate oxidase. Dehydroascorbate (Dha) was determined by using reduced glutathione.

RESULTS

Effect of Mitochondrial Inhibitors on Ascorbate Content, Photosynthesis and Respiration. Treatment with antimycin A, or oligomycin or salicylhydroxamic acid (SHAM) decreased the Asc/Dha ratio (Fig. 1A). All the inhibitors increased the total ascorbate pool, by 15 to 40%. The increase was pronounced with SHAM.

Photosynthetic O_2 evolution decreased upon treatment with all the three inhibitors (Table 1). Respiration was affected marginally.

Effect of Treatment with GAL. Feeding pea leaf discs with 25 mM L-galactono-1,4-lactone (GAL) elevated the total ascorbate pool by nearly 3-fold (Fig. 2B). The presence of antimycin A or oligomycin or SHAM increased further the total ascorbate. The Asc/Dha ratios were high in GAL-treated samples, even in presence of oligomycin or antimycin A (Fig. 2A).

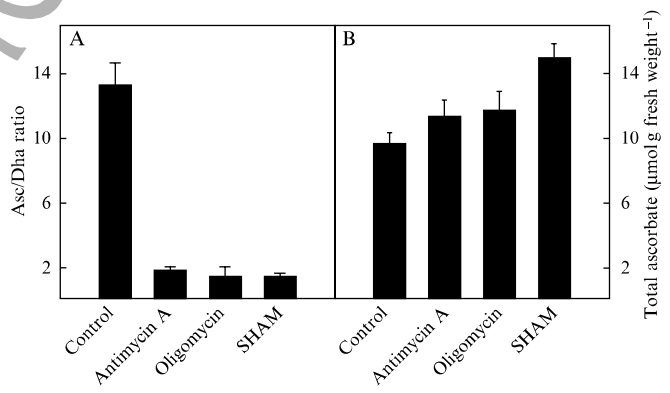

Figure 1: Ascorbate content of pea leaf discs incubated in mitochondrial inhibitors (antimycin A 1 μM, oligomycin 1 $\mu g\, ml^{-1}$, SHAM 2 mM) for 2 h, followed by 10 min in dark. The leaf discs were then washed and incubated in water for 30 min in light of (300 $\mu mol\, m^{-2}\, s^{-1}$).

Table 1: Rates of photosynthesis and respiration in leaf discs of pea after treatment with mitochondrial inhibitors. Figures in brackets indicate % control, i.e., in the absence of inhibitor

	Rate ($\mu mol\, O_2\, m^{-2}\, s^{-1}$)	
Treatment	Respiration	Photosynthesis*
Control	1.1 ± 0.07 (100)	20.3 ± 0.72 (100)
Antimycin A (1 μM)	1.0 ± 0.07 (90)	16.7 ± 1.36 (82)
Oligomycin (1 $\mu g\, ml^{-1}$)	1.1 ± 0.67 (101)	15.5 ± 0.98 (76)
SHAM (2 mM)	0.6 ± 0.08 (57)	17.1 ± 0.99 (84)

* At a light intensity of 300 $\mu mol\, m^{-2}\, s^{-1}$.

